

https://dspace.org/

Hydrometallurgical separation of titanium and iron in ilmenite

Habile, Lungisizwe

2021
https://hdl.handle.net/10539/32948

Downloaded from a DSpace repository. https://dspace.org/

MSc Engineering Dissertation:

Hydrometallurgical Separation of Titanium and Iron in Ilmenite

---



WITS UNIVERSITY

Prepared by:

Lungisizwe Habile (792332)

Supervisor: Prof. Herman Potgieter*

Co-Supervisor: Prof. Walter Purcell**

** - Visiting Professor School of Chemical & Metallurgical Engineering

**School of Chemical and Metallurgical Engineering, 2020*

Declaration

I hereby declare that this work is my own unaided work. It is being submitted to the University of the Witwatersrand for the degree of MSc in Engineering (Chemical).The work has not been examined or submitted to any other University.

Acknowledgments

I am grateful to the Lord for constantly providing me with strength and patience to conduct my research work. My supervisor, Prof Herman Potgieter together with my co-supervisor Prof. Walter Purcell have always been providing guidance since the beginning of this my research work. I therefore express my sincere gratitude towards them for assisting me and guiding me to complete my research work successfully.

I would also like to thank Mrs Sonia Mavhungu, Mr Motlatsi Phali and Mrs Janet Smith who are the laboratory staff for assisting with analyses and solving technical issues. I am also thankful to the Wits School of Chemical and Metallurgical Engineering for providing facilities required to conduct my research work.

I express my sincere gratitude to the CSIR for funding this project since 2019. I thank my family and friends who have given me love and emotional support throughout my research work.

Abstract

The recovery of titanium from ilmenite has been under investigation and researched for many years. This study aims at finding the optimal dissolution route for ilmenite and the separation of the titanium and iron components therein, while maintaining a balance between the economics and optimum operational conditions. Investigated parameters were the leaching of ilmenite using different acids, together with hydrogen peroxide additions. Separation methods that were investigated after leaching included selective precipitation, solvent extraction and the use of ion-exchange resins. Two acids were used for the leaching of ilmenite, namely concentrated sulphuric acid and phosphoric acid. The second dissolution attempt was carried out using a mixture of hydrogen peroxide and the acids mentioned above. Each sample was prepared using 0.5g of ilmenite and 10ml of acid. Hydrogen peroxide concentrations of 2; 5; 10; 15 and 20 vol % H_2O_2 were used, respectively. A combination of H_2SO_4 and 15 vol % H_2O_2 was selected as the optimum mixture for dissolution. The temperature for the dissolution increased rapidly to temperature of about 155 °C and no heat was added until the end of the 30min period. The optimum mixture achieved 81 % Ti dissolution, with only trace amounts of Fe present in the solution.An evaluation of the different separation methods was undertaken. Selective precipitation using Phenantroline (phen) and NaTPB (sodium tetra-phenyl borate) as precipitation reagents was carried out. Each of these reagents were used at varied volume concentrations of 2 %, 5 %, 10 %, 15 % and 20 %. The precipitated titanium oxide was recovered through filtration. No precipitation occurred when phen was used. When 2 % NaTPB was used, the amount of Fe remaining in solution at the end of a 30 min period, was approximately 85 %. The recovery of Ti was close to 100 % and no Ti remained dissolved in solution. Solvent extraction was also investigated. Acetylacetone (acacH) and 1-octanol were used as chelating reagent and extraction solvent respectively.90-95 % Fe was recovered in the aqueous layer and titanium to the organic layer. Cationic and anionic resins were also used in order to investigate the separation of titanium and iron. Dowex marathon C hydrogen was used as a cationic resin, with Amberlite IRA-900 and Amberlite IRA-67 as strong and weak anionic resins, respectively. A recommended elution flow rate of approximately 0.7 mL/min was employed. It was found that using Dowex marathon C hydrogen at 15 % achieves better separation of Ti and Fe than both IRA-900 and IRA-67. A process flowsheet was designed with a mass efficiency of approximately 50 %. Solvent extraction using 2 % acetylacetone in 1-octanol was used as a separation medium. A plant utility structure was also constructed as the plant is aimed at being a Greenfield plant. A techno-economic evaluation found that the proposed plant for the process could yield returns of approximately 18 %.

Table of Contents

Declaration i

Acknowledgments ii

Abstract iii

Nomenclature viii

1.1 Background **1**

1.2. Problem Statement **3**

1.3. Aims and Objectives **4**

1.4. Hypothesis **4**

CHAPTER 2—LITERATURE REVIEW AND THEORETICAL BACKGROUND 5

2.1.Possible Ilmenite Dissolution Techniques 5

2.1.1.Ilmenite Dissolution Additives-Gaseous Oxygen and Liquid Oxygen 5

2.1.2. Ilmenite Dissolution Additives-Hydrogen Peroxide 6

2.1.3. Ilmenite Dissolution Additives-Fluorine and other Halogens 8

2.1.4. Oxidizing Reagent Selection Criteria 9

2.1.5. Ilmenite Dissolution through HCl-Alcohol and HCl-Water Systems 11

2.1.6. Ilmenite Dissolution through Bioleaching 11

2.1.7. Plasma Manufacturing of TiO_2 12

2.1.8. Ilmenite Dissolution Rates 13

2.2.Methods involving Iron and Titanium Separation 14

2.2.1. Hydrometallurgical Processing Technology of Titanomagnetite Ores **14**

2.2.2 Preparation of Synthetic TiO_2 Through Sulphation of Ilmenite Followed by Impurity Removal **15**

2.2.3. Selective Precipitation **16**

2.2.3.1 Past Studies Conducted on Selective Precipitation 17

2.2.4. Solvent Extraction Separation **19**

2.2.4.1. Past Studies Conducted on Solvent Extraction 19

2.2.5. Ion-Exchange Resins **20**

2.2.5.1. Ion-Exchanger Capacity and Eluting Starting Conditions 21

2.2.5.2. Ion-Exchanger pH and ionic strength 21

2.2.5.3. Past Studies Conducted on Ion Exchange Resins 22

CHAPTER 3—EXPERIMENTAL PROCEDURES AND MATERIALS 24

3.1. Equipment **24**

3.2. Materials **24**

3.3. Experimental Procedure **24**

3.3.1. Dissolution of Ilmenite 24

3.3.2. Selective Precipitation 25
3.3.3. Solvent Extraction Separation 25
3.3.4. Ion-Exchange Resins 25
3.4. Quantification Technique **26**
3.4.1. Atomic absorption spectroscopy 26
3.5. Data Analysis **27**
3.6. Experiment Summary-Block Flow Diagram **28**
4.1. Leaching **29**
4.1.1. Factors Influencing Ilmenite Dissolution **34**
4.1.1.1. Temperature **34**
4.2. Separations **35**
4.2.1. Selective Precipitation 35
4.2.2. Solvent Extraction 39
4.2.3. Ion Exchange Resins 42
4.3. Residue Analysis **54**
4.4. Experimental Conclusion **56**
CHAPTER 5—PROCESS FLOWSHEET & UTILITY STRUCTURE 57
5.1. Experiments Conclusion & Information Taken To Prelimi-nary Process **57**
5.3. Overview of the plant description and flowsheet **59**
5.4. Plant Utility Structure **62**
5.4.1 Steam Generation 62
5.4.2. Cooling Tower 64
5.5. Economic Comparison **66**
CHAPTER 6 – CONCLUSIONS AND RECOM-MENDATIONS 68
6.1. Conclusions **68**
6.2. Recommendations for Future Work **69**
6.3. Value and Contribution of this Work **69**
7. References 70
8. Appendix 74
8.1. Appendix A- Results in terms of concentration **74**
8.2. Appendix B-Lab Plan **77**
8.2.1. Dissolution **77**
8.2.2. Separation **78**
8.3.Appendix C-Images of Prepared Solutions **80**
8.4.Appendix D-Mass & Concentration Profile Tables (Raw Data) **83**
8.4.1. Dissolution **83**
8.4.2.Separation **84**

8.6 Appendix F-SEM Results 87

List of Tables

Table 2.1: Summary of liquid oxygen properties (Air Products, 2005). 6
Table 2.2: Summary of hydrogen peroxide properties (PubChem, 2016) 8
Table 2.3:NaPT selective precipitation results (Purcell, 2019). 18
Table 2.4:Ion-exchange results obtained through the use of bauxite and bentonite clay (Das, 1990). . 22
Table 4.1: Ti and Fe % dissolution in in H_2SO_4 and various H_2O_2 amounts 33
Table 4.2: Titanium selectivity in ilmenite leaching with various H_2O_2 additions. 33
Table 4.3: Relative supersaturation precipitation values of NaTPB additions 37
Table 4.4: Kinetic fittings for NaTPB selective precipitation of Ti from solution 37
Table 4.5: Selective precipitation of Titanium from solution with various NaTPB additions. 38
Table 4.6: Fe and Ti Distribution ratios and Separation Factors in aqueous and organic layers with various Acac additions 41
Table 4.7: 1st order separation correlation for Fe using DMCH 42
Table 4.8: 1st order separation correlation for Ti using DMCH. 43
Table 4.9: 1st order separation correlation for Fe using IRA-67. 45
Table 4.10: 1st order separation correlation for Ti using IRA-67. 46
Table 4.11: 1st order separation correlation for Fe using IRA-900. 47
Table 4.12: 1st order separation correlation for Ti using IRA-900. 48
Table 4.13: Fe and Ti ion exchange separation parameters. 49
Table 4.14: Fe and Ti % recoveries on filtered cake. 54

List of Figures

Figure 2.1: Formation of hydrogen peroxide using 2-anthraquinol (Arkema, 2016). 7
Figure 2.2: Representation of the Kroll process and its reactions (Centre for Industry, 2016) 8
Figure 2.3: Dissolution of ilmenite using HCl-C_2H_5OH, HCl-CH_3OH and HCl-H_2O over 9hr (Turker, 1988) 11
Figure 2.4: Dissolution of ilmenite using P.citrinum, A.niger and B.megaterium (Theeraporn, 2013). 12
Figure 2.5: Schematic diagram of the plasma manufacturing of TiO_2 (Nel, 2010). 13
Figure 2.6: Ilmenite dissolution rate at varied H_2SO_4 concentrations (Woranart, 2013). 13
Figure 2.7: Ti and Fe extraction efficiency at varied HF concentrations (Sachkov, 2017). 15
Figure 2.8: Illustrated Acetylacetone-titanium bonding (Erik, 1993). 19
Figure 2.9: Optimum ion-exchange separation through low eluting flow rates (Khan, 2012) 21
Figure 3.1: Schematic representation of an atomic absorption spectrometer (Beatriz, 2019). 25
Figure 3.2: Experimental block flow diagram for titanium recovery.investigation 27

Figure 4.1: Fe(mass%) dissolved in solution when using H_2SO_4 and H_2O_2 at varied vol%, 25°C, pH of 2 and stirring at 180rpm. 28
Figure 4.2: Ti(%) dissolved in solution when using H_2SO_4 and H_2O_2 at varied vol%, 25°C, pH of 2 and stirring at 180rpm. 30
Figure 4.3: Fe(%) dissolved in solution when using H_3PO_4 and H_2O_2 at varied vol%, 25°C, pH of 2 and stirring at 180rpm. 30
Figure 4.4: Ti(%) dissolved in solution when using H_3PO_4 and H_2O_2 at varied vol%, 25°C, pH of 2 and stirring at 180rpm. 31
Figure 4.5: Dissolution temperature profile of ilmenite 34
Figure 4.6: Fe (mass %) remaining in solution when using NaTPB at 25°C, pH of 2 and stirring at 180rpm. 35
Figure 4.7: Ti (mass %) remaining in solution when using NaTPB at 25°C,pH of 2 and stirring at 180rpm. 36
Figure 4.8: Fe (%) in aqueous layer using acetylacetone (acac) in 1-octanol at 25°C, pH of 4 and stirring at 180rpm. 38
Figure 4.9: Ti (%) in aqueous layer using 20% acetylacetone (acac) in 1-octanol. 39
Figure 4.10: Ti % in aqueous layer using acetylacetone (acac) in 1-octanol at 25°C,pH of 4 and stirring at 180rpm. 40
Figure 4.11: General extraction of metal M (Christian, 1991). 40
Figure 4.12: Cumulative Fe(%) eluted at 25°C using a cationic resin Dowex Marathon C Hydrogen (DMCH vol%), 0.5M H_2SO_4 eluent at 0.7ml/min. 42
Figure 4.13: Ti(%) eluted at 25°C using a cationic resin Dowex Marathon C Hydrogen (DMCH) 0.5M H_2SO_4 eluent at 0.7ml/min. 43
Figure 4.14: Fe(%) eluted at 25°C using an anionic resin Amberlite IRA-67 with 0.5M H_2SO_4 eluent at 0.7ml/min. 44
Figure 4.15: Ti(%) eluted at 25°C using an anionic resin Amberlite IRA-67 0.5M H_2SO_4 eluent at 0.7ml/min. 46
Figure 4.16: Fe(%) eluted at 25°C using an anionic resin Amberlite IRA-900, 0.5M H_2SO_4 eluent at 0.7ml/min. 47
Figure 4.17: Ti(%) eluted at 25°C using an anionic resin Amberlite IRA-900, 0.5M H_2SO_4 eluent at 0.7ml/min. 48
Figure 4.18: Summary of the maximum elution of Fe using the various cationic ion-exchange resins. 50
Figure 4.19: Summary of the maximum elution of Fe using the various anionic ion-exchange resins. 51
Figure 4.20: Breakthrough curve for 20% DMC 51
Figure 4.21: Breakthrough curve for 20% IRA-67 52

Figure 4.22: Breakthrough curve for 20% IRA-900……..……..…52
Figure 4.23: SEM image of precipitate formed when applying a 5%NaTPB mixture. Analysis at 1mm, 25 nA and 15kV. 53
Figure 4.24: Graphical precipitate composition results of Fe and Ti for 5%NaTPB mixture. 54
Figure 5.1 Process flowsheet 60
Figure 5.2: Rankine Cycle diagram. 61
Figure 5.3 Plant utility structure 64

Nomenclature

AA	Atomic absorption
Acac	Acetylacetone
DMCH	Dowex Marathon C Hydrogen
HAZOP	Hazard and Operability
ICP	Inductively Coupled Plasma
MTPD	Metric Tonnes per Day
SEM	Scanning Electron Microscope
NATPB	Sodium tetraphenyl borate
Phen	Phenanthroline
TOPO	Tri-octylphosphine oxide
λ(wt%)	Fe total removal efficiency or TiO_2 loss.
C	Concentration.
V	HCl leaching volume.
M	Mass
W	Constant

CHAPTER 1—INTRODUCTION

1.1 Background

Titanium is one of the most valuable metals to be discovered in the history of metals. This metal has a high economic value, as it is an important component in the operations of many industries. According to recent studies, power plant condensers are constructed using titanium as it provides resistance to corrosion (Emsley, 2014). Furthermore, desalination plants and many structures that are submerged in seawater use titanium coatings, as it provides good resistance to corrosion by seawater.

Titanium is as strong as steel but less dense—which makes it an excellent alloying agent with metals such as iron and aluminium (Emsley, 2014). As is known, these alloys are used in aircrafts, missiles, car engines and even in bicycles, as it can withstand extreme temperatures and pressure. This shows that titanium is indeed a pillar in most industries. It is therefore crucial to constantly consider ways of improving the beneficiation of this metal in order to meet its increasing demand (while minimizing impact to the environment).

Titanium also has a biological role, as it was found to attach well to bone (Emsley, 2014) and has surgical applications such as joint replacements. In the paint industry, titanium is used as a pigment in the form of titanium oxide (Siddle, 1975). Titanium oxide is also used in solar observation studies as it provides good reflection of infrared radiation. Furthermore, titanium oxide is used in sunscreens as it is a good reflector of UV light, thus preventing UV radiation from damaging the skin (Emsley, 2014).

Titanium was discovered in 1791 by Reverend William George (Emsley, 2014). Upon this discovery, the sand that contained this metal was called menachanite, which appeared black in colour. Titanium is the 9th most abundant metal in the earth's crust (Emsley, 2014). It is found in igneous rocks and sediments which break off from these rocks — which explains why it is found in beach sand. Titanium occurs mostly in ores such as ilmenite, rutile and sphene (Siddle, 1975).

South Africa has the second largest reserves of titanium in the world (Creamer Media's, 2013). This makes South Africa potentially one of the largest titanium producing countries in the world. The Council for Scientific and Industrial Research (CSIR) recently started recovering titanium by using the Kroll process (Creamer Media's, 2013). This process involves obtaining

pure titanium from chlorination, electrolysis and magnesium reduction. The CSIR titanium pilot plant was launch on the 7th of June 2013 to produce Ti metal. The production capacity of this plant is 2kg/hour, which is an annual production rate of 15.8 ton/year (Creamer Media's, 2013). The CSIR aimed to improve this production rate to 500 ton/year (semi-commercial) by 2017. To make it a fully commercial plant, the plant is to be scaled up to a production rate of 20 000 ton/year.

This improvement of the Kroll process for the pilot plant was essential. This is because the pilot plant was found to produce pure titanium at lower temperatures than the Kroll process (Creamer Media's, 2013). Lower temperature requirements meant less energy required to run the process, thus providing a good trade-off between plant economics and optimum operational conditions. The processing and selling of titanium is a profitable industry, which in turn can result in a boost to the country's economy. One of the raw materials fed to the plant is ilmenite, a mineral worth R4.06/kg (Creamer Media's, 2013). Pure grade titanium powder costs about R324/kg (Alibaba.com, 2020). The calculation of the **overview** of the annual profit margin based on raw material-product value mentioned above would be as follows (assuming a typical 70% mass efficiency):

$$Annual\ Profit\ Margin = [Product\ price \times rate_P] - [Raw\ material\ cost \times\ rate_R]$$

$$= \left[\left(\frac{R324}{kg}\right) * \left(\frac{1000kg}{ton}\right) * \left(\frac{500ton}{yr}\right)\right] - \left[\left(\frac{R4.06}{kg}\right) * \left(\frac{1000kg}{ton}\right) * \left(\frac{650ton}{yr}\right)\right]$$

= R 159 361 000/yr.

Where:

$rate_P$ = CSIR semi-commercial annual production rate.

$rate_R$ = Annual raw material assuming 70 % mass efficiency.

From the basic profit margin, which excludes operation costs, one can conclude that the plant can be highly profitable. Possible reasons for such a high plant profitability are:

- South Africa has access to low cost ilmenite.
- High abundance of ilmenite with high titanium content guarantees long periods of operation.
- Exceptional economics of scale of the pilot plant as the unit produces considerable amounts of product for a given amount of feed.

It is important to note that the CSIR titanium pilot plant does have room to improve its profit margin. One such possibility is to turn the plant into a green field plant, which means that the plant will generate its own power, cooling and heating utilities (Chen, 2014). This will in turn reduce the cost of utilities, thus leading to an increase in profit. Green field plants are expensive, but results in high savings in the long run. Furthermore, a green field plant produces surplus power, which can be sold to generate more revenue or can be stored and used as backup in downtimes.

It is for these reasons that the CSIR is on the continuous lookout for the optimization of all the units of its plant. The optimization will in turn aid with obtaining high production (while upholding product quality) from a given amount of feed material. The optimization normally involves batch and semi batch processes, such as conducting laboratory experiments to find optimal separation techniques (Martinez, 2016). Upon approval of these techniques, they are then converted into viable processes.

This study aims at finding titanium recovery methods that are less energy intensive than current ones. The experiments will be divided into two sections, namely the dissolution of the ore using acids and separation of titanium oxide and iron oxide using hydrometallurgical separation techniques. Hydrometallurgical separation techniques such as selective precipitation, solvent extraction separation and ion-exchange resins (by eluting) will be the separation routes that will be tested experimentally for the separation of these metal oxides.

1.2. Problem Statement

The CSIR is on the continuous lookout for the optimization of all the units of its plant. Titanium dioxide has to be separated from beach sand. The ilmenite bearing ore is mined and recovered through a number of processes before it can be beneficiated into titanium and titanium alloys employed in especially the aerospace industry. The flux dissolution and chlorination routes are energy intensive as it requires high temperature operations. Less energy intensive and more sufficient iron and titanium separation processes can substantially reduce production costs of titanium, and there is a strong motivation to investigate such options.

1.3. Aims and Objectives

This study aims at finding the optimal dissolution route for ilmenite and separation of titanium oxide and iron oxide, which occur in this ore, while maintaining a good trade-off between economics and optimum operations. The objectives of this study are as follows:

- Evaluate ore dissolution techniques. Identify and select the most efficient, cost effective and eco-friendly dissolution technique.
- Identify the separation reagents, mixing ratios and determine the most efficient method by selecting the one with the highest TiO_2 recovery.
- Convert the most efficient method into a conceptual process and conducting an economic evaluation thereafter.

The dissolution of ilmenite involves the use of acids such as sulphuric acid and phosphoric acid. This study will further investigate the ore dissolution by adding hydrogen peroxide to the mixture. Various techniques of separating metal oxides have been proposed. These techniques include selective precipitation, solvent extraction separation and use of ion-exchange resins, and these will be investigated and compared in this study. The conceptual process design involves the construction of material flow through major equipment together with a conceptual plant utility structure for greenfield plant application.

1.4. Hypothesis

This work proved that it is possible to separate iron and titanium in ilmenite more economically and efficiently than other processes which have been used to date. This will improve the economic beneficiation of titanium from ilmenite with the CSIR process.

1.5. Dissertation Structure

This dissertation consists of 6 chapters. The first few chapters are chapter 1 and 2, which provide the project overview and literature review respectively. These chapters are important as they outline the need for research in the recovery of titanium and typical industry operational methods. Chapter 3, 4 and 5 are experimental methods, results and discussion, and proposed design of a plant. Chapter 6 summarises the conclusion and make suggestions for further work, respectively.

CHAPTER 2—LITERATURE REVIEW AND THEORETICAL BACKGROUND

A. Theoretical Background

2.1.Possible Ilmenite Dissolution Techniques

Ilmenite has to be dissolved first before the separation of its compounds can be carried out. The degree of ore dissolution is therefore a contributing factor to the amount of desired compounds that can be recovered for a given amount of ore. Companies are on the lookout for techniques that help obtain optimal dissolution if not complete dissolution. As discussed in **section 2.6**, complete ore dissolution is achieved through the use of heated sulphuric acid (200 °C). This heating requires energy, which in turn increases operational costs.

When process plants are designed, energy requirements are kept as low as possible. It has been proven that processes carried out at room temperature are far cheaper to run compared to processes with high temperatures and/or high pressure requirements (Krishen, 1965). One of the aims of this work will be to investigate whether addition of an oxidizing agent(s) could enhance the dissolution of ilmenite at room temperature. Taking into consideration the properties of ilmenite as provided in **Table 2.3,** a survey on possible oxidizing agents was conducted and is presented in **section 2.1** to **2.3**. Recovery and quantification techniques are outlined in subsequent sections.

2.1.1.Ilmenite Dissolution Additives-Gaseous Oxygen and Liquid Oxygen

Oxygen is an oxidizing agent which can react with nearly all metals and organic materials. In reaction with metals, the product formed is usually a metal oxide. In processes that require oxygen, air separation units (ASU) are required in order to produce pure oxygen. This is normally done in order to increase oxygen content for increased conversions or dissolution rates. Preferably oxidizing agents for dissolution of solids are oxidizing agents in the liquid state, as this provides wetting of the solid material (Air Products, 2005). Wetting of the solid material often helps soften the material, which contributes to increased dissolution rate.

Opting for liquid oxygen comes with advantages and disadvantages. Oxygen is often stored as a liquid as it is less bulky and less costly in this state compared to high pressure gaseous storage (Air Products, 2005). The downside of liquid oxygen is that it is a cryogenic liquid. This means that its boiling point is below -90 °C, which is too cold for processes to be carried out at room

temperature or above. Furthermore, materials of construction for processes that involve the use of oxygen should have high ignition temperatures and be nonreactive towards oxygen (Air Products, 2005). Materials with such properties are very expensive and also expensive to repair.

Table 2.1**:** *Summary of liquid oxygen properties (Air Products, 2005).*

Molecular Formula	O_2
Molecular Weight g/mol	31,999
Boiling Point @ 1 atm	-183 °C
Freezing point @ 1 atm	-218 °C
Critical Temperature	-118,4 °C
Critical Pressure	49,6 atm
Density, Liquid @ BP, 1 atm	1141 kg/m^3
Density, Gas @ 20°C ,1 atm	1,33 kg/m^3
Specific Gravity, Gas (air=1) @ 20°C, 1 atm	1,11
Specific Gravity, Liquid(water=1) @ 20°C, 1 atm	1,14
Specific Volume @ 20°C and 1 atm	0,754 m^3/kg
Latent Heat of Vaporization at BP	213 kJ/kg
Expansion Ratio, Liquid to Gas, BP to 20°C	1 to 860
Solubility in Water @ 25°C,1 atm	3,16 % by volume

2.1.2. Ilmenite Dissolution Additives-Hydrogen Peroxide

Hydrogen peroxide is a compound that is a liquid at room temperature. It is commonly used in bleaching and is normally supplied at 40 %(w/w) (Arkema, 2016).This liquid is miscible in water and is colourless in its pure form.

2.1.2.1 Production of Hydrogen Peroxide

Hydrogen peroxide is produced using a process called the Autoxidation process. This process comprises of 4 stages, namely hydrogenation of an anthraquinone, oxidation of the resulting anthraquinol, extraction of hydrogen peroxide solution and lastly purification and concentration of hydrogen peroxide (Arkema, 2016).

Hydrogenation of an anthraquinone:

2-ethylanthraquinone is mixed with a solution containing a polar and non-polar solvent, including a catalyst such as nickel (Arkema, 2016). Hydrogen gas at 320 K is then introduced to the mixture in order to hydrogenate 2-ethylanthraquinone.The product formed in this stage is 2- ethylanthraquinol. The catalyst is recovered by filtration and is recycled in order to reduce catalyst requirements (Arkema, 2016).

Oxidation of the resulting 2- ethylanthraquinol:

Air is used to oxidize the 2-ethylanthraquinol.The oxygen in air reacts with 2-ethylanthraquinol to form hydrogen peroxide and 2-ethylanthraquinone (Arkema, 2016).The process is represented by **Figure 2.1**.

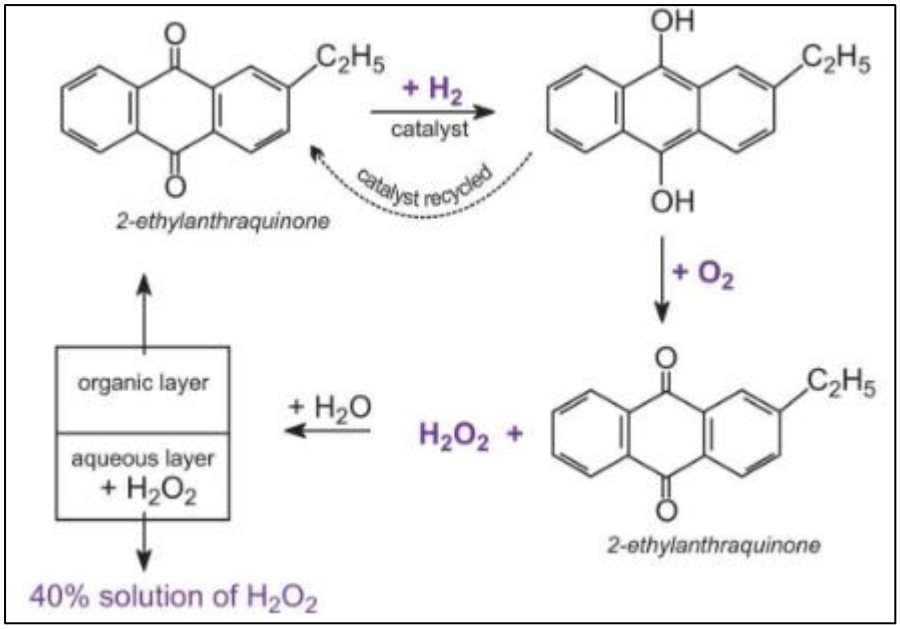


***Figure 2.1**: Formation of hydrogen peroxide using 2-ethylanthraquinol (Arkema, 2016).*

Reaction 1 is the overall reaction represented by **Figure 2.1** (Arkema, 2016):

$H_2 + O_2 \rightarrow H_2O_2$……..(1)

Extraction of hydrogen peroxide solution:

The extraction of hydrogen peroxide involves the addition of water. The addition of water extracts hydrogen peroxide as an aqueous solution with 40% hydrogen peroxide content.

Purification and concentration of hydrogen peroxide:

The standard hydrogen peroxide purity is 40 % (Arkema, 2016). The aqueous hydrogen peroxide is therefore taken for purification. The purification involves the use of organic solvents and the pumping of air into the aqueous solution in order to remove residual anthraquinone.

Table 2.2**:** *Summary of hydrogen peroxide properties (PubChem, 2016)*

Molecular Weight	34.014 g/mol
Hydrogen Bond Donor Count	2
Hydrogen Bond Acceptor Count	2
Colour	Colourless Liquid
Odour	Slightly sharp odour
Taste	Bitter, slightly acidic
Boiling Point @ 1 atm	152.2 °C
Solubility @ 22.2°C	100 mg/mL or greater
Specific Gravity @ 20°C	1.11
Vapor Density (Relative to air)	1.02
Autoignition Temperature	Not Flammable

2.1.2.3. 'Piranha Solution'

A 'piranha solution' is a mixture of sulphuric acid and hydrogen peroxide. This solution is widely used in the microelectronics industry (Stevic, 2018). The solution cleans silicon wafers by removing photoresist residues. The solution is also used to smoothen homemade circuit boards. A mask is often used to cover a blank copper board. A piranha solution is then applied in order to rapidly remove the uncovered copper. Furthermore, this solution can be used to clean glassware in laboratories. However, most institutions have prohibited the use of piranha solution as a cleaning agent due to its danger as an aggressive oxidizing reagent. (Stevic, 2018).

The formation of the piranha solution results in an increased temperature. This is because the reaction between sulphuric acid and hydrogen peroxide is strongly exothermic to form H_2SO_5 and H_2O as seen in reaction 2 (Stevic, 2018).

$H_2SO_4 + H_2O_2 \rightarrow H_2SO_5 + H_2O$……..…[ΔH= -880kJ/mol] (2)

2.1.3. Ilmenite Dissolution Additives-Fluorine and other Halogens

Fluorine is highly reactive and is considered the most reactive element in the periodic table (Robertson, 2019). It attacks all metals and is regarded as a dangerous reagent to use and should be handled with utmost care. On the other hand, an element with such properties proves to be a good oxidizing agent, which can be used to dissolve stubborn solid compounds (Robertson, 2019).

2.1.3.1 Fluorine uses

Fluorine is the 13th most abundant element found in the earth's crust (Robertson, 2019). This element is obtained in its elementary form through electrolysis of hydrogen-difluoride. The uses of fluorine are as follows (Robertson, 2019):

- Nuclear power industry. For the manufacturing of uranium hexafluoride which is used to separate uranium isotopes.
- For the manufacturing of sulphur hexafluoride, which is used as an insulating gas in the electric industry.
- Manufacturing of high temperature plastics such as Teflon.
- Etching of light bulb glass (used as hydrofluoric acid).

2.1.4. Oxidizing Reagent Selection Criteria

Various factors affect the choice of an oxidizing agent. These factors include solubility, rate of oxidation for a given material, reusability, availability and associated costs. According to literature, it is important to consider these factors in order to achieve an efficient and cost effective process (Neil, 1996).

Solubility:

The oxidizing reagent to be used should be soluble in the liquid to be used to dissolve the material subject to dissolution (Neil, 1996). Solubility is closely linked to the dissolution rate and rate of oxidation. The more soluble an oxidizing agent is, the higher the oxidant concentration available in solution for oxidation to take place hence increase dissolution rate (Neil, 1996).

Rate of Oxidation:

An ideal oxidizing reagent is one which results in a high oxidation rate (Sinnott, 2005). Materials mixed with such reagents tend to dissolve much more quicker, thus saving time and money.

Reusability:

The easier it is to recycle the oxidizing reagent, the better. The oxidizing reagent is regarded as a process supporting material. Process supporting materials are additional materials used to carry out a process excluding major raw material. According to literature, a recycling process supporting material reduces the overall supporting material requirements (Sinnott, 2005). This results in reduced operational costs.

Availability:

It is ideal to select a reagent that is readily available to the plant site (Arthur, 1984). This is an important factor as it gives rise to other factors such as transportation costs. The use of a reagent

that will constantly require shipment from other countries will negatively affect the company's annual profit.

Associated Costs:

Raw material costs are one of the main contributing factors in raw material selection. Alternative cheaper raw materials for the process could already save much costs. It would therefore be ideal to select oxidizing reagents that are cheap and effective (Arthur, 1984).

Oxidizing reagents that are closely in line with almost all of these 5 factors are a perfect match.

2.1.5. Kroll Process

The Kroll process was designed to produce zirconium and was named after William Kroll in 1940 (Titanium processing Center, 2017). The Kroll process is also used to produced Ti from $TiCl_4$ and can be represented by the following sketch:

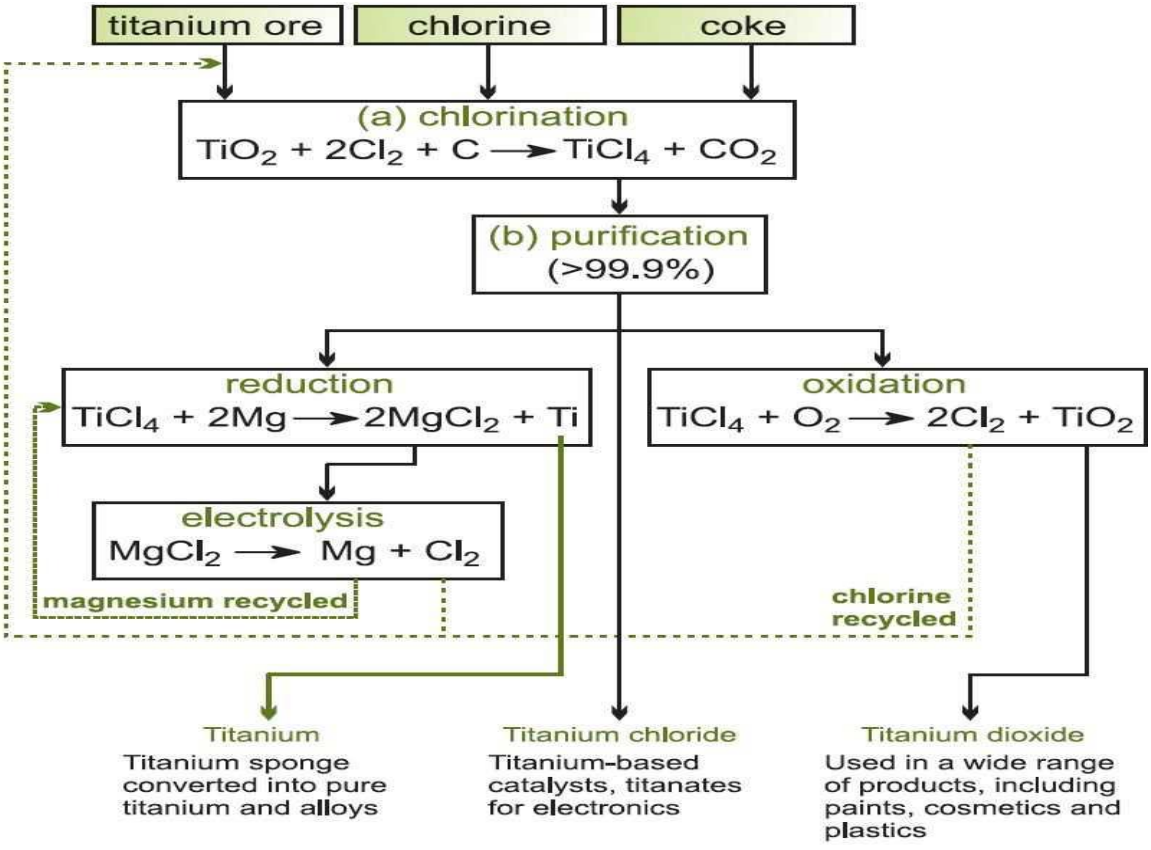


Figure 2.2: *Representation of the Kroll process and its reactions (Centre for Industry, 2016)*

The separation of MCl_2 and titanium is carried out under vacuum distillation at approximately 0.1 Pa and 1000 °C, reaching a titanium separation rate of 111 kg/hr.

B. LITERATURE REVIEW

2.1.5. Ilmenite Dissolution through HCl-Alcohol and HCl-Water Systems

This method involves the dissolution of ilmenite at room temperature. HCl-alcohol combinations that are used, are HCl-C_2H_5OH and HCl-CH_3OH. HCl-water mixtures that are used is basically various concentrations of HCl-H_2O (Turker, 1988). The HCl-C_2H_5OH and HCl-CH_3OH systems dissolve a noticeable amount of Fe and a higher amount of titanium. These differences in Fe and Ti dissolved amounts reduces separation complexity and thus separation costs. This is a theoretical ilmenite leaching model that uses linear order multivariable model for validity checks.

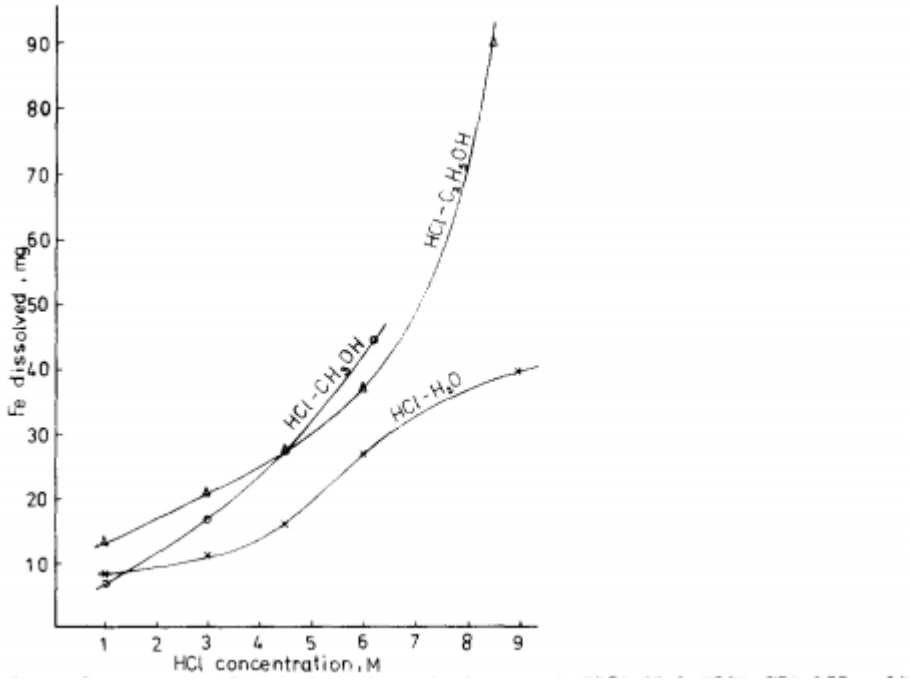


Figure 2.3: *Dissolution of ilmenite using HCl-C_2H_5OH, HCl-CH_3OH and HCl-H_2O over 9hr (Turker, 1988)*

The HCl-alcohol systems is prepared by using absolute C_2H_5OH and CH_3OH. The respective alcohols where saturated with HCl gas. The results illustrated above were obtained with ilmenite concentrate mesh fraction of 200. A 2.5 g ilmenite sample was added to 125ml of leaching solution (Turker, 1988) with stirring.

2.1.6. Ilmenite Dissolution through Bioleaching

Ilmenite bioleaching involves the use of micro-organisms to digest ilmenite. The micro-organisms that are used are *bacillus megaterium (B.megaterium), penicillium citrinum (P.citrinum)* and *asperillus niger (A.niger)* (Theeraporn, 2013). Spores of the respective organisms are transferred to a flask placed in a rotary shaker at 30 °C and 200rpm. A 35 day

period results in a Fe extraction of 0.45 % and a Ti extraction of 0.28 % when *P.citrinum* and *A.niger* are used. Under the same conditions, but for a period of 3 days, using *B.megaterium* achieves a Fe extraction of 0.2 % and a Ti extraction of 0.4 % (Theeraporn, 2013).

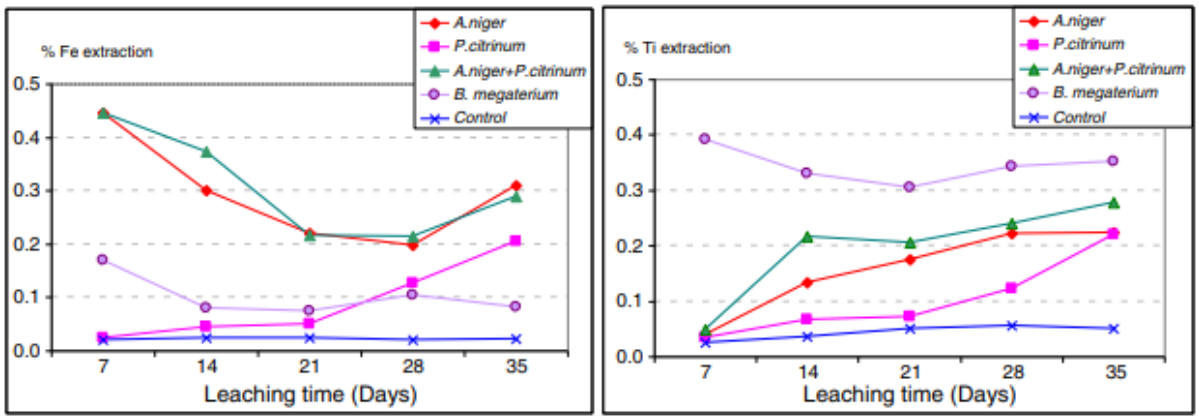


Figure 2.4: *Dissolution of ilmenite using* P.citrinum, A.niger and B.megaterium *(Theeraporn, 2013).*

2.1.7. Plasma Manufacturing of TiO_2

Carbo-chlorination is normally used in order to produce $TiCl_4$. Distillation is then used to purify the $TiCl_4$. A CH_4 flame reactor is used to carry out the oxidation reaction where TiO_2 at pigment grade is formed. Plasma manufacturing of TiO_2 is a modification of this method. **Reaction 3** represents a plasma –assisted oxidation reaction of $TiCl_4$ (Nel, 2010).

$TiCl_4 + O_2 \rightarrow TiO_2 + 2Cl_2$ …….. (3)

The advantage of this method is that after condensation and coagulation, the Cl_2 can be recovered easily and recycled to the feed stream of the carbo-chlorination unit. The process for plasma manufacturing of TiO_2 is shown schematically in **Figure 2.5** (Nel, 2010):

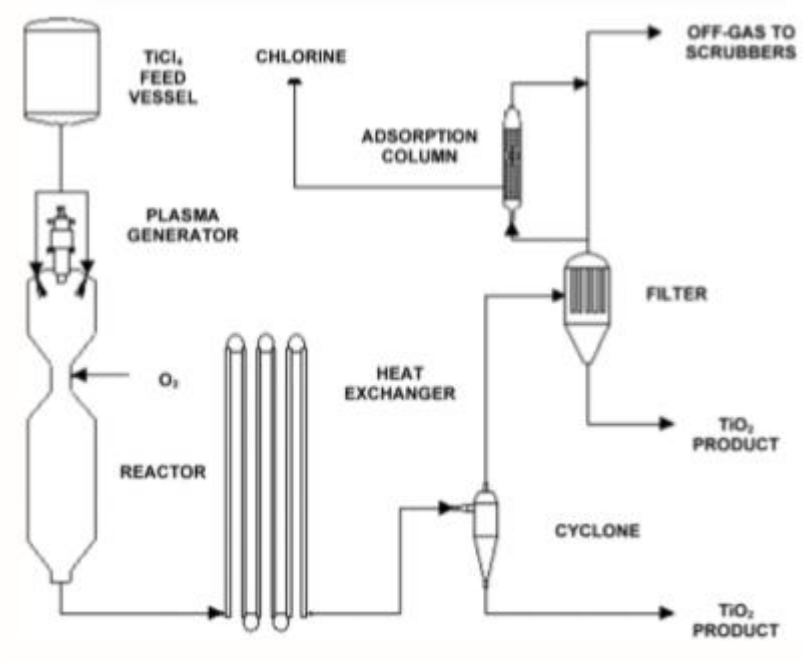


Figure 2.5: *Schematic diagram of the plasma manufacturing of TiO_2 (Nel, 2010).*

2.1.8. Ilmenite Dissolution Rates

The rate of dissolution of ilmenite plays an important role in the amount of metal that can be recovered for a given period. The higher the dissolution rate, the higher the concentration of metal available in solution for recovery (Woranart, 2013). This in turn reduces the dissolution recycle load, hence reducing process complexity and costs. Research conducted using sulphuric acid has proven that the dissolution rate of ilmenite increases with the increase in sulphuric acid concentration (Woranart, 2013). **Figure 2.6** represents this process.

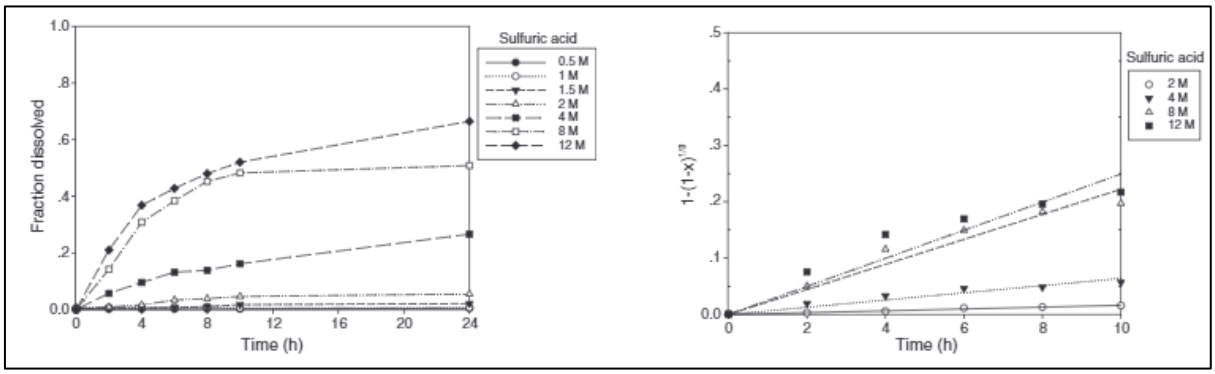


Figure 2.6: *Ilmenite dissolution rate at varied H_2SO_4 concentrations (Woranart, 2013).*

2.2.Methods involving Iron and Titanium Separation

Methods of recovering titanium from ores such as ilmenite are discussed in the sections below.

2.2.1. Hydrometallurgical Processing Technology of Titanomagnetite Ores

This method involved the hydrometallurgical processing where dissolution and separation occurs simultaneously (Sachkov, 2017). Hydrometallurgical processing of the titanomagnetite ores of the Chineisk deposit was used to test the possibility of recovering high amounts of titanium and iron respectively. The concentration of the leaching solution and acidity were varied. Ammonium fluoride was used as a leaching solution. After optimization, 0.42mol/L ammonium fluoride solution was found to be the optimum leaching concentration. The amount of Ti and Fe recovery were found to be 62.8 wt% and 3.5 wt% respectively. Acidity was changed using HF at different concentrations. After pH optimization, titanium recovery was found to be 63.7 %, with a Fe/Ti ratio increment of 3.4 times that in the original ore. This study proved that leaching concentration and acidity influences hydrometallurgical process selectivity. The interaction between the ore, NH_4F and HF is described by the reaction (Sachkov, 2017):

$$FeTiO_3{\cdot}Fe_3O_4 + 6NH_4F + 6HF + 0.25O_2 = (NH_4)_3FeF_6 + (NH_4)_2TiF_6 + Fe_3O_4 + 3.5H_2O + NH_3 \quad ..(4)$$

The experiments were conducted in polyethylene containers with continuous stirring for 20 hours. A Nutsche filter was used to separate the solid residue. The residue was then dried at a temperature of 120 °C. X-ray diffraction data was used to calculate the Ti and Fe weight percentage in the solid phase of the ore together with the Fe/Ti ratio. The extraction efficiency of these components was calculated as follows (Sachkov, 2017)**:**

$$w = \frac{\text{m(component in the liquid phase)}}{\text{n(component in the initial phase)}} \times 100\% \quad \ldots\ldots\ldots\

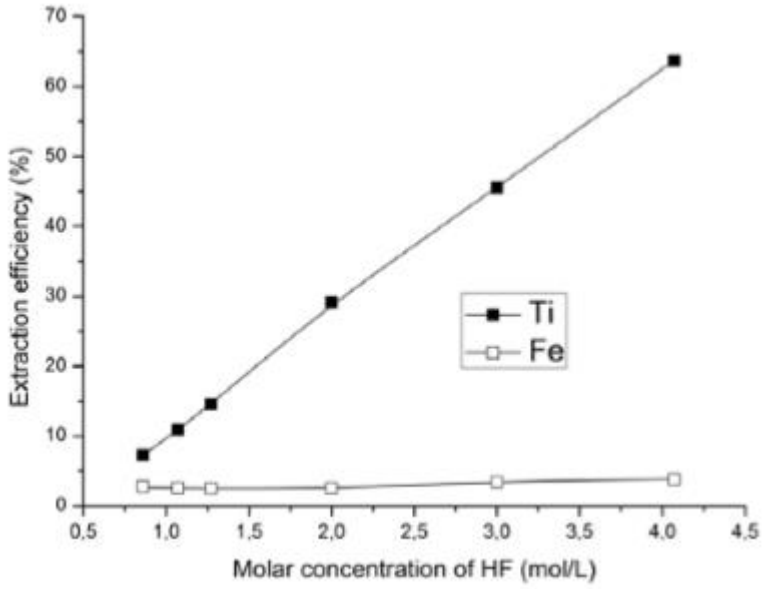


Figure 2.7: *Ti and Fe extraction efficiency at varied HF concentrations (Sachkov, 2017).*

Effective separation of Fe and Ti was achieved by varying the concentration of the leaching reagents. More Ti was recovered in solution at high HF concentrations, while most of Fe remained in the solid phase.

2.2.2 Preparation of Synthetic TiO_2 Through Sulphation of Ilmenite Followed by Impurity Removal

This method involved the preparation of synthetic rutile from ilmenite (Liu, 2017). During the roasting of ilmenite using $(NH_4)_2SO_4$, $(NH_4)_2SO_4$ and ilmenite were mixed at different mass ratios in order to obtain the optimum mixing ratio. The heating range was kept between 250 and 420 °C under an inert N_2 atmosphere. The sulphated ilmenite was allowed to cool to 25 °C. Further roasting of the sulphated ilmenite (thermal decomposition experiments) was carried out at roasting temperatures ranging from 440 °C to 570 °C. The sulphated ilmenite was subjected to 10 % H_2SO_4 and H_2O leaching at 50 °C. This was done in order to determine the sulphation conversion. **Equations 2** and **3** were used to calculate the sulphation conversion and decomposition percentage respectively.

$$\eta = \left(\frac{C_1 \times V_1 \times 10^{-3}}{M_1 \times W_1}\right) \times 100\% \quad \text{..... (2)}$$

$$\varphi = \left(1 - \frac{C_2 \times V_2 \times 10^{-3}}{M_1 \times W_1 \times \eta}\right) \times 100\% \quad \text{..... (3)}$$

Where:

η(%) - Sulphation conversion.

C - Concentration.

V_1 - Volume of leaching solution.

W - Mass percentage.

φ - Decomposition percentage of Fe and Ti containing sulfates.

V_2 - Volume of water leaching solution.

The last stage of this method involved the removal of impurities. The remaining solid material was treated with distilled water at a liquid/solid ratio of 10 ml/g at 50 °C for 1 hour. Sulphates that were removed, were $FeSO_4$, $MgSO_4$ and $CaSO_4$. Fe_2O_3 from the initial leaching experiment was removed by dissolving the water leached residue in a HCl solution. The temperature and liquid/solid ratio was set at 15-98 °C and 50 ml/g respectively, and the leaching lasted 180min. SiO_2 impurity was removed by dissolving the HCl leached residue in a 5 wt% NaOH solution at 102°C and a liquid/solid ratio of 50ml/g respectively. After HCl leaching, the Fe total removal efficiency and TiO_2 loss were calculated as follows:

$$\lambda = \frac{C_2 \times V_2 \times 10^{-3} + C_3 \times V_3 \times 10^{-3}}{M_1 \times W_1} \times 100\% \quad \text{..... (4)}$$

Where

λ(wt%) – Fe total removal efficiency or TiO_2 loss.

C - Concentration.

V - HCl leaching volume.

M - Mass

W - Constant

2.2.3. Selective Precipitation

The separation of ions in an aqueous solution through the use of a reagent that precipitates one or more ions while leaving other ions in solution, is called selective precipitation (Chipich, 1988). This method has been incorporated in the early purification stages of titanium from its ore. Ilmenite is composed of a high percentage of $FeTiO_3$, with trace amounts of $MnTiO_3$ and $MgTiO_3$ (Hobart, 2005). Phenanthroline and sodium tetraphenyl borate (NaTPB) are used as

precipitation reagents (Dennis, 2001). The main method together with the reactions involved are given in the following paragraphs.

The process of obtaining titanium in pigment grade from ilmenite involves the dissolution of ilmenite using a highly concentrated hot solution of sulphuric acid of about 95 wt% (Krishen, 1965). Ilmenite ore with relatively high content of manganese is first treated though magnetic separation. High manganese content is normally a rare case. Ilmenite is therefore directly treated with sulphuric acid at temperatures around 200̊ °C (Krishen, 1965). The reaction which occurs is as follows:

$$FeTiO_3 + 2H_2SO_4 \rightarrow TiO \cdot SO_4 + FeSO_4 + 2H_2O \quad \text{..... (5)}$$

The titanium oxysulphate seen in **Reaction 5** is further boiled with water to produce hydrous titanium oxide as depicted in **Reaction 6** (Krishen, 1965):

$$TiO \cdot SO_4 + 2H_2O \rightarrow TiO \cdot (OH)_2 + H_2SO_4 \quad \text{..... (6)}$$

Filtration is used to recover the hydrous titanium oxide. In this process, hydrous titanium oxide is washed free of iron oxides and acidic substances. A rotary oil-fired furnace is used to calcine the hydrous titanium oxide in order to form TiO_2. The refractive index of this oxide is expected to be under 2.5-2.71 (Krishen, 1965). This process depends on high amounts of sulphuric acid, as it requires 2 tons of 95 wt% sulphuric acid to produce 1 ton of titanium oxide (Krishen, 1965).

The normal operation is to introduce precipitation reagents right after **reaction 5** (Chipich, 1988). These precipitants include phenanthroline and NaTPB. The precipitation reagents are first dissolved in ethanol. Ethanol was found to be a good precipitation enhancing agent (Dennis, 2001). The precipitation reagent mixture is mixed with the ilmenite dissolved in sulphuric acid. At correct precipitant mixing ratios (depending on ilmenite amount), titanium oxide is precipitated. This leaves iron and sulphates in solution (Carvalho, 2002). The precipitate is then recovered using filtration.

2.2.3.1 Past Studies Conducted on Selective Precipitation

A study of the precipitation method for the separation of titanium and iron (as oxides) in ilmenite was conducted recently (Purcell, 2019). Dissolution was conducted using acid/base dissolution followed by flux dissolution. For different sets of experiments phenanthroline(phen), sodium tetraphenylborate(NaTPB) and 2-mercaptopyridine N-oxide sodium salt (NaPT) were used as precipitation reagents. Phen and NaTPB were also mixed and

the mixture was used as a precipitant in order to test the degree of separation. Phen had a very low precipitation selectivity. NaTPB also resulted in a low precipitation selectivity. The mixture of phen and NaTPB also showed a poor precipitation selectivity. NaPT gave good precipitation selectivity results as the precipitate contained 100 % Fe while the filtrate contained 99.6 % Ti. For this study, the precipitate was dried at 100 °C before being analysed. **Table 2.3** show the results that were obtained for the NaPT experiment.

***Table 2.3*:**NaPT selective precipitation results *(Purcell, 2019)*

Mole ratio (Metal: NaPT)	% Ti(III) Recovery	
	Precipitate[a]	Filtrate
1:3	95.2	6.1
1:5	100	0.00
1:7	100	0.00
	% Fe(II) Recovery	
1:2	92.6	8.3
1:3	100	0.00
1:5	100	0.00

Another study involved selective precipitation techniques used to recover refined iron oxide pigments for the production of paint from a synthetic acid mine drainage solution. Treatment plants sell the iron oxides in order to subsidize treatment costs. The study used stepwise selective precipitation process using oxidation, pH and filtration to recover iron oxide pigments of varying colours and properties. Various chemical and physical design variables were varied in order to evaluate the changes on iron oxide morphology. These variables included drying duration, reaction temperature, alkaline addition rate and target pH. Drying duration resulted in the transformation of amorphous phases of iron oxide to hematite, increased redness in paint streaks and improved crystallinity. No changes were observed with alkaline addition. Without changing the crystallinity of the samples, increasing the reaction temperature darkened the colour of pigments and pigment surface area was increased. According to the study, increased pigment surface area increases coating ability (Ryan, 2017).

The pH of 3 achieved the highest purity and a distinct yellow colour, which depicted jarosite properties. Paint streaks from other samples darkened. The pH range up to 7 did not precipitate

nickel and manganese—implying that they required more basic conditions in order to be precipitated (Ryan, 2017).

2.2.4. Solvent Extraction Separation

Solvent extraction uses a phenomenon called chelation. Chelation is the bonding of two or more molecules to a specific metal ion (Chemicool, 2017). A chelating agent contains sites where two or more atoms (from different sites) of the chelating agent form bonds with the ions of a specific metal. **Figure 2.8** represents the bond co-ordination of acetylacetone as an example of a chelating agent bonding to titanium:

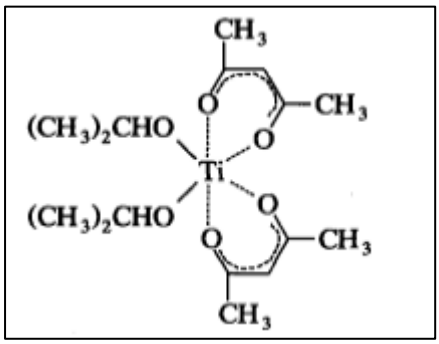


Figure 2.8: *Acetylacetone bonding to titanium (Erik, 1993).*

Ilmenite is mixed with acids such as HCl, H_2SO_4 and H_3PO_4 (Erik, 1993). The chelation of titanium includes other chelating agents, such as sodium mercaptopyridine N-oxide (NaPT) and tri-octylphosphine oxide (TOPO) (Hauchard, 1997). The chelation agents are mixed with extraction solvents before being added to the ilmenite solution. The extraction solvents serve a purpose of separating the metal complexes from the aqueous solution. Extraction solvents that were found to have optimum separation when using the mentioned chelating agents are kerosene, methyl isobutyl ketone (MIBK) and 1-octanol (Dipaloy, 2015).

2.2.4.1. Past Studies Conducted on Solvent Extraction

Simultaneous recovery of total Fe and Ti from ilmenite was studied through the use of solvent extraction as a separation method (Alafara, 2011). Acid concentration and temperature was investigated in the dissolution of the ore where HCl (2M) was used to dissolve the ore. An amount of 84.4 % ilmenite was dissolved within 120 min. Values of the Arrhenius equation's variables were calculated for this reaction with the well-known equation:

$$k = Ae^{\frac{-E_a}{RT}} \quad \text{.....(7)}$$

E_a = 38.4kJ/mol | A = 11.8s^{-1} | k = 0.85

In this study 97 % titanium extraction efficiency was observed through the use of 1.5 M NaTPB in kerosene and 10g/L ilmenite in the leach liquor. After chelation, the separation was conducted by removing iron using 3 M ammoniacal solution at pH 3.5. HCl (0.1M) was used to recover the stripped titanium solution.

Another solvent extraction study was conducted using NaPT, acetylacetone and TOPO in acidic medium (Purcell, 2019). This study was conducted in order to compare the Ti recovery of these reagents. TOPO had the lowest success rate for recovering Ti (below 90%), while the other chelation reagents had yields above 95 %.

Furthermore, a recent study used solvent extraction on the separation of titanium from vanadium and iron in leach solutions of vanadium slag. The extraction was carried out using trioctyl tertiary amine (N235). The effects of various conditions on the separation was investigated as the leach solutions contained high amounts of vanadium and iron impurities. More than 82% Ti was extracted when using 35 %(v/v) N235 and 65 %(v/v) sulfonated kerosene as the extractants (Zhang, 2019). Vanadium and iron were co-extracted at 5 % and 10 % respectively. Over 97 % Ti,7 % vanadium and 18 % iron were extracted at the end of the 3-stage extraction process. Vanadium and iron impurities were removed using 1.25 mol/L ammonium sulfate as a washing reagent followed by stripping using 1.0 mol/L of ammonia. The stripping achieved a Ti recovery of approximately 90 % from the purified organic liquor (Zhang, 2019).

2.2.5. Ion-Exchange Resins

Ion-exchange chromatography is a charge separation method. This method separates ions and polar molecules based on their affinity for the ion-exchange resin (Khan, 2012). Cation and anion exchangers are used in this method. Both these exchangers can come in categories of either strong or weak basic and acidic. There are typical ion-exchangers that are used for the recovery of titanium (Khan, 2012). In the case of cation exchangers, Dowex Marathon C hydrogen, which is classified as a strongly acidic resin, is used. Clinobrite Zeolite is normally used as a weakly acidic resin. In the case of anions exchangers, Amberlite IRA-900 is used as a strongly basic resin while Amberlite IRA-67 is used as a weakly basic resin. These resins are mixed with water to form a slurry. The slurry is then passed into a column and a solution of the titanium ore is added to the column. Phosphoric acid is normally used to elute the desired metal in the sample. Typical acid eluting flow rates are approximately 0.7 ml/min (Khan, 2012). Eluting at high flow rates results in insufficient contact time for the ion-exchange to occur.

Lowering the eluting flow rate increases the contact time, which in turn leads to optimum ion separation (Khan, 2012). **Figure 2.9** represents this phenomenon.

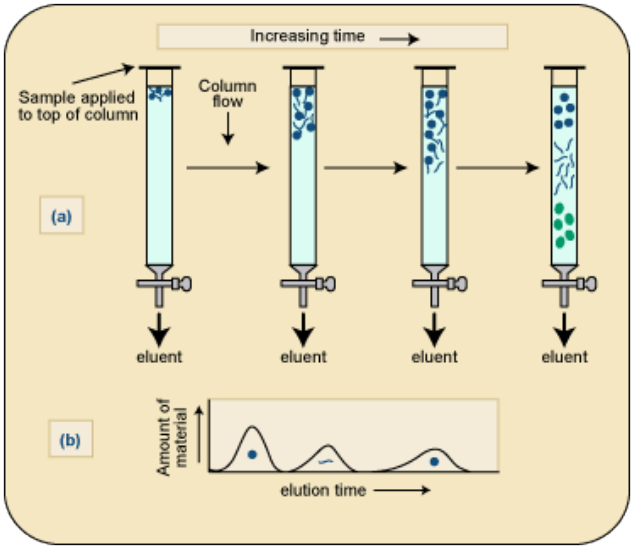


Figure 2.9: *Optimum ion exchange separation through low eluting flow rates (Khan, 2012)*

2.2.5.1. Ion-Exchanger Capacity and Eluting Starting Conditions

The capacity of an ion-exchanger refers to the amount of ions that the exchanger can take up in the eluting process (Khan, 2012). The typical industry elution is called isocratic elution. Isocratic elution refers to elution starting conditions where only the undesired substances are adsorbed. Only the desired substance is eluted. The regeneration of the ion-exchange adsorbents is achieved through washing the column bed with a salt solution in order to regain the ionic strength of the ion-exchanger (ionic strength of about 2 M is recommended); (Khan, 2012).

2.2.5.2. Ion-Exchanger pH and ionic strength

The ion-exchange separation process requires specific conditions of the buffer substance and ion-exchangers. The pH of the buffer substance should be 1 pH unit below the isoelectric point for anionic exchangers or alternatively; 1pH unit above the isoelectric point in the case of cation exchangers (Khan, 2012). It is important to ensure that the charge sign of the buffer substance is the same as that of the functional groups of the ion-exchanger. This is done in order to avoid the ions of the buffer substance from taking part in the ion-exchange process (Khan, 2012). The function of the buffer substance is to carry out the elution of the desired substance down the elution column.

The isocratic elusion is achieved through the adjustment of ionic strength and pH (pH is related to ionic strength) around the isoelectric point of the sample substances. The pH is set at the isoelectric point of the desired substance (Khan, 2012). This prevents the desired substance from being adsorbed together with all the substances in the sample. Only the desired substance is therefore eluted down the elution column.

It is important to have the ion-exchanger at low ionic strengths. This is done in order to minimise competition between charged groups of the ion-exchanger—which allows more bonding of the unwanted substances in the sample (Khan, 2012). This shows that carrying out this process at low ion-exchanger ionic strengths aids with operating at optimum ion-exchanger capacity.

2.2.5.3. Past Studies Conducted on Ion Exchange Resins

A study on the recovery of titanium from dissolved ilmenite was conducted using ion-exchange resins. The solution containing titanium and iron was poured in an eluting column where titanium was eluted using H_2SO_4 (0.5M) and H_2O_2(0.05%) (Liebenberg, 1947). The remaining iron was eluted using HCl(0.2M) and acetone(55%). Another study was conducted where titanium was eluted in a similar manner as in the study described above, at an eluting rate of 0.5 mL/min (Das, 1990). In this study, the ore was bauxite which also contained aluminium which has a similar sorption than iron. In order to prevent simultaneous elution of iron and aluminium, a fluoride masking agent was added to the bed. HCl was used to elute the iron as usual. The elution of aluminium then followed using H_2SO_4 (4mol/L). **Table 2.4** represents a summary of the results that were obtained through the use of different ores.

***Table 2.4*:**Ion exchange results obtained through the use of bauxite and bentonite clay *(Das, 1990)*.

Sample	Compound	Reported value (%)	Found (%)[b]	Recovery (%)
Bauxite (B.A.S)	Al_2O_3	51.2[a]	50.9	99.4
	Fe_2O_3	17.5	16.9	96.5
	TiO_2	2.25	2.18	96.8
Bauxite (I.A.C)	Al_2O_3	49.1[a]	48.6	98.9
	Fe_2O_3	13.5	13.0	96.2
	TiO_2	10.0	9.92	99.2
Bentonite clay (SINP)	Al_2O_3	24.14	23.9	99.0
	Fe_2O_3	6.85	6.2	90.5
	TiO_2	1.74	1.7	97.7

[a] By difference, [b] Mean of triplicate analysis

The recovery of titanium from bauxite (I.A.C) by Das had the best titanium recovery (99.2%). The current study investigated the separation of titanium and iron from pure ilmenite. The separation was conducted using Dowex Marathon C hydrogen, Amberlite IRA-900 and Amberlite IRA-67 as ion-exchange resins. These resins were used at different concentrations/amounts in a slurry in order to improve the separation of titanium and iron. The separation was conducted over time (30 min) in order to produce separation profiles which were easy to track as it unfolds. Furthermore, the separation profile aid with finding time intervals where separation processes reach their plateau, and these time intervals then become the target points of optimization.

Another study conducted on ion-exchange resins involved the recovery of metals by an ion-exchange process using chelating resin and sodium dithionite. According to literature, recovering metals from nickel laterite leach solution is difficult as the solution contains high amounts of iron (Amilton, 2019). Ferric iron causes separation inefficiencies as it precipitates at above pH 2 and causes co-precipitation of copper and cobalt. The ferric ion is normally reduced to ferrous iron which precipitates just at pH 5 only. This study focussed on the effect that iron reduction has on the resin. It was found that metal adsorption increased with the reduction of ferric iron to ferrous iron. The chelating was selective to copper at pH 2 which aided with reducing the separation complexity. The order of selectivity of the chelating resin varied as the pH was increased—with high nickel and cobalt adsorption at pH 3.5 but with low selectivity (Amilton, 2019).

The above literature review has shown that dissolution of ilmenite is most successful through acid leaching—using sulphuric acid. Selective leaching seems to fall short. Hydrogen peroxide has been reported to be a good leaching aid and this study will focus at finding optimum selective leaching through hydrogen peroxide additions. Furthermore, the study will use different reagents as compared to the ones used in literature, in pursuit of achieving optimum separation.

CHAPTER 3—EXPERIMENTAL PROCEDURES AND MATERIALS

This chapter provides information regarding the equipment, materials and experimental procedures used in this project.

3.1. Equipment

The experiments were conducted using different sets of equipment, including AAS, ICP, SEM and glassware of various sizes.

3.2. Materials

The substances required to carry out each method vary depending on the method that was being used. The list below provides the materials required to run all the experiments. **Section 3.4** provides the experimental procedure and the specific substances used in each method.

- Sodium tetraphenyl borate (NaTPB).
- Phenanthroline.
- Ethanol.
- Sulphuric acid, hydrochloric acid and phosphoric acid.
- Acetylacetone (acac).
- 1-octanol.
- Dowex marathon C hydrogen.
- Amberlite IRA-900.
- Amberlite IRA-67.
- Hydrogen peroxide.

3.3. Experimental Procedure

This section gives the procedures that were followed to conduct the experiments. Note that the experiments were divided into 2 stages. The first stage involved finding be best ilmenite dissolution technique. The second stage involved finding the best iron and titanium separation method after the best dissolution technique from stage 1 was used to dissolve the ilmenite.

3.3.1. Dissolution of Ilmenite

Two acids were used for the dissolution of ilmenite, namely concentrated sulphuric acid and concentrated phosphoric acid. The dissolution was carried out at room temperature. The second dissolution attempt was carried out using a mixture of hydrogen peroxide and the acids

mentioned above. Each sample was prepared using 0.5g of ilmenite and 10ml of acid. The samples were prepared in triplicate. Hydrogen peroxide optimization was carried out using 2;5; 10; 15 and 20 vol% H_2O_2-acid mixtures respectively. The dissolution of ilmenite was investigated over time. Over a period of 30 minutes, small samples were extracted from each mixture in order to find the dissolution profile of ilmenite in terms of the amounts of Ti and Fe (refer to Section 4).

3.3.2. Selective Precipitation

Phenantroline and NaTPB were added to the ilmenite solution. These reagents were expected to selectively precipitate titanium oxide (Chipich, 1988). Each of these reagents were used at varied volume concentrations of 2 %, 5 %, 10 %, 15 % and 20 % as a percentage of the dissolved solution of ilmenite. Varying the reagent concentration aids with finding the trend between precipitation reagent concentration and the amount of the desired component to be precipitated (which is titanium oxide in this case). The precipitated titanium oxide was recovered through filtration.

3.3.3. Solvent Extraction Separation

Acac was used as a chelating reagent. These reagents were first dissolved in 1-octanol (extraction solvent) before it was added to the ilmenite-acid aqueous solution. Continuous stirring is essential for achieving optimum chelation (Hauchard, 1997). A separating funnel was used to separate the organic layer from the aqueous layer. The organic layer was then back extracted using water in order to recover titanium. An atomic absorption spectroscopy was used for analysis.

3.3.4. Ion-Exchange Resins

Cationic and anionic resins were used in order to achieve the separation of dissolved titanium and iron ions. Dowex marathon C hydrogen was used as cationic resins. Amberlite IRA-900 and Amberlite IRA-67 were used as strong and weak anionic resins, respectively. The resins were mixed with water to form a slurry. The slurry was transferred to a column to create an ion-exchange bed. The ilmenite solution was poured onto the ion-exchange bed. Thereafter, the bed was eluted with phosphoric acid at varied phosphoric acid concentrations of 8-10M. The recommended elution flow rate of about 0.7 mL/min was employed (Khan, 2012). The masses of the respective ion-exchange resins used were varied at 0.4,1, 2.2, 3.52 and 5g. Breakout curves were plotted in order to determine the breakout point and volume of effluent treated per unit mass of exchange resin used. These values were used to compare the performance of the different exchange resins.

3.4. Quantification Technique

3.4.1. Atomic absorption spectroscopy

Atomic absorption spectroscopy can be used to determine the concentration of a metal in a given sample (Beatriz, 2019). In the metal recovery industry, this spectroscopy technique is often used in laboratories for routine metal analyses. The atomic absorption spectrometer uses a nitrous flame or air flame to atomise the atoms in the sample (Beatriz, 2019). This occurs in three steps. The flame evaporates the liquid sample into a dry sample. Vaporisation of the dry sample into a gas occurs right after the conversion of the liquid sample into a dry sample. The last step is atomisation where the compounds are broken down into atoms. The atomic absorption spectrometer then uses the absorption of light through this atomic cloud to measure the concentration of the gas phase atoms. According to literature, this is a highly recommended method as it is fast and easy to use (Beatriz, 2019). **Figure 3.1** represents the schematic diagram an atomic absorption spectrometer.

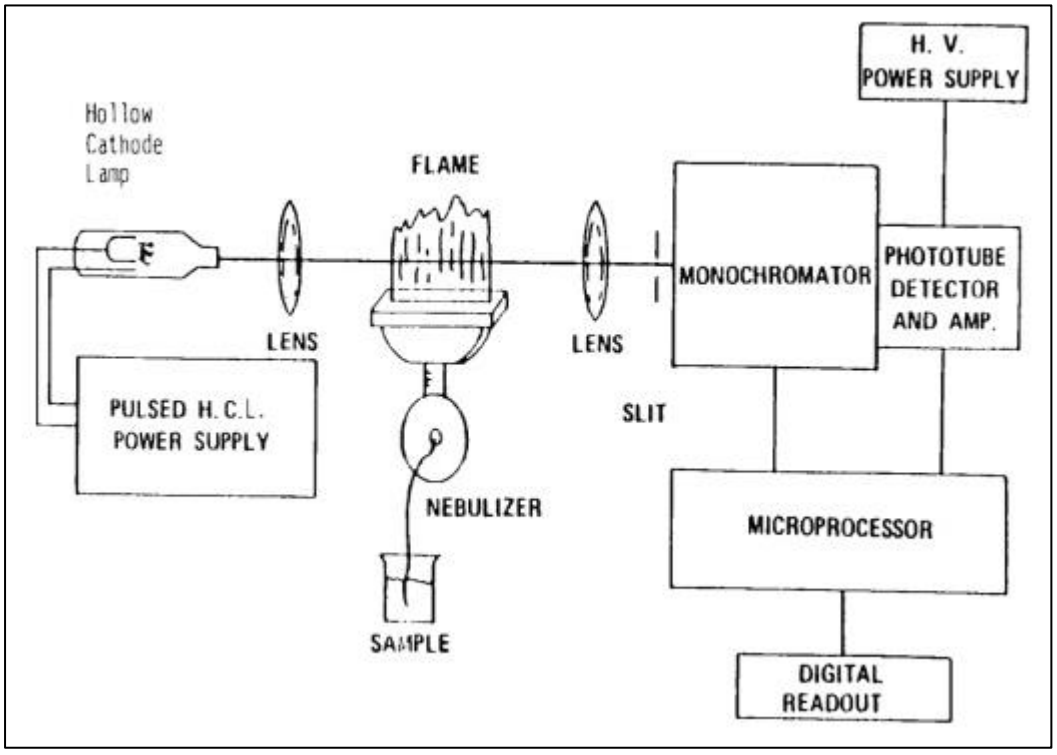


Figure 3.1: *Schematic representation of an atomic absorption spectroscopy (Beatriz, 2019).*

Using the titanium and iron spectroscopy cathode lamps, concentrations of the samples of the study at hand were obtained. To ensure instrument accuracy, calibration was undertaken using blank samples and actual samples for all set of runs. Using the AA, the samples were analysed in the order described in **section 3.3.1** to **3.3.4**.

3.4.2. SEM Analysis Description

Sigma FE SEM (field emisson scanning electron microscope) was used. The sample was placed on a double sided carbon tape on aluminium stub and analysed with EDS (Energy disperse spectrometry) mounted on a ZEISS stage. The analysis was semi-quantative and samples were uncoated. Furthermore, results indicated that Fe and Ti, if present, were below the detection limit of the technique. The images were recorded in SE (secondary electron) mode. Each sample was analysed in several areas. The samples were analysed at 15 kV since they were uncoated and photos were taken at 10 kV and 0.4 A.

3.5. Data Analysis

At the end of each run, the AA spectrometer produced a SpectraAA report which was used for quantifying titanium, and this allows one to calculate the titanium oxide content which could be achieved from each part of the investigation. Thereafter, the results were presented in graphical format and discussed. The method yielding the highest titanium recovery was considered the most efficient. This method was then considered to design a viable process.

3.6. Experiment Summary-Block Flow Diagram

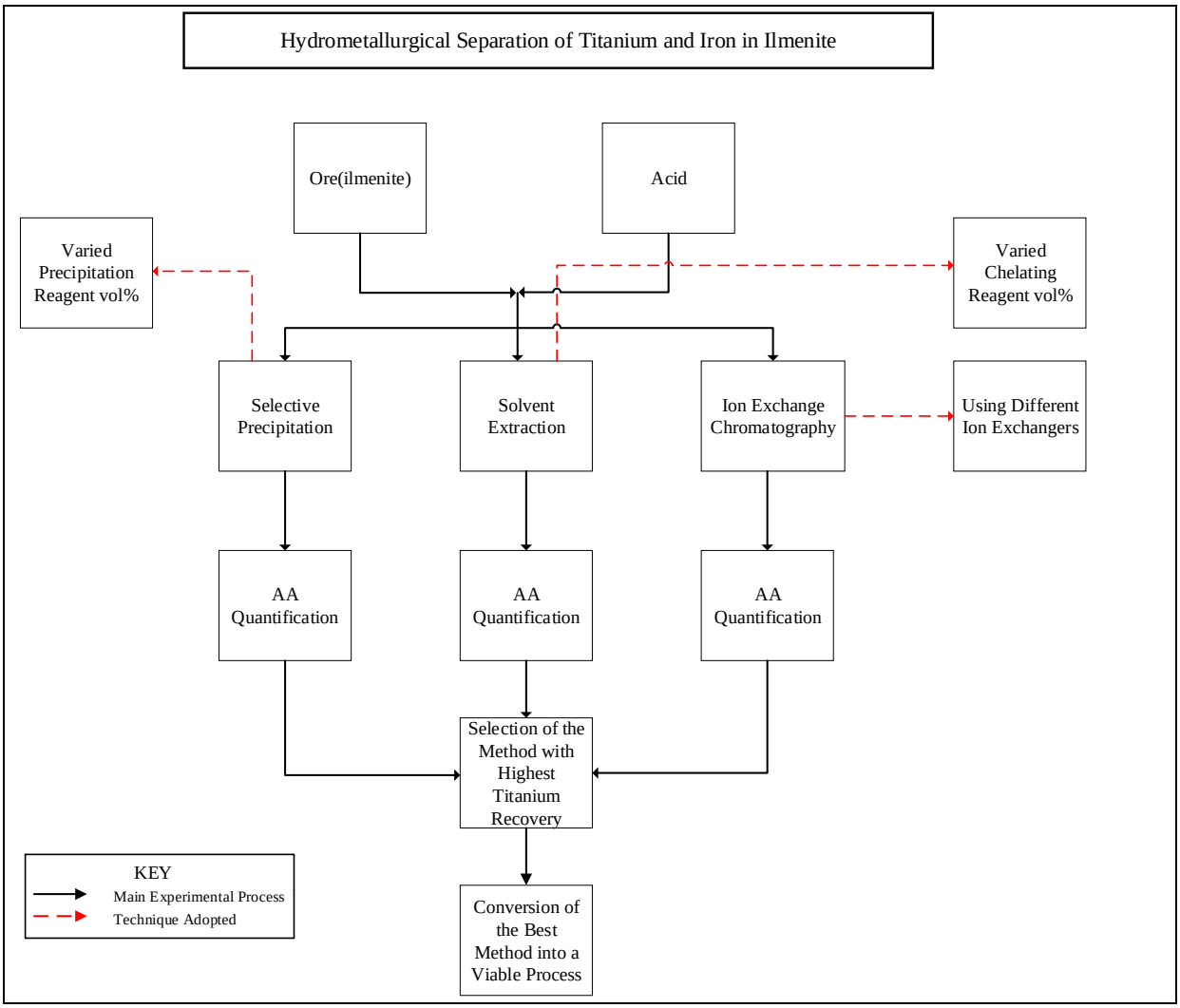


***Figure 3.2**: Experimental block flow diagram for titanium recovery.*

CHAPTER 4—RESULTS AND DISCUSSION

The results obtained from the ore dissolution phase and the results from the separation phase (selective precipitation, solvent extraction and ion exchange resins) are described in this chapter. From each phase, the method that produced optimum results was recommended. A 18.4 M and 14.8 M of H_2SO_4 and H_3PO_4 was used for leaching respectively.

4.1. Leaching

The experiments for the dissolution of ilmenite were conducted as described in **section 3.3.1**.

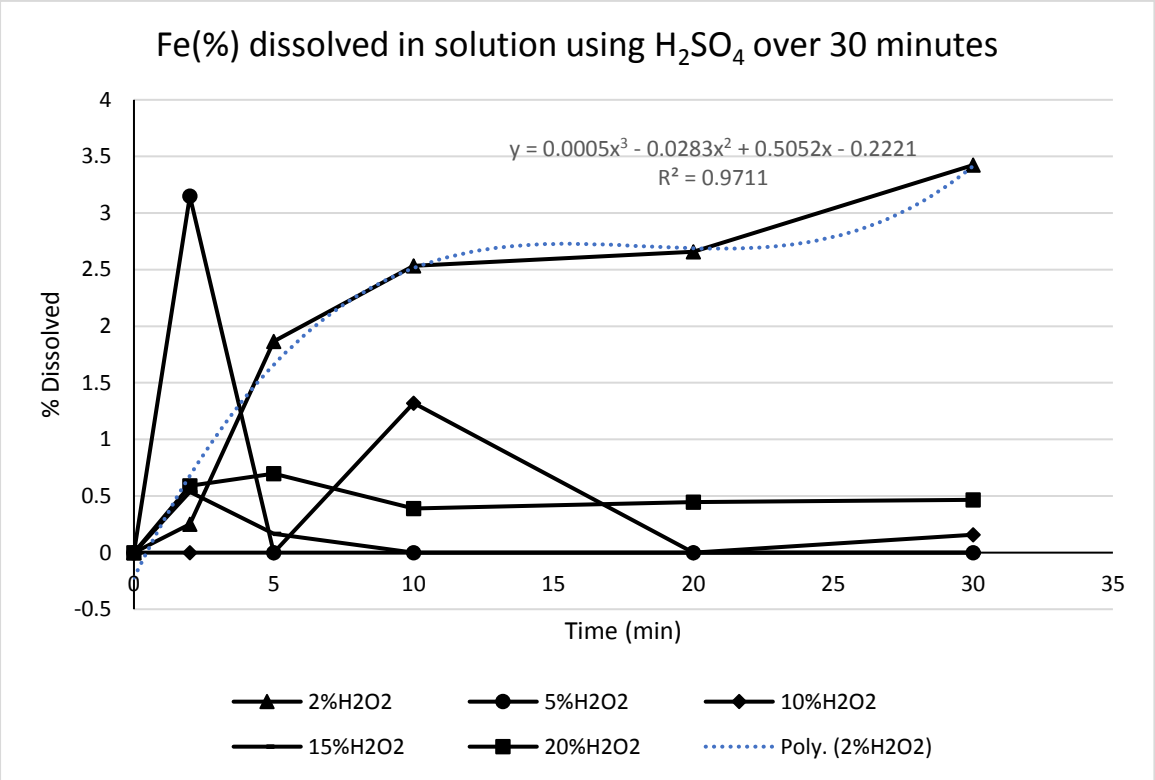


***Figure 4.1**: Fe(mass%) dissolved when using H_2SO_4 and H_2O_2 at varied vol%, 25 °C, pH of 2 and stirring at 180 rpm.*

The dissolution of ilmenite was carried out at room temperature at a pH of 2 and a stirring speed of 180 rpm. The reaction between H_2O_2 and H_2SO_4 resulted in a rapid temperature increase from 25 °C to 155 °C within approximately 8 seconds due to the exothermic nature of the reaction. This temperature increase and formation of H_2SO_5 initiated the ilmenite dissolution. The results depict that less iron was dissolved in solution for the mixtures with higher H_2O_2 concentrations than at the lowest hydrogen peroxide concentration (vol%). First, second and third order equations were fitted to the graphs where the highest R^2 presented by the respective correlation coefficients of the fits of equations on each graph was recorded. The mixture of 2 % H_2O_2 had the highest Fe dissolution at the end of 30 min (3.4%). A third order

polynomial was fitted and gave a R^2 value of 0.97, which represents a reasonable fit. As a result, the dissolution was found to be of third order with rate constant of 0.026 $M^{-1}min^{-1}$. The highest Fe recovery (3.4%) of this study was approximately 24 times less than another literature reported value of 84 % (Mukhopadhyay, 2007).

From these observations, the optimum H_2O_2 concentration range would approximately be 5 to 15 %, provided that more titanium can be dissolved in this range. This would make the separation less complex because little iron would be present in the solution. The mass of titanium was analysed in order to obtain the titanium mass profile. **Figure 4.2** represents the titanium mass profile for the various sulphuric acid-hydrogen peroxide mixtures described above.

The samples of the results in **Figure 4.1** were also analysed for the amount (mass %) of titanium dissolved. The results from **Figure 4.2** depict that increasing amounts of titanium was dissolved in solution for the mixtures with increasingly higher H_2O_2 concentrations (vol%). The mixture of 2 % H_2O_2 had the least Ti dissolved at the end of 30 min, i.e. approximately 48 %. Higher percentage dissolutions were only observed in the 15 and 20 % H_2O_2 mixtures. This signified that more H_2O_2 was required in order to dissolve more Ti. The mixture of 20% H_2O_2 had the highest amount of Ti dissolved (85%). This compares favourably with other results reported in literature where leaching conducted without adding H_2O_2 yielded only 41 % titanium dissolution (Mukhopadhyay, 2007). Another study reported 57 % titanium dissolution when using 8 M H_2SO_4 with 6 hours of stirring (Jonglertjunya, 2013). **Figure 4.2** shows the amount of titanium dissolved in solution.

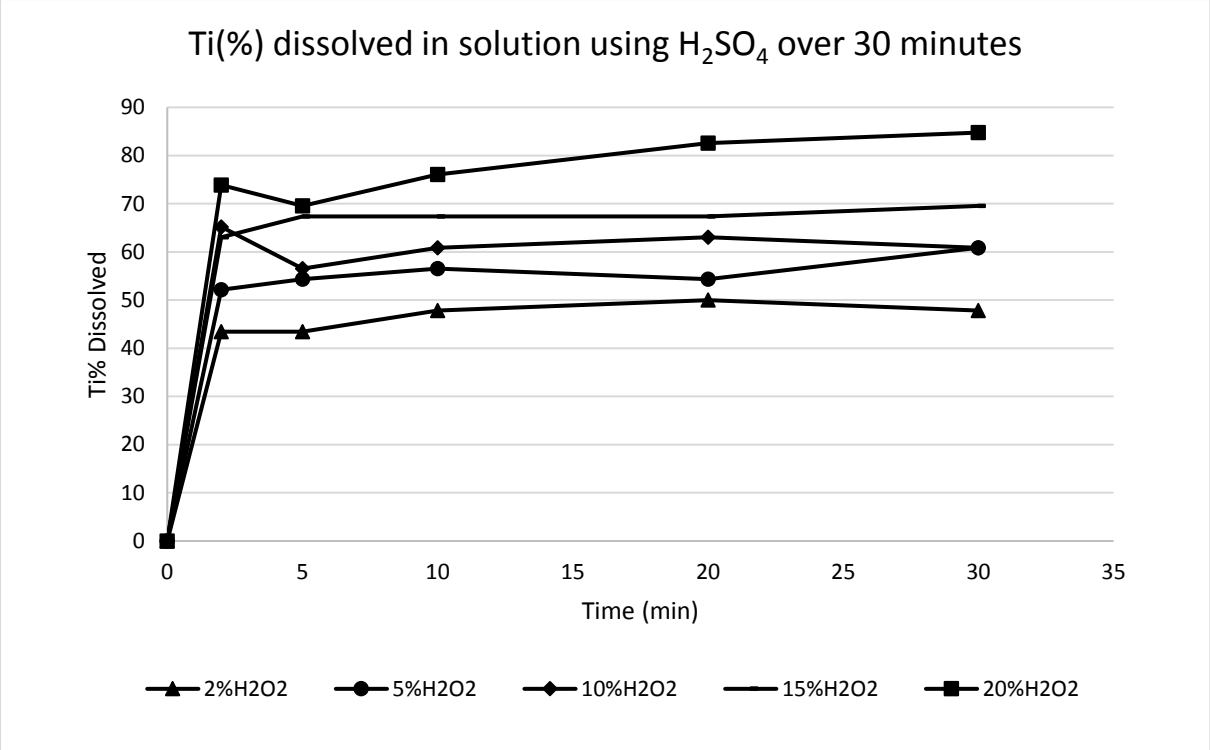


Figure 4.2: *Ti(%) dissolved when using H_2SO_4 and H_2O_2 at varied vol%, 25 °C, pH of 2 and stirring at 180 rpm.*

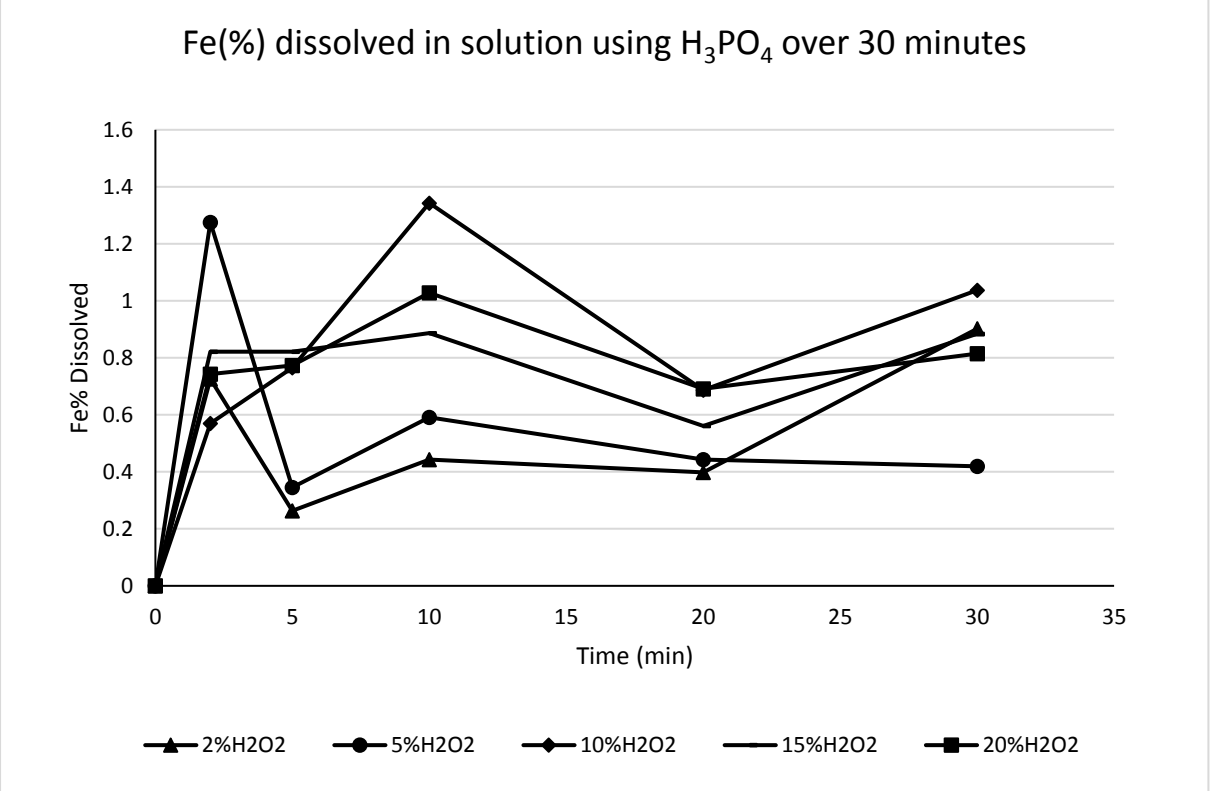


Figure 4.3: *Fe(%) dissolved when using H_3PO_4 and H_2O_2 at varied vol%, 25 °C, pH of 2 and stirring at 180 rpm.*

When the acid was changed from H_2SO_4 to H_3PO_4 with all the other experimental conditions staying the same, such as starting temperature, pH and stirring speeds constant, the results represented schematically in Figure 4.3 was obtained. When H_3PO_4 was used, the optimum H_2O_2 concentration range for the minimum amount of iron dissolution was narrower than when H_2SO_4 was used, i.e. there is less variation in the amounts of iron dissolved at the various time intervals. A maximum of 1 % of Fe was dissolved in solution with a 10 % H_2O_2 addition. Another study of titanium dissolution from ilmenites with phosphoric acid found that 31 % of Fe dissolved (Jailson, 1997). The H_2O_2 additions to the acid were successful in surpressing Fe dissolution when compared with other previous reports in literature which also show that H_2O_2 has a high affinity to Ti than Fe.

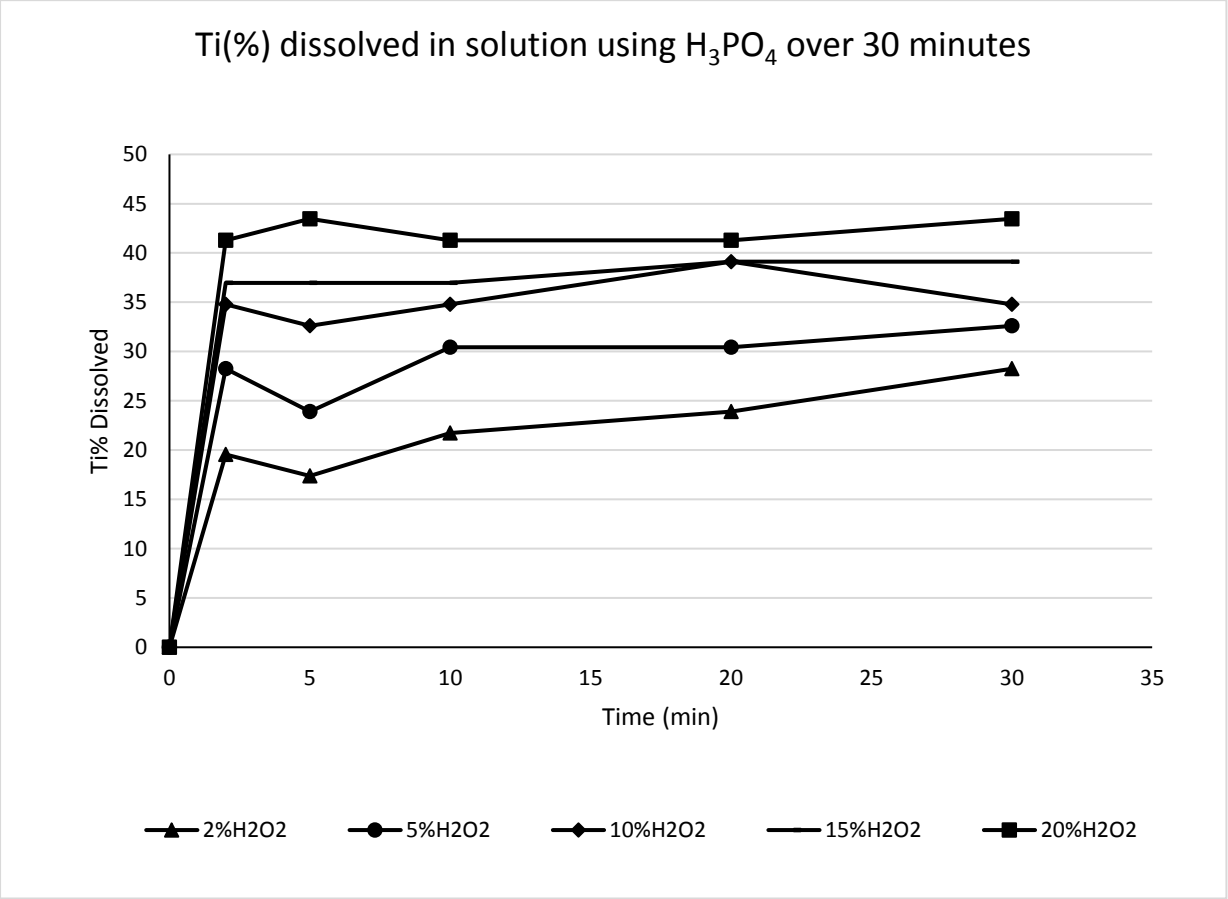


***Figure 4.4**: Ti(%) dissolved in solution when using H_3PO_4 and H_2O_2 at varied vol%, 25 °C, pH of 2 and stirring at 180 rpm.*

The H_3PO_4 runs were also analysed for the amount (mass %) of titanium dissolved from the ore. H_3PO_4 with various H_2O_2 additions resulted in less dissolved Ti compared to when H_2SO_4

and H_2O_2 were used. The dissolution seems to be complete within less than 10 minutes, where after it stays fairly constant for most of the runs. Based on the 2-20% H_2O_2 concentration range, the maximum dissolved Ti for a H_3PO_4 and H_2O_2 combination was approximately 48 %, compared to almost 81 % when H_2SO_4 and H_2O_2 were used. This could be due to the differences in reaction temperature generated during the dissolution process. While the H_3PO_4 and H_2O_2 dissolution showed no temperature change, the H_2SO_4 and H_2O_2 dissolution reaction resulted in a temperature change of about 130 °C (**see section 4.2.1**).

This project aims at separating titanium and iron and recovering as much titanium as possible. Based on these leaching results, hydrogen peroxide clearly aids with dissolving more titanium while simultaneously suppressing the amount of iron obtained. This observation can help to devise conditions which would make the separation of these metals feasible. When employing H_2SO_4 and H_2O_2, it was important to also determine the H_2O_2 concentration that helps achieve a good trade-off between the dissolution of the two metals. **Table 4.1** represents the recovery (%) summary of the Fe and Ti when H_2SO_4 or H_3PO_4 with and without H_2O_2 were used.

Table 4.1: Ti and Fe % dissolution in H_2SO_4 and various H_2O_2 amounts.

Using H_2SO_4 + H_2O_2 After 30min					
Metal	2vol%	5vol%	10vol%	15vol%	20vol%
Fe(% dissolution)	3.4	0.0	0.2	0.0	0.5
Ti(% dissolution)	55.8	71.0	71.0	81.1	98.9
Using H_3PO_4 + H_2O_2 After 30min					
Fe(% dissolution)	0.9	0.4	1.0	0.9	0.8
Ti(% dissolution)	33.0	38.0	40.6	45.6	50.7
[Without adding H_2O_2; After 30min]					
Using only H_2SO_4					
Fe(% dissolution)	1.5				
Ti(% dissolution)	20.0				
Using only H_3PO_4					
Fe(% dissolution)	0.6				
Ti(% dissolution)	23.0				

The dissolution of ilmenite in industry results in a solution that has significant amounts of both iron and titanium in solution (Woranart, 2013). The average Fe dissolution was approximately 1 % and typically in excess of 71 % for Ti in sulphuric acid and hydrogen peroxide mixtures. For phosphoric acid with hydrogen peroxide additions, the average Fe dissolution was approximately 1 % and was around 42 % for Ti. H_2SO_4 was selected as the best acid for ilmenite dissolution as it yields a higher Ti recovery than H_3PO_4. H_2SO_4 and 15 vol% H_2O_2 was selected as the optimmum mixture for dissolution. This mixture achieved a reasonably high Ti dissolution (81%) with only trace amounts of Fe (error margin about 2.4%).

The selectivity of titanium for each NaTPB addition was calculated using **Equation 8** and is presented in **Table 4.2** where a selectivity of 33.1 was achieved.

$$Ti\ Selectivity = \left(\frac{\left(\frac{[Ti]}{[Fe]}\right)_{in\ the\ aqueous\ phase}}{\left(\frac{[Ti]}{[Fe]}\right)_{in\ raw\ material}} \right) \quad \text{..... (8)}$$

Table 4.2: Titanium selectivity for ilmenite leaching at various H_2O_2 additions.

Titanium Selectivity	
H_2O_2 Addition	**Selectivity**
2 %	14.1
5 %	24.1
10 %	28.4
15 %	33.1
20 %	30.2

4.1.1. Factors Influencing Ilmenite Dissolution

4.1.1.1. Temperature

Piranha solutions (combinations of sulphuric acid and hydrogen peroxide) result in exothermic dissolutions when prepared/applied and thus increased temperatures (**Equation 9**), as well as create highly oxidising environments (Chen, 2008). This mixture was prepared at room temperature in a conical flask containing ilmenite. The temperature increased rapidly to a temperature of about 155 °C during the dissolution reaction (monitored using a 250 °C thermometer). Figure 4.5 represents the dissolution temperature profile. This spontaneous

temperature increase reduces heating requirements for dissolution, since the typical industry ilmenite dissolution temperature is 200 °C (Woranart, 2013).

$H_2SO_4 + H_2O_2 \rightarrow H_2SO_5 + H_2O$ …….…… [ΔH= -880kJ/mol].(9)

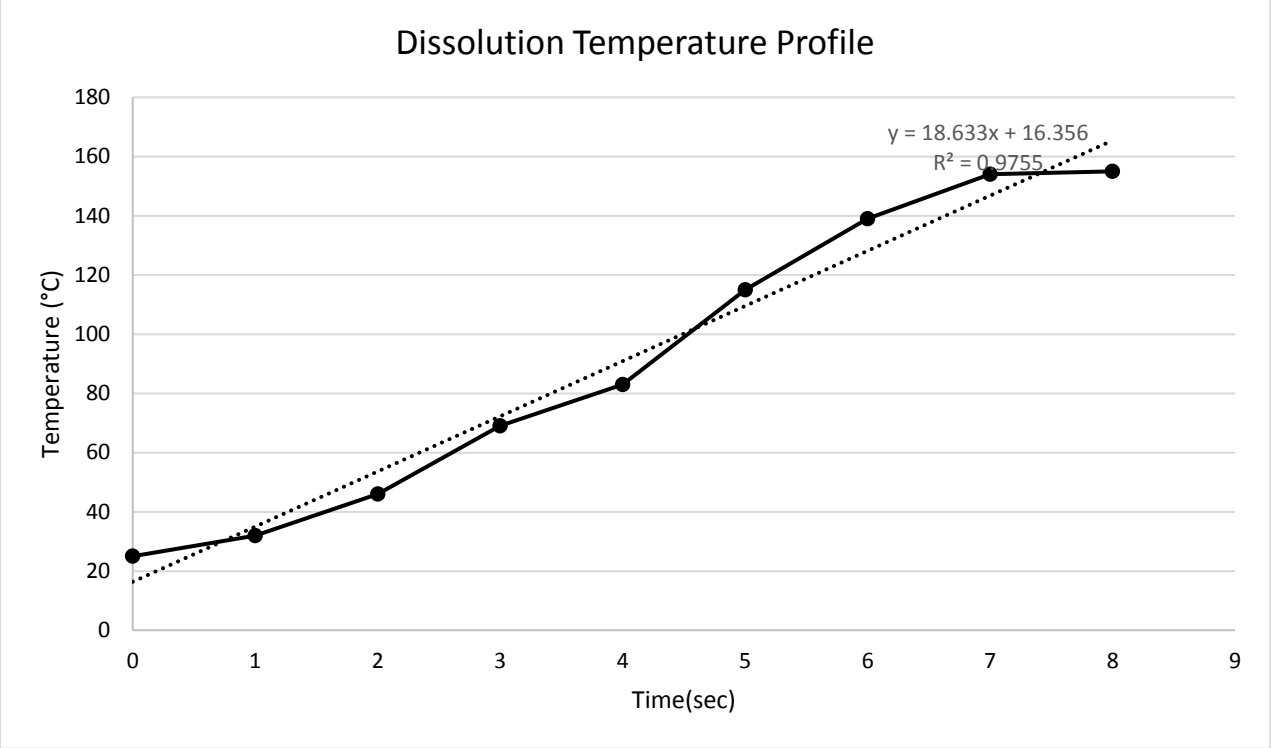


***Figure 4.5**: Dissolution temperature profile of ilmenite.*

A straight line was fitted to the profile. The correlation coefficient of this profile was 0.98 (close to 1). This means that the temperature rise during dissolution was directly proportional to the time.

4.2. Separations

4.2.1. Selective Precipitation

Selective separation was carried out at room temperature below a pH of 2 and at a stirring speed of 180rpm. Selective precipitation was investigated using 5 mixtures at varied precipitation reagent concentrations. Phenanthroline (phen) and sodium tetraphenyl borate (NaTPB) were used as precipitation reagents. Each reagent was added at concentrations of 2, 5, 10, 15 and 20 vol%. There was hardly any precipitation observed when phen was used. A recent study reported a similar outcome when only phen was used (Purcell, 2019).This is because phen tents to form homogeneous mixtures with metal ion solutions. Selective separation conducted using NaTPB produced some precipitates. The mass of Fe and Ti remaining in solution were

measured at different time intervals as shown in the figures below and used to calculate the precipitated yields.

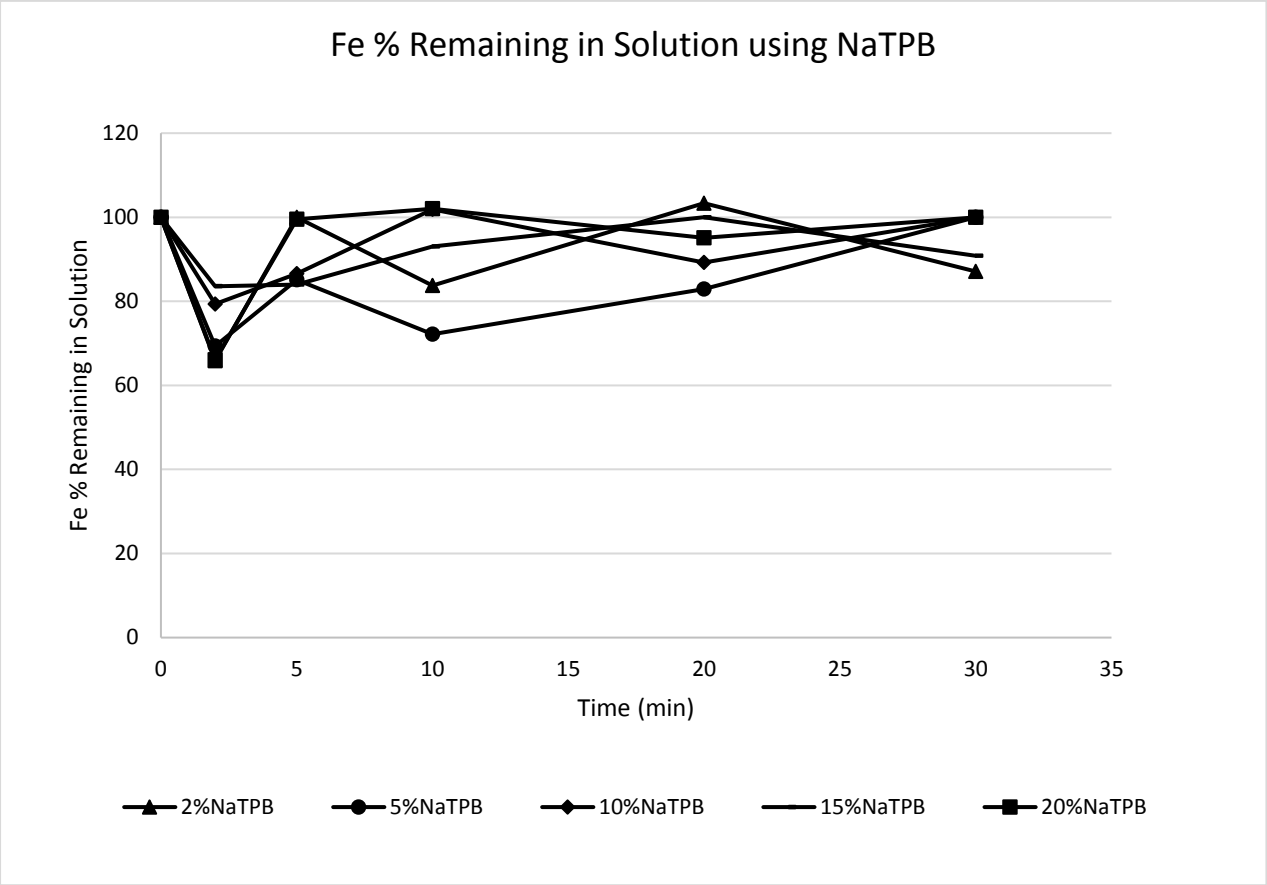


***Figure 4.6**: Fe mass % remaining in solution when using NaTPB at 25 °C, pH of 2 and stirring at 180 rpm.*

The results in **Figure 4.6** depict that there were insignificant amounts of Fe that were precipitated. For example, 2 % NaTPB resulted in approximately 85 % of Fe remaining in solution at the end of 30 min. This meant that only 15% of Fe was recovered from the solution. All the other mixtures (5;10;15 and 20%) had similar responses—with less than 25 % Fe precipitated. This observation was found to be closely in line with the reported value of 25.1 % Fe precipitated from a study where a combination of phen and NaTPB were used as precipitants at a ratio of 1:3, respectively (Purcell, 2019). The recovery of Ti was close to 100 % as there was no Ti remaining in solution. This can be seen from **Figure 4.7**, which shows the results of the Ti that was not precipitated.

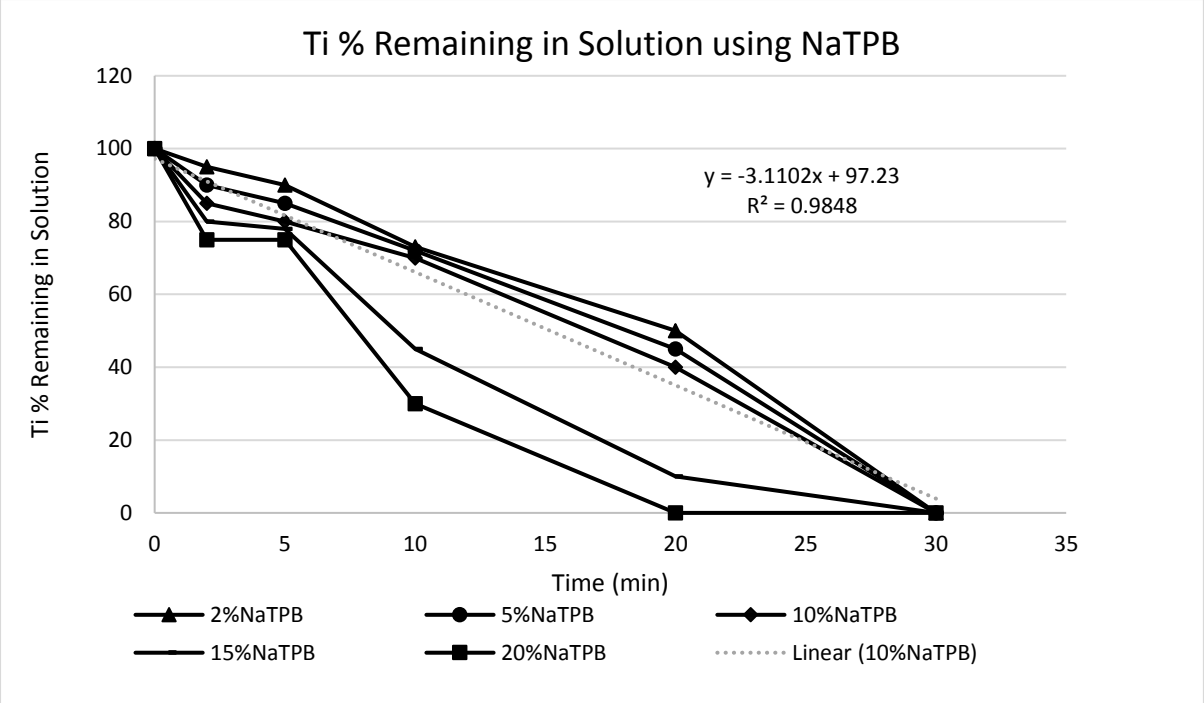


***Figure 4.7**: Ti mass % remaining in solution when using NaTPB at 25 °C, pH of 2 and stirring at 180 rpm.*

The samples of NaTPB experiments were also analysed for the amount (mass %) of titanium that remained in solution after precipitation over the 30 min period. All the NaTPB concentrations achieved a 100 % Ti precipitation. In fact, there was a generally linear relationship between the time needed for precipitation and the amount of Ti remaining in solution, with the higher concentrations of NATPB resulting in faster precipitation than the lower ones. The 20 % NaTPB solution achieved a 100 % Ti precipitation within 20 min. The Ti precipitation results from the study where a combination of phen and NaTPB (1:3) was used, reported Ti precipitation of approximately 35 % (Purcell, 2019). The precipitation of the study at hand was found to be first order with rate constant of 0.021 $M^{-1}min^{-1}$.The super-saturation of the particles at equilibrium for the study at hand was described using the relative super-saturation equation (RSS) given in **Equation 10** (Skoog, 2014).The K_{sp} values were calculated using **Equation 11**.

$$RSS = \frac{Q-S}{S} \quad \ldots\ldots (10)$$

$$K_{sp} = [Fe^{2+}][Ti^{4+}] \quad \ldots\ldots (11)$$

***Table 4.4*:** RSS Precipitation values of NaTPB addition to ilmenite solution.

NaTPB Addition	K_{sp} (mg^2/L^2)	RSS
2%	92.2	0.7
5%	-	0.9
10%	92.3	1.12
15%	-	1.31
20%	92.7	1.66

The increasing RSS values with increasing concentrations of NaTPB corresponds to the acceleration in the mass precipitation of the Ti with time, which is observed in **Figure 4.7**. The kinetics of the selective precipitation of Ti from solution by NaTPB is summarised in **Table 4.4** and indicates a reasonably good fit with a 1st order process, except in the case of the highest concentration NaTPP used.

***Table 4.4*:** Kinetic fittings for NaTPB selective precipitation of Ti from solution

Selective Precipitation Kinetic Order Fitting	
%NaTPB.[order]	R^2
2.[1st]	0,97
5.[1st]	0,98
10.[1st]	0,98
15.[1st]	0,93
20.[1st]	0,86

The selectivity of titanium for each NaTPB addition was calculated using **Equation 8** (presented earlier) and is presented in **Table 4.5** where the highest selectivity of 7 was achieved.

Table 4.5: Titanium selectivity for selective precipitation at various NaTPB additions.

Titanium Selectivity	
NaTPB Addition	**Selectivity**
2 %	5.13
5 %	6.7
10 %	6.8
15 %	5.8
20 %	7.0

4.2.2. Solvent Extraction

Solvent extraction was carried out at room temperature at a pH of 4 and at a stirring speed of 180rpm. Solvent extraction was investigated using 5 mixtures at varied acetylacetone concentrations in 1-octanol. Each solvent extraction mixture resulted in an aqueous and organic layer when added to the ilmenite solution.Fe has high affinity to the aqueous layer while Ti has a higher affinity to the organic layer hence the trends below.

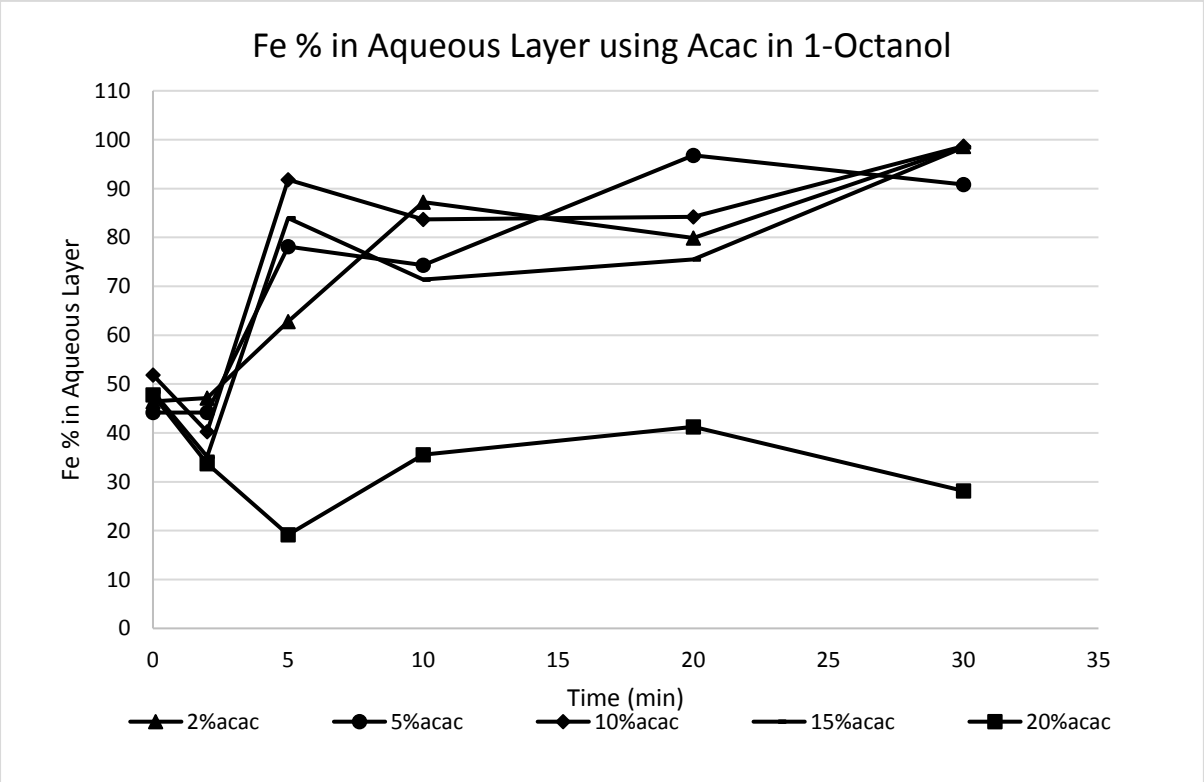


***Figure 4.8**: Fe % in aqueous layer using acetylacetone (acac) in 1-octanol at 25 °C, pH of 4 and stirring at 180 rpm.*

Over a period of 30 min, more of the Fe was found in the aqueous layer than the organic layer. Of the total Fe present in each mixture, 90-99% Fe reported to the aqueous layer over the 30min period, except in the case of the highest acac concentration used (20%). This observation was closely in line with the 99.1 % Fe extraction reported in a recent study, where the extraction solvent was a combination of 1-octanol and MIBK (Purcell, 2019). The separation was found to be second order with rate constant of 0.03 $M^{-1}min^{-1}$. All the titanium in the respective mixtures was chelated and extracted into the organic layer, leaving only trace amounts of Ti in the aqueous layer (see **Figure 4.9**). An amount of 30 % of the Fe reported to the aqueous layer when the mixture with 20 %acac was used. This would mean that for this study, the maximum acac concentration to use for successful Fe separation is around 5-10 % acac as depicted by **Figure 4.8**. Furthermore, the 20 % acac mixture was the only mixture that caused some of Ti to report to the aqueous layer as shown in **Figure 4.9 and 4.10.** This means that the threshold acac concentration for minimum Ti extraction into the aqueous layer should be around 5-10% acac applied over at least 30 minutes.

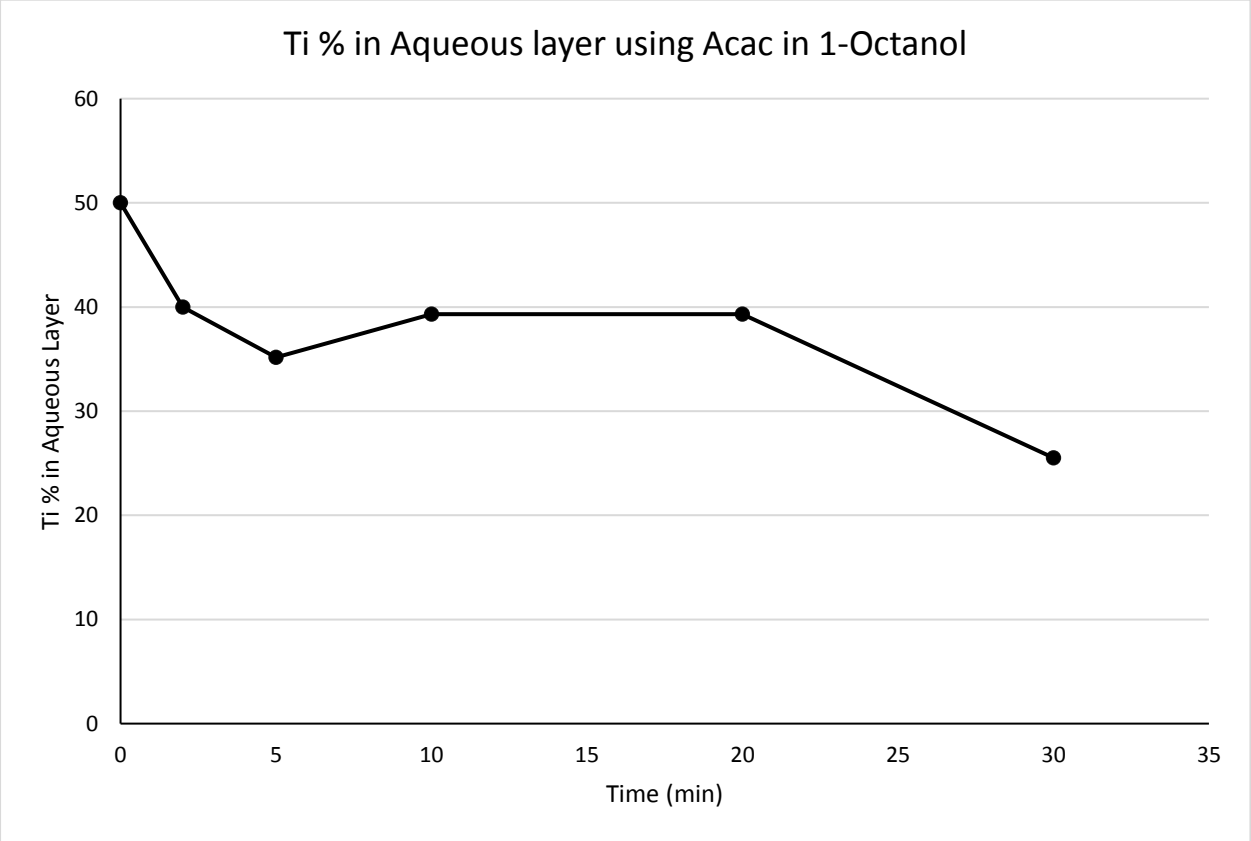


***Figure 4.9**: Ti % in aqueous layer using 20% acetylacetone (acac) in 1-octanol.*

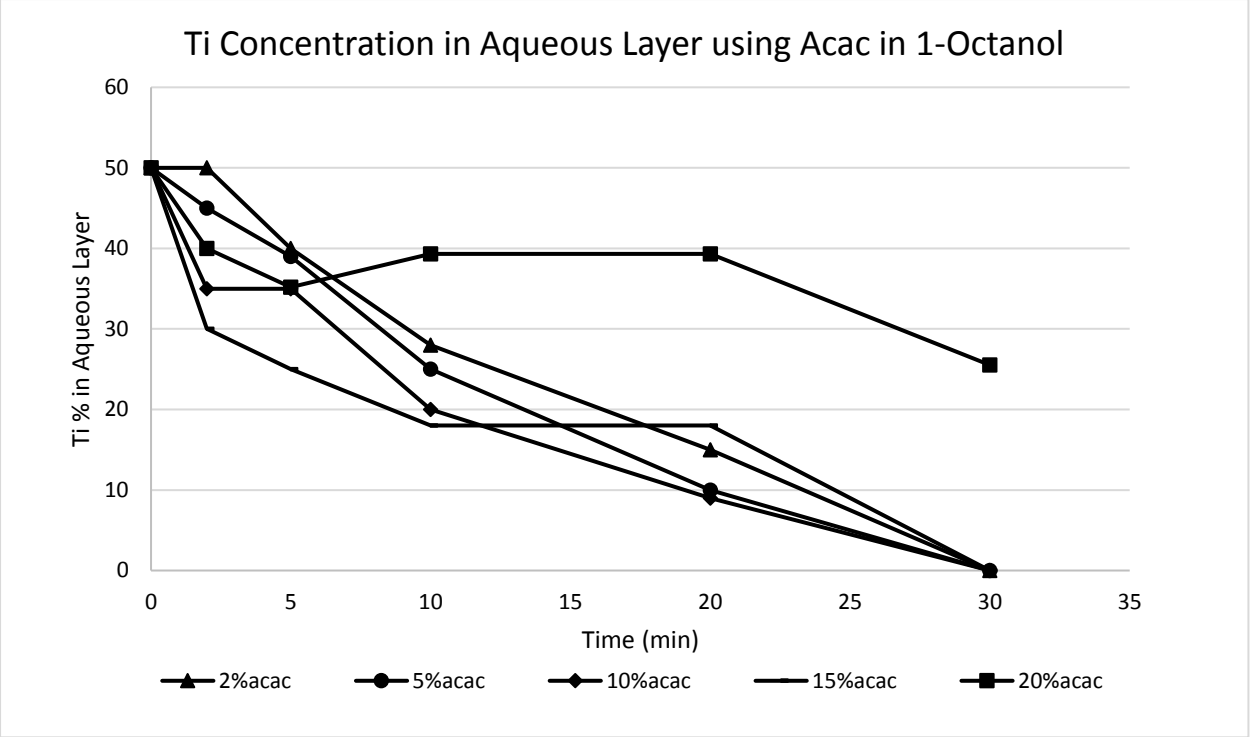


***Figure 4.10**: Ti % in aqueous layer using acetylacetone (acac) in 1-octanol at 25 °C, pH of 4 and stirring at 180 rpm.*

A study conducted by Alafari (2011) showed similar results where NaTPB was used together with kerosene as an extraction solvent. In this study, 97 % titanium extraction efficiency was observed through the use of 1.5M NaTPB in kerosene and 10 g/L ilmenite in the leach liquor (Alafara, 2011). **Figure 4.11** together with **Equation 12** were used to determine the distribution ratios for Ti and Fe between the aqueous and organic layer (Christian, 1991).

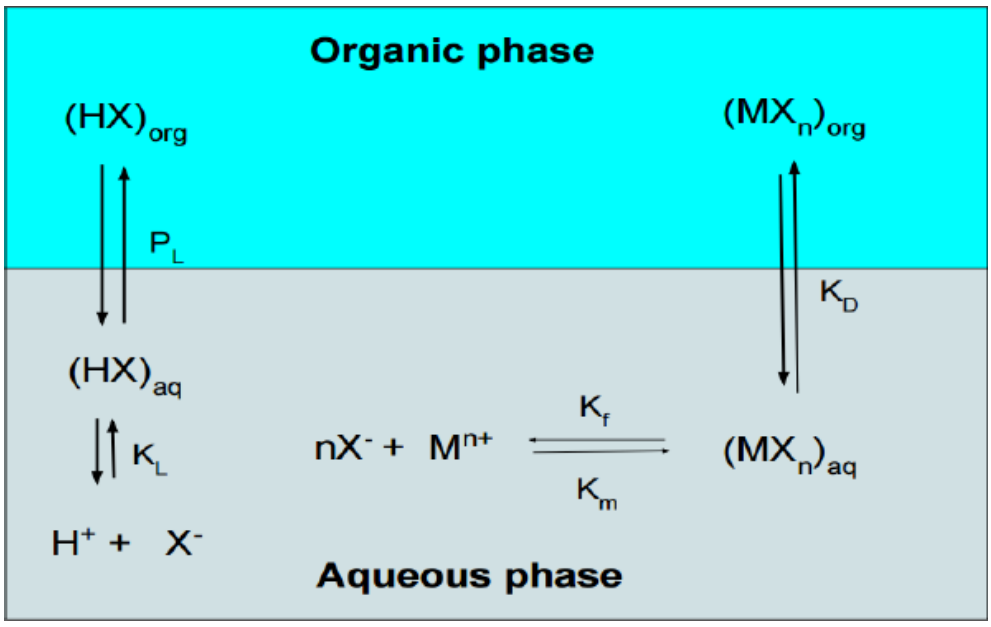


***Figure 4.11**: General extraction of metal M (Christian, 1991).*

$$K_D = \frac{[M]_{org}}{[M]_{aq}} \quad \text{..... (12)}$$

The separation factor was calculated from the distribution ratios. **Equation 13** represents the separation factor equation, which can also be interpreted as a separation efficiency equation (Solvent Extraction, 2016).

$$\alpha = \frac{K_{D(A)}}{K_{D(B)}} \quad \text{.....(13)}$$

***Table 4.6*:** Fe and Ti Distribution ratios and xeparation factors at various Acac additions between aqueous and organic layers.

Acac added	Distribution ratio (Kd),Fe	Distribution ratio (Kd),Ti	Separation Factor
2 %	3.4×10^{-3}	2×10^{1}	5.9×10^{3}
5 %	4.8×10^{-2}	5×10^{2}	10×10^{3}
10 %	2.9×10^{-3}	3.2×10^{3}	11×10^{5}
15 %	3.1×10^{-3}	2.3×10^{1}	7.4×10^{3}
20 %	6.2×10^{4}	1.9×10^{-3}	3.1×10^{-3}

From the values in this table, it seems that 10 % acac is the preferred concentration to get the maximum separation between Fe and Ti when extracting the Ti from the aqueous layer into the organic layer of 1-octanol. This confirms the visual trends seen in the various graphs in **Figures 4.8 – 4.10**.The differences in recoveries to the different layers can be explained by the differences in affinities between Fe, Ti and the aqueous and organic layers.

4.2.3. Ion Exchange Resins

The results of the Ti and Fe recoveries with various ion-exchange resins are presented in the discussion below. A summary of the maximum elution for the various ion-exchangers is provided in **Figure 4.13** and **4.14**. The behaviour of Fe elusion with a cationic resin is depicted in **Figure 4.12**:

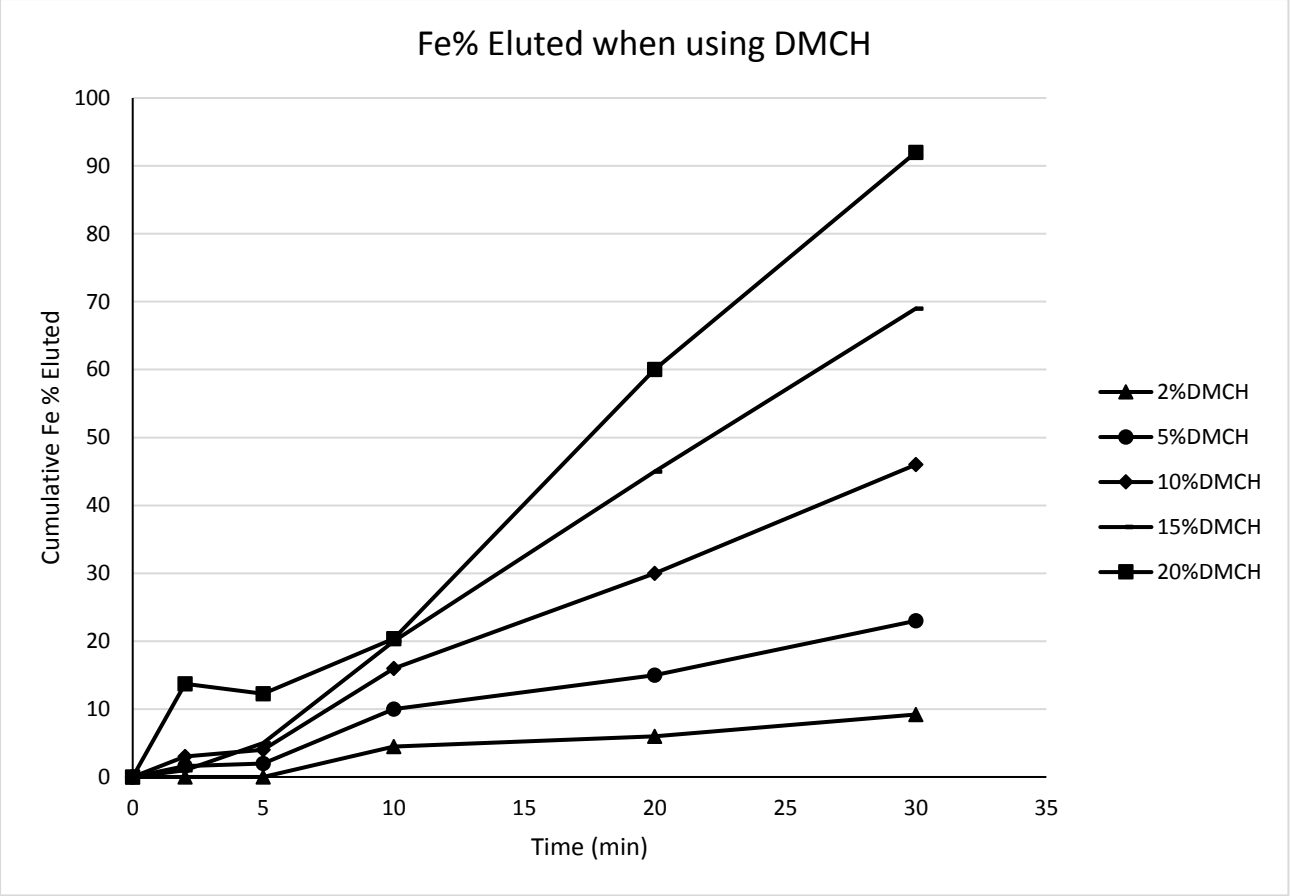


Figure 4.12: *Cumulative Fe % eluted at 25 °C using a cationic resin Dowex Marathon C Hydrogen (DMCH vol%), with 0.5M H_2SO_4 eluent at a flowrate of 0.7 ml/min.*

Table 4.7**:** 1st order separation correlation for Fe using DMCH .

DMCH Separation Order fitting	
%DMCH.[order]	R^2
2.[1]	0,94
5.[1]	0,98
10.[1]	0,99
15.[1]	0,99
20.[1]	0,97

As recommended in literature, 0.5M H_2SO_4 at an elution flow rate of 0.7ml/min was used to elute the Ti-Fe containing solution using Dowex Marathon C Hydrogen (DMCH) cationic exchange resin (Khan, 2012). All the runs were given at most 30min to obtain significant recoveries as higher residence time reduce production rate . 20 %DMCH was found to have the highest amount of eluted Fe, i.e.it retains the least amount of Fe and releases the most during the elution process, while retaining most Ti as compared to the other ion exchange resin

amounts used which is attributed to its higher affinity for Ti ions compared to Fe ions. **Figure 4.12** depicts that approximately 90 % of Fe was eluted after 30 minutes when a slurry of 20 vol.% DMCH was used. This compares favourably with other results reported in literature, where separation conducted using Dowex Marathon WBA achieved only 65 % Fe elution at 1.7 ml/min eluent flow rate (Purcell, 2019). The recovery differences between these studies could be because of the different ion- exchange resins that were used. The elution of titanium is shown in **Figure 4.13**.

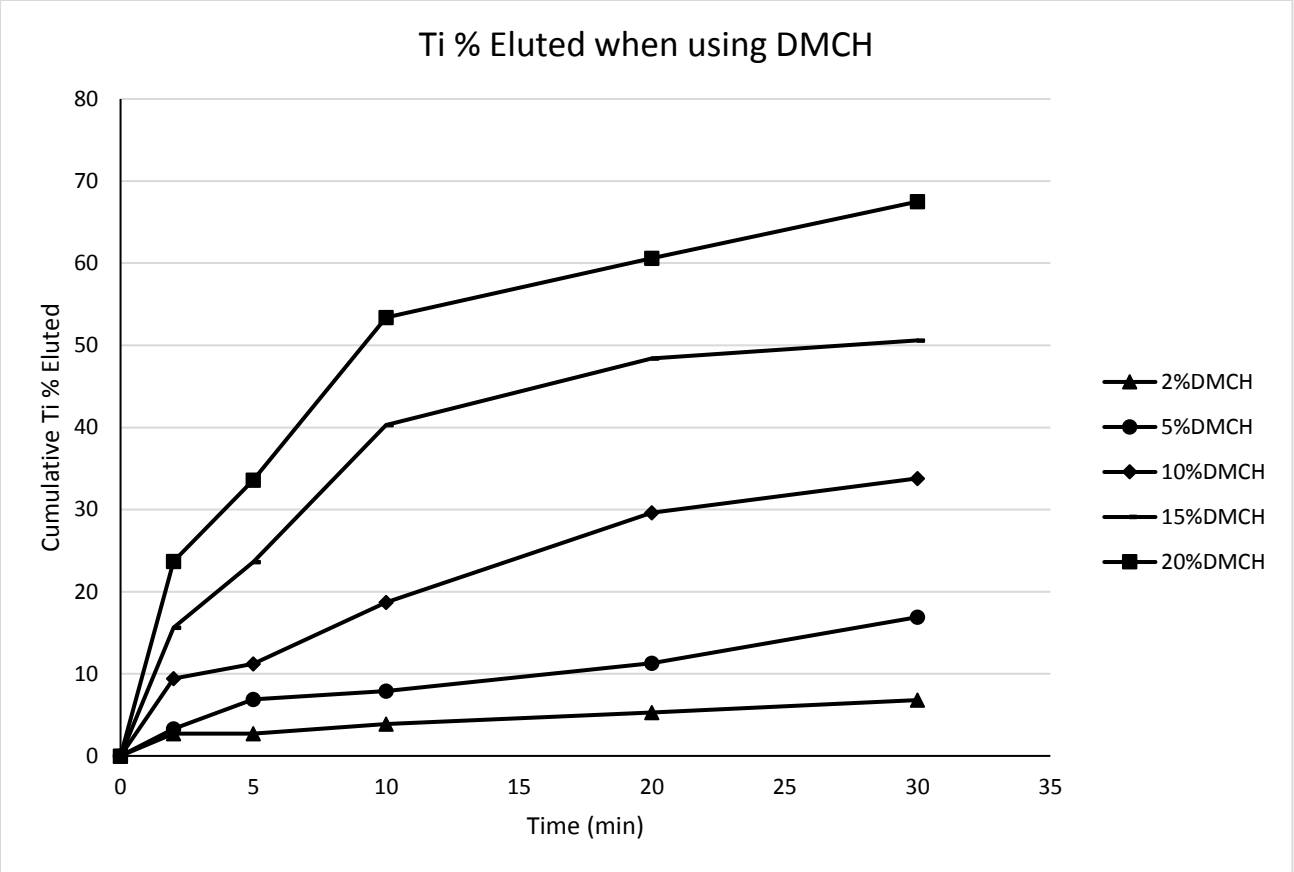


Figure 4.13: *Ti% eluted at 25 °C using a cationic resin Dowex Marathon C Hydrogen (DMCH) 0.5M H_2SO_4 eluent at 0.7 ml/min.*

Table 4.8**:** 1st order separation correlation for Ti using DMCH in ion exchange.

DMCH Separation Order fitting	
%DMCH[order]	R^2
2.[1]	0,88

5.[1]	0,94
10.[1]	0,93
15.[1]	0,79
20.[1]	0,78

The eluted mixtures were also analysed for titanium under the same conditions**. Figure 4.13** represents the amount of Ti that was eluted. and indicates that approximately 68% of Ti was eluted after 30 minutes when a slurry containg 20 vol.% DMCH was used. The 20 vol.% DMCH bed resulted in 90 % eluted Fe and 68 % eluted Ti. The Ti selectivity of this method was found to be low (3.2) and comparable with the low selectivity reported in literature (Purcell, 2019). Considering the fact that the separated mixture comes from a solution that favours more Ti dissolved than Fe, the separation load on this method was reduced by approximately 60 % (Martinez, 2016). **Table 4.13** represents a summary of the respective ion-exchange separation performance parameters.

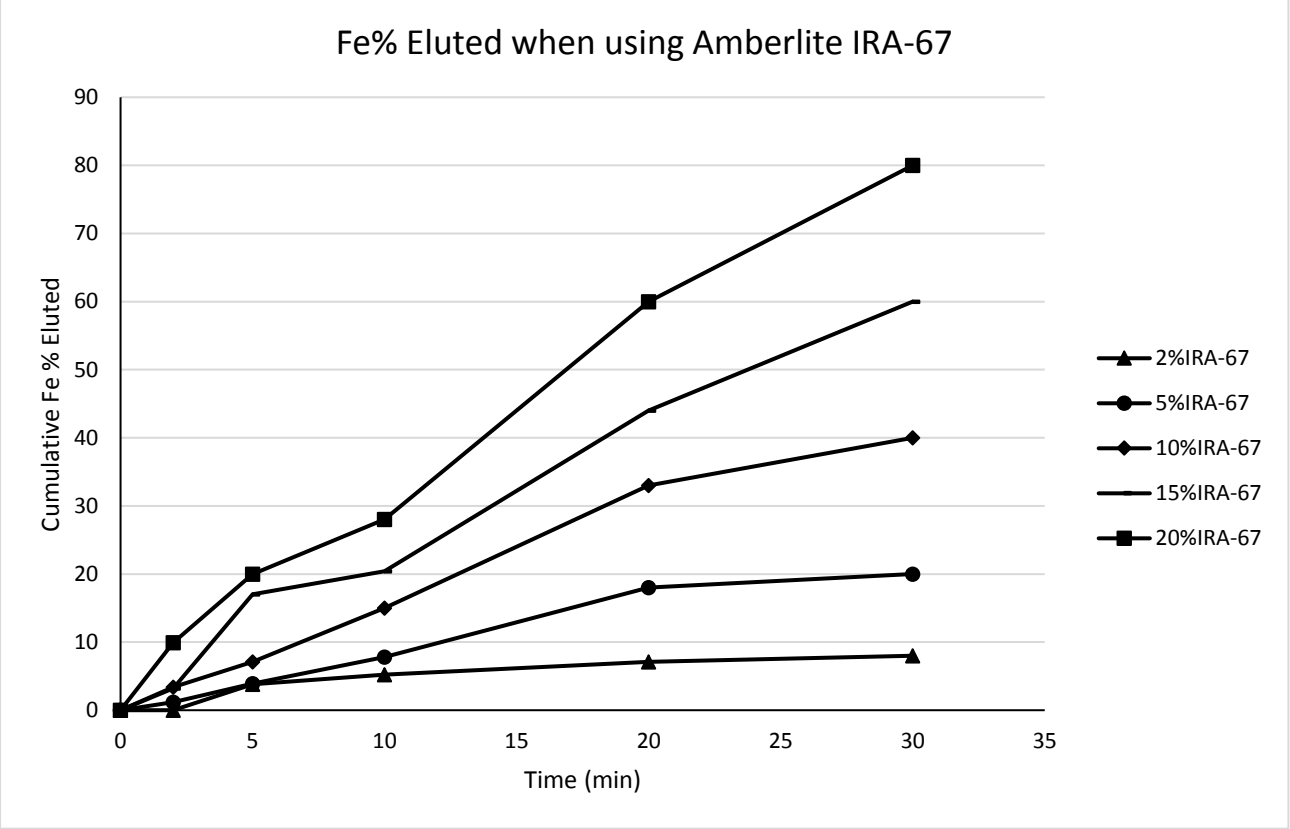


Figure 4.14: *Fe% eluted at 25 °C using a anionic resin Amberlite IRA-67 with 0.5M H_2SO_4 eluent at 0.7 ml/min.*

Table 4.9: 1st order separation correlation for Fe using IRA-67

IRA-67 Separation Order fitting	
%IRA-67[order]	R^2
2.[1]	0,84
5.[1]	0,96
10.[1]	0,98
15.[1]	0,98
20.[1]	0,99

The ionic exchange separation was also tested using an anionic resin (Amberlite IRA-67), while the other separation conditions such as eluent type and flow rate were kept constant. The highest Fe elution was observed with a slurry of 20 vol.% IRA-67, which yielded 79 % after 30 minutes, i.e 21 % Fe remained adsorbed on the anionic bed. This observation outlined that the amount (%mass) of adsorbed Fe using IRA-67 was double the Fe adsorption of the Dowex Marathon C Hydrogen cationic exchange resin. Opposite ionic charges have more affinity for each other, and this could be an explanation for the increased Fe adsorption on the anionic bed (Sachkov, 2017). A study that used Amberlite anionic exchange resin and 1M H_3PO_4 eluent at 1.7 ml/min obtained similar results with approximately 75 % Fe elution (Purcell, 2019). Amongst other factors, the 4 % difference in these two studies could be caused by the differences in bed length and ultimately bed contact surface area. The longer the ionic exchange column, the more time there is allowed for ionic adsorption as well as elution (Khan, 2012).

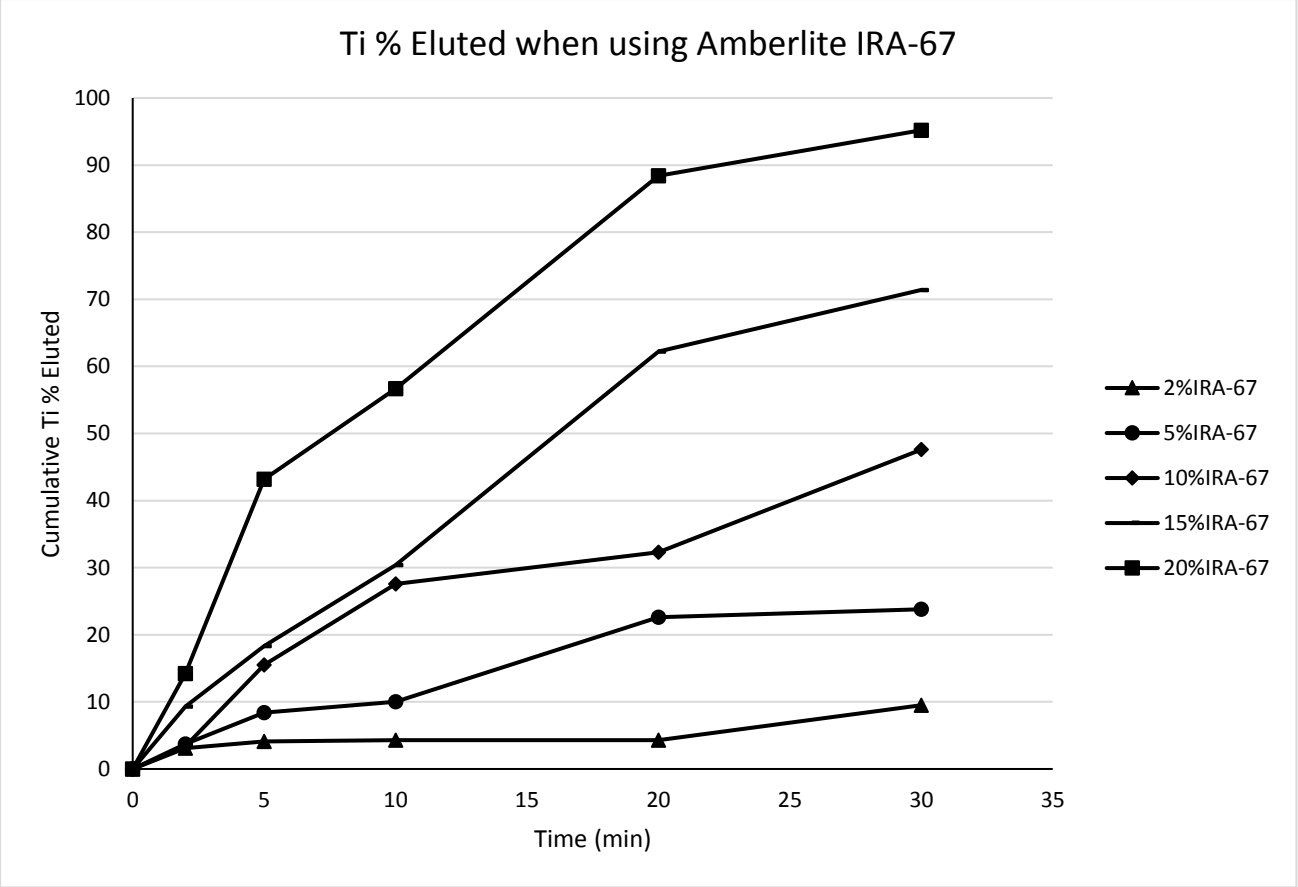


Figure 4.15: *Ti% eluted at 25 °C using a anionic resin Amberlite* ***IRA-67*** *0.5M H_2SO_4 eluent at 0.7 ml/min.*

Table 4.10**:** 1st order separation correlation for Ti using IRA-67.

IRA-67 Separation Order fitting	
%IRA-67.[order]	R^2
2.[1]	0,78
5.[1]	0,93
10.[1]	0,99
15.[1]	0,97
20.[1]	0,99

Ti elusion was also investigated for IRA-67. The analysis was therefore based on constant experimental conditions. The eluted Ti and Fe for the slurry containing 20 vol.% IRA-67 was 95 % and 80 % after 30 minutes respectively. This observation reported a lower selectivity

(1.2) compared to DMCH. Using Amberlite-402, a recent study also obtained a low selectivity (1.06) with approximately 80 % and 75 % of Ti and Fe eluted respectively (Purcell, 2019). The observation between these studies shows that when using Amberlite, the elusion difference between Ti and Fe was not significant enough to cause efficient separation. However, this observation depicts that when using anionic exchange resins, using Amberlite IRA-67 appears to be slightly better than using Amberlite-402 as IRA-67 reported a marginally higher selectivity.

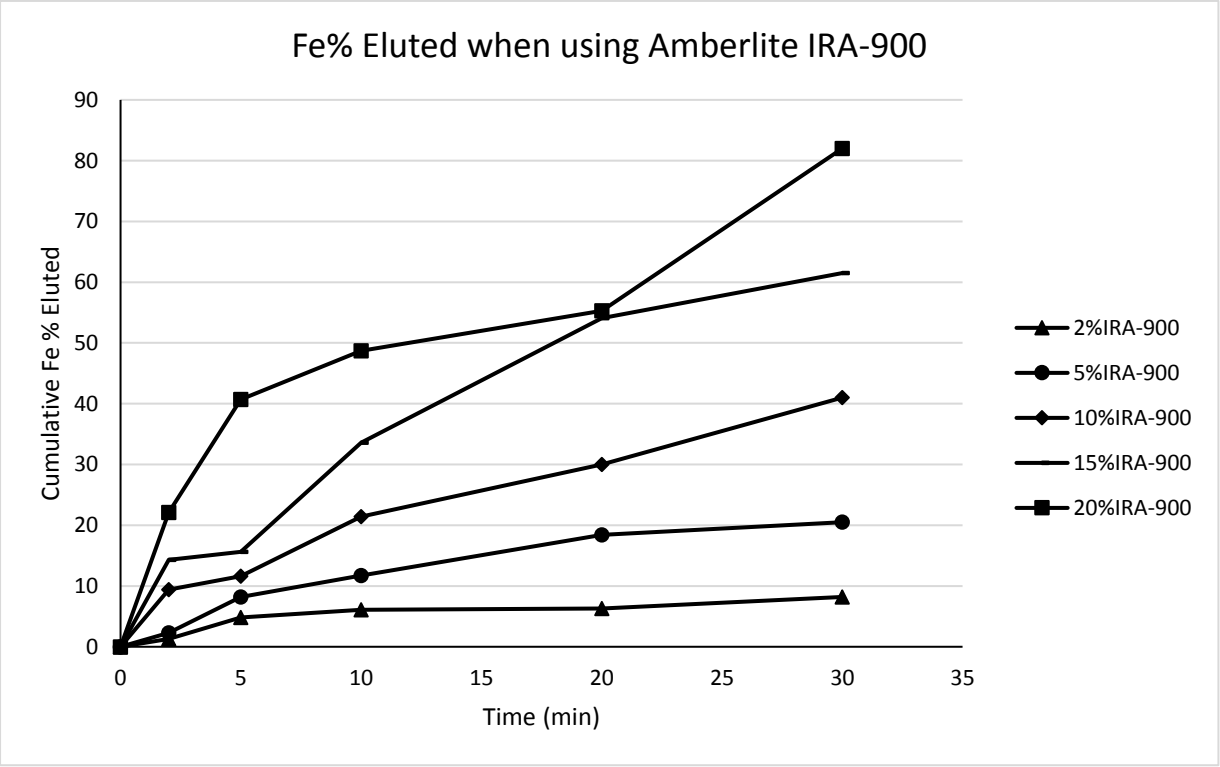


Figure 4.16: *Fe% eluted at 25 °C using a anionic resin Amberlite* ***IRA-900****, 0.5M H_2SO_4 eluent at 0.7 ml/min.*

Table 4.11: 1st order separation correlation for Fe using IRA-900.

IRA-67 Separation Order fitting	
%IRA-900.[order]	**R^2**
2.[1]	0,78
5.[1]	0,91
10.[1]	0,99
15.[1]	0,94

20.[1]	0,85

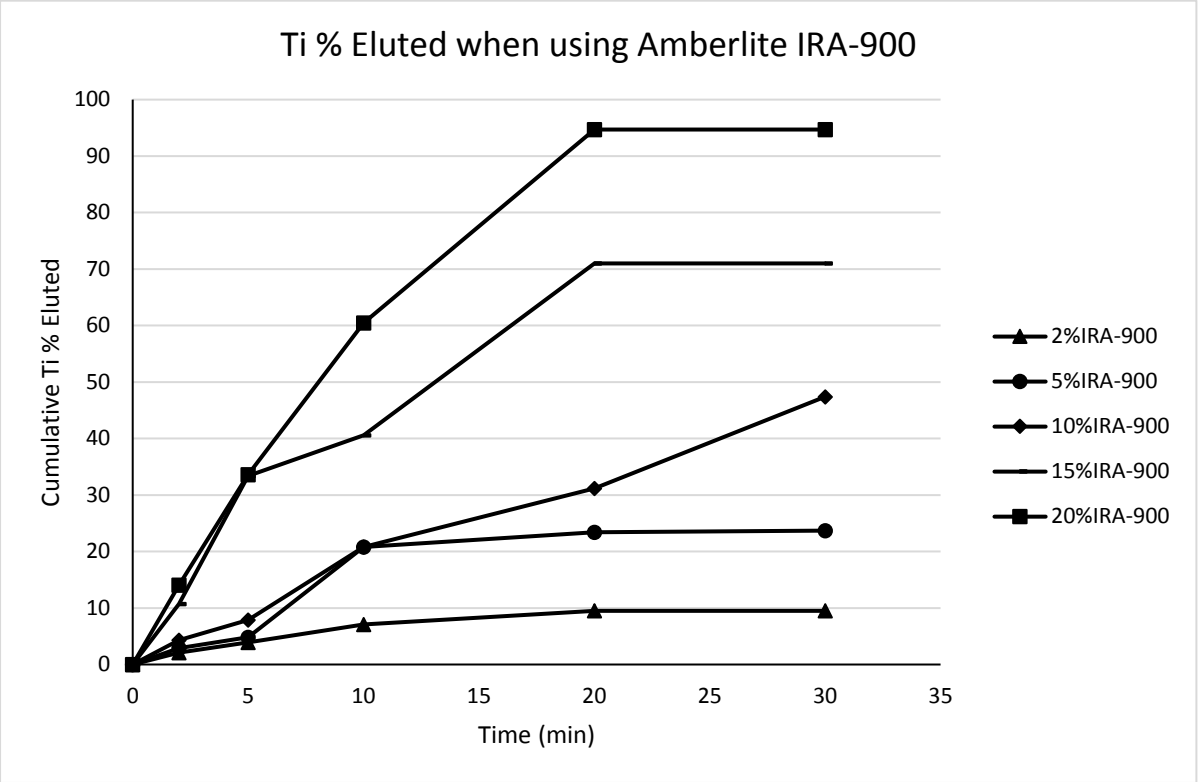


Figure 4.17: *Ti % eluted at 25 °C using a anionic resin Amberlite* ***IRA-900****, 0.5M H_2SO_4 eluent at 0.7 ml/min.*

Table 4.12**:** R^2 fitting information for Ti using IRA-900.

IRA-900 Separation Order fitting	
%IRA-900.[order]	**R^2**
2.[1]	0,83
5.[1]	0,78
10.[1]	0,99
15.[1]	0,98
20.[1]	0.88

Anionic exchange resins were further investigated using Amberlite IRA-900 which has a higher ionic strength compared to Amberlite IRA-67, with ionic strengths around 0.3 and 0.01M respectively (Mamchenko, 2000). The 20 vol.% IRA-900 bed resulted in 82 % eluted Fe and 95 % eluted Ti. This observation depicted that IRA-900 achieved the lowest selectivity

(1.16) compared to DMCH and IRA-67. The tendency of anionic exchange resins to produced low elusion differences between Ti and Fe was also observed in a study where the elusion difference was 5 % through the use of Amberlite IR-130C (Purcell, 2019). However, Amberlite IRA-900 performed better than Amberlite IR-130C as Amberlite IRA-900 achieved an elution difference of 26 % (95-69%). At high resin ionic strengths, competition between different metals of identical charge sign can lead to closely identical adsorption recoveries (Sanjeev, 2013). The similar elusion percentages of Ti and Fe presented in **Figure 4.16** and **4.17** were due to closely identical adsorption that existed between Ti and Fe across the ionic bed.

Table 4.13 represents the ion-exchange separation parameters, which describe the separation efficiency of each ion-exchange resin. The migration of species in the column was obtained through the calculation of the retention factor (k) as represented by **equation 14** (Skoog, 2014).

$$k = \frac{t_r - t_0}{t_0} \quad \text{..... (14)}$$

Where t_o is the time taken by the mobile phase to pass through the ion-exchange column and t_r is the retention time of the eluted material in the column. Considerable separation is represented by a separation factor that is greater than 1.The separation factor (α) was determine as described in **section 4.2.2**.The column length was calculated as it represents the number of theoretical plates (N) which in turn affects separation efficiency (Skoog, 2014). The larger the value of N, the better the separation. W represents the theoretical peak width which is the time taken to reach the highest elusion concentration (amount) point or fairly constant and/or rapid decreasing rate of concentration (Skoog, 2014).

$$N = 16\left(\frac{t_r}{w}\right)^2 \quad \text{..... (15)}$$

***Table 4.13*:** Fe and Ti ion exchange separation parameters.

Ion exchange separation parameters					
Resin Addition(%)	Element	k	α	W(min)	N
Dowex Marathon C Hydrogen (DMCH)					
2	Ti	17,3	5,4	10	45
	Fe	4,8	1	10	80
5	Ti	27,2	4,4	30	67
	Fe	2,1	3,9	30	5,8
10	Ti	32,6	6,7	20	33
	Fe	1,5	1	30	80
15	Ti	26,3	9,5	20	79

	Fe	4,9	1,1	30	98
20	Ti	20,4	4,3	30	26
	Fe	1,3	1	30	116
Amberlite IR-67					
2	Ti	21,6	4,6	5	68
	Fe	4,5	1	5	10,6
5	Ti	16,2	4,3	20	38,7
	Fe	2,7	1	20	76,5
10	Ti	25,3	5,6	30	88
	Fe	2,2	1	30	6,8
15	Ti	10,6	5,5	20	3,7
	Fe	3,1	1	30	9,3
20	Ti	30,8	6,1	30	98
	Fe	3,9	1	30	3,5
Amberlite IR-900					
2	Ti	13,9	4,9	10	12
	Fe	4,4	1	5	56
5	Ti	12,1	3,4	10	43
	Fe	4,4	1	20	3,6
10	Ti	15,1	3,3	30	66
	Fe	6,3	1	30	49
15	Ti	11,7	4,3	20	31
	Fe	7,2	1	30	34
20	Ti	23	2,2	20	14
	Fe	8,8	1	30	29

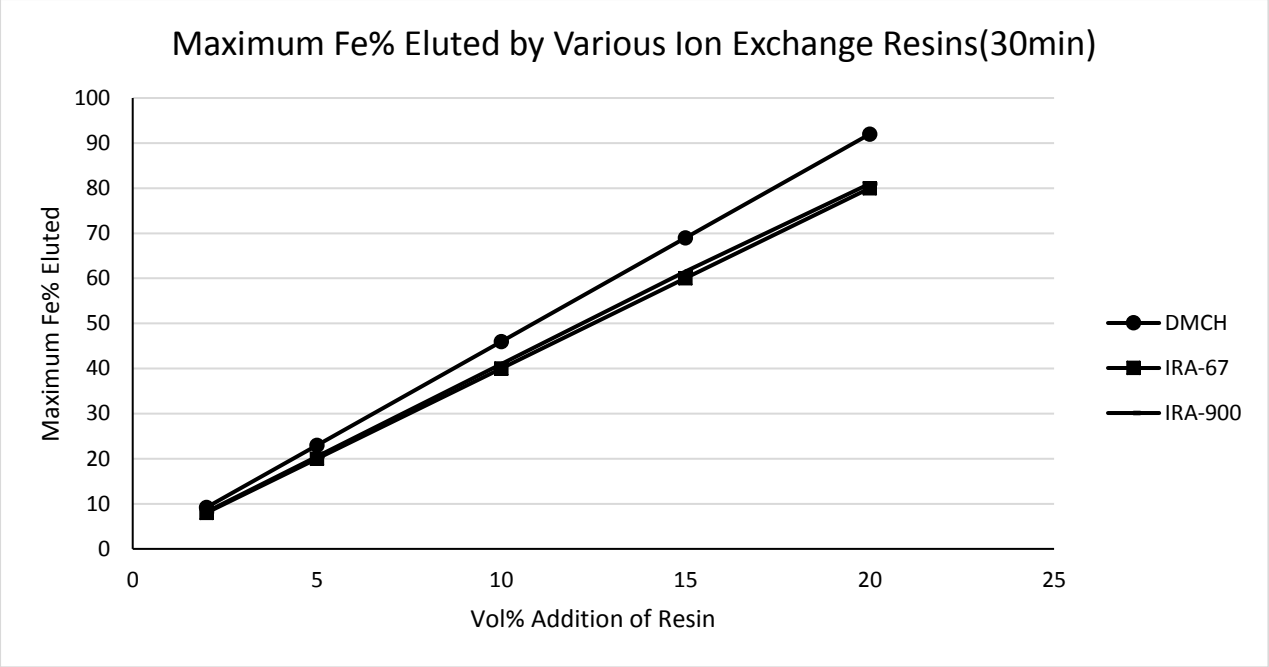


***Figure 4.18**: Summary of the maximum elution of Fe using the various ion exchange resins.*

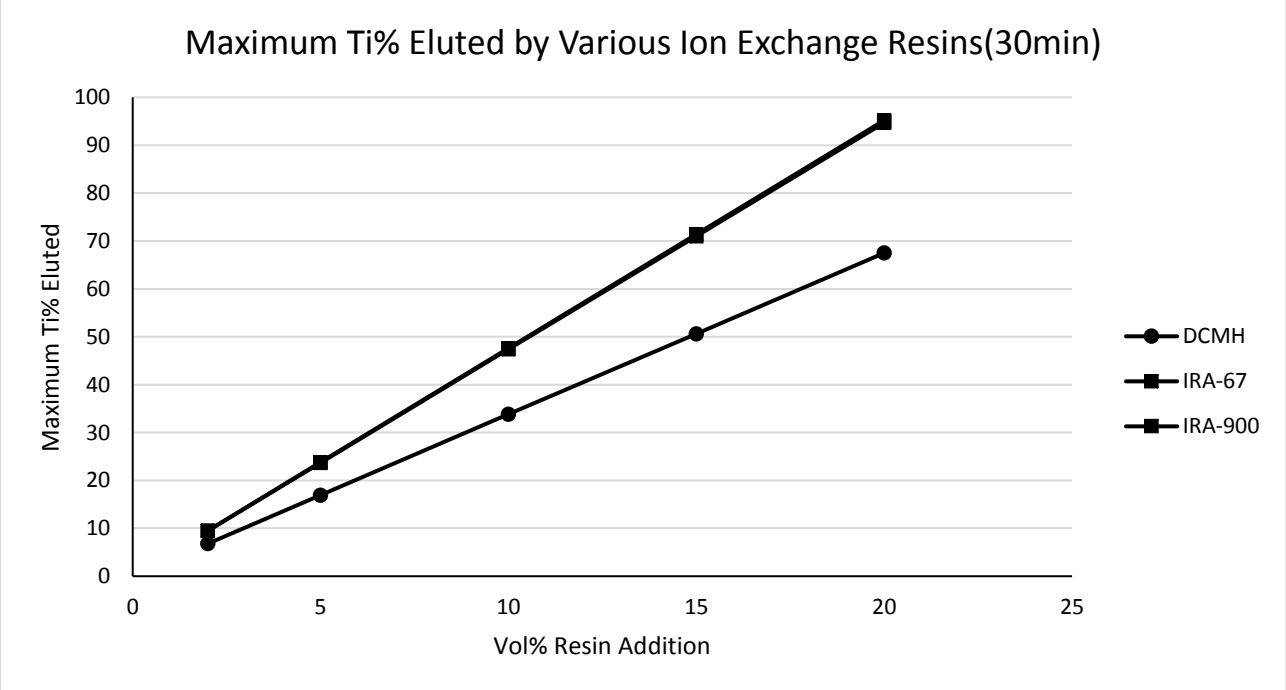


***Figure 4.19**: Summary of the maximum elution of Fe using the various ion exchange resins.*

Significantly high elusion differences we obtained for the different ion exchange resins, separation was therefore seen to be possible**. Figure 4.18** and **4.19** depict that DCMH gave the highest Fe elution and lowest Ti elution respectively.. For improved separation, a series of elution columns or an extension of a single column would have to be considered. Breakthrough

curves were plotted for the three ion exchange resins in order to determine the breakthrough points.

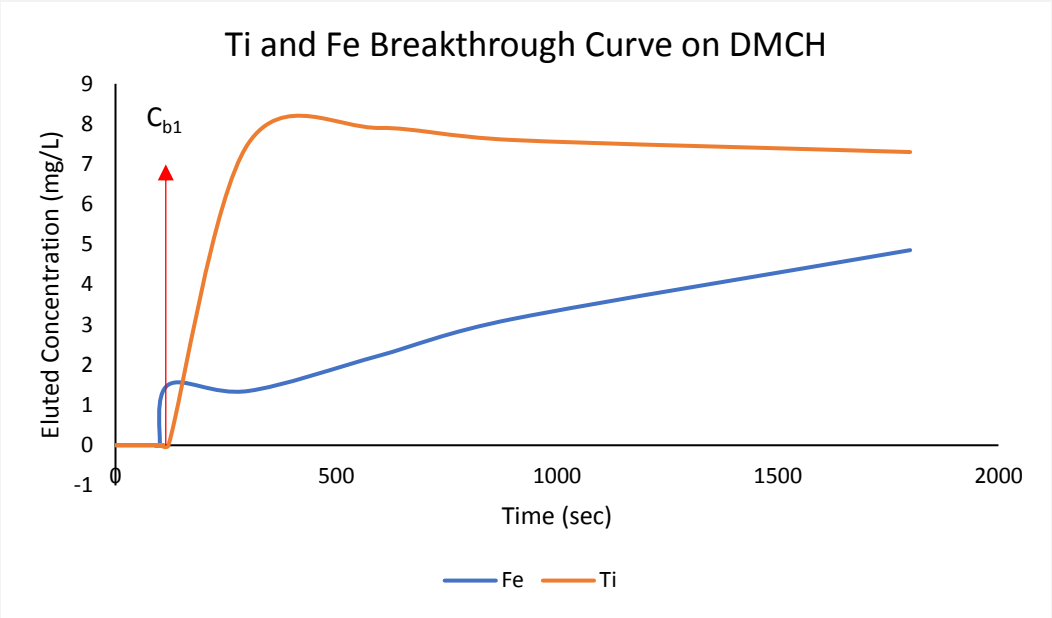


Figure 4.20: Breakthrough curve for 20% DMCH.

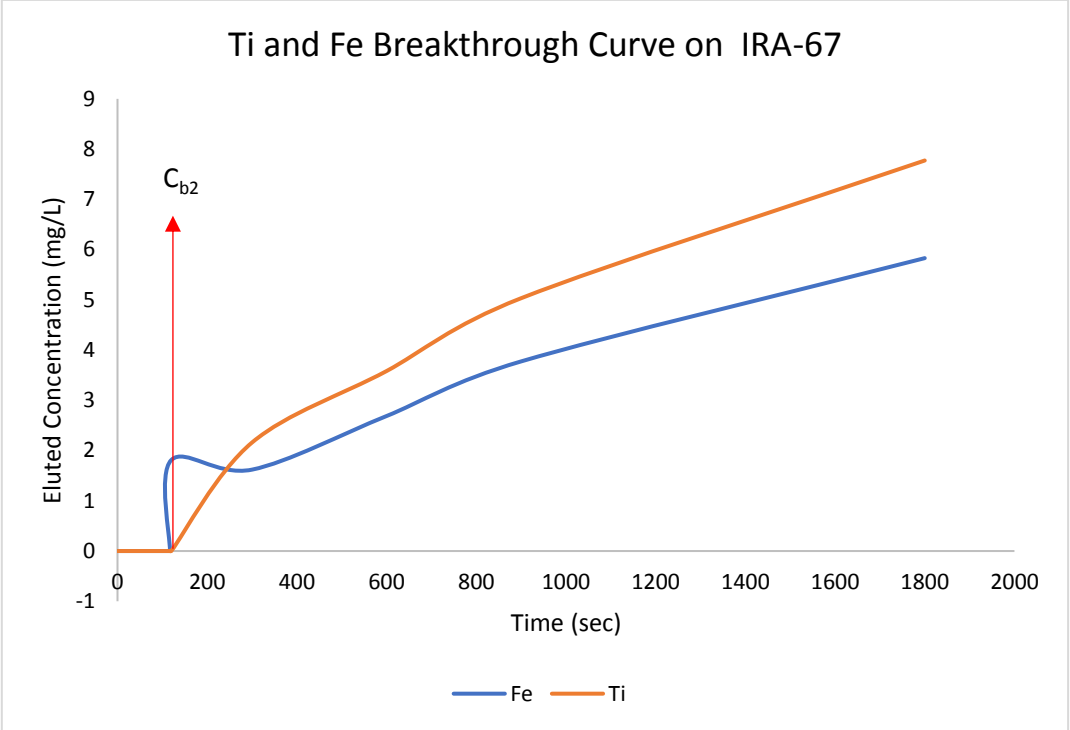


Figure 4.21: Breakthrough curve for 20% IRA-67.

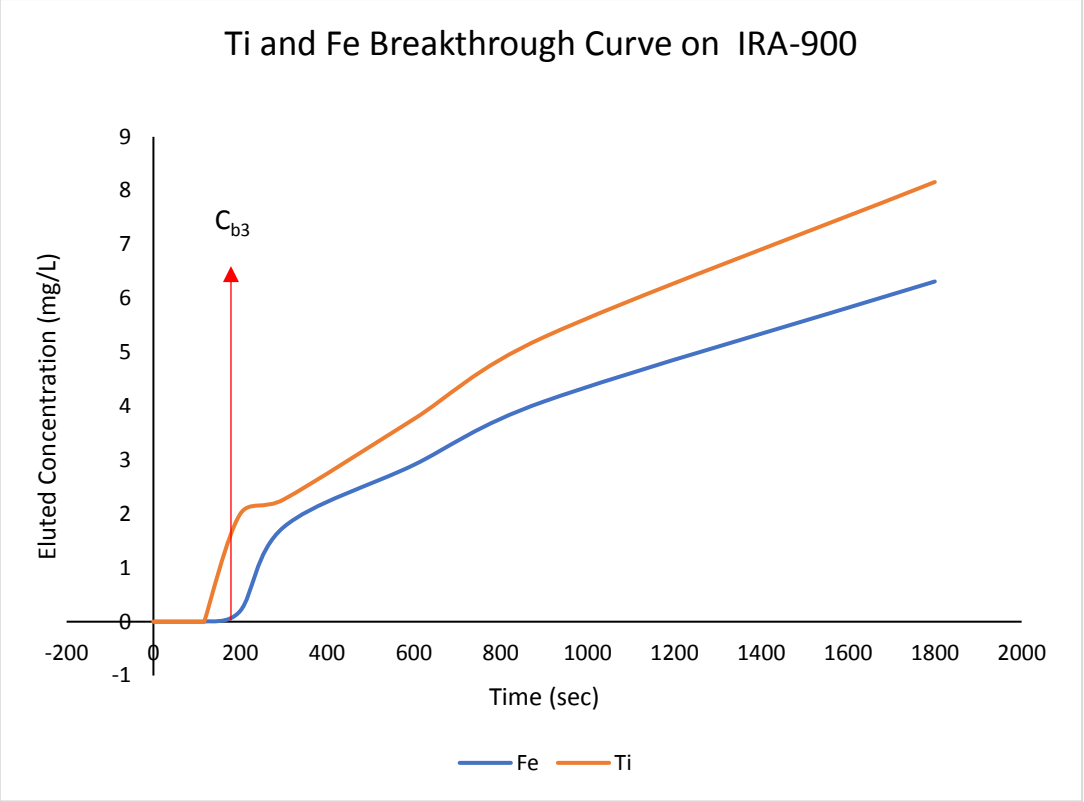


Figure 4.22: Breakthrough curve for 20 % IRA-900.

C_{b1}, C_{b2} and C_{b3} represents the breakthrough points of the respective ion exchange resins. DMCH and IRA-67 obtained a breakthrough point at 120 seconds (2 minutes) while IRA-900 was at 3.3 minutes. As seen in figure 4.20-4.22, the breakthrough points allowed for a fairly complete separation of Ti and Fe.

4.3. Residue Analysis

Some of the separation methods resulted in the formation of a precipitate cake, which was analysed by SEM for its composition. When phenanthroline was used as a precipitant in selective precipitation, there was no precipitation observed. However, when NaTPB was used, there was some precipitate seen, as the images below indicate. (see also appendix C).

4.3.1. Selective Precipitation

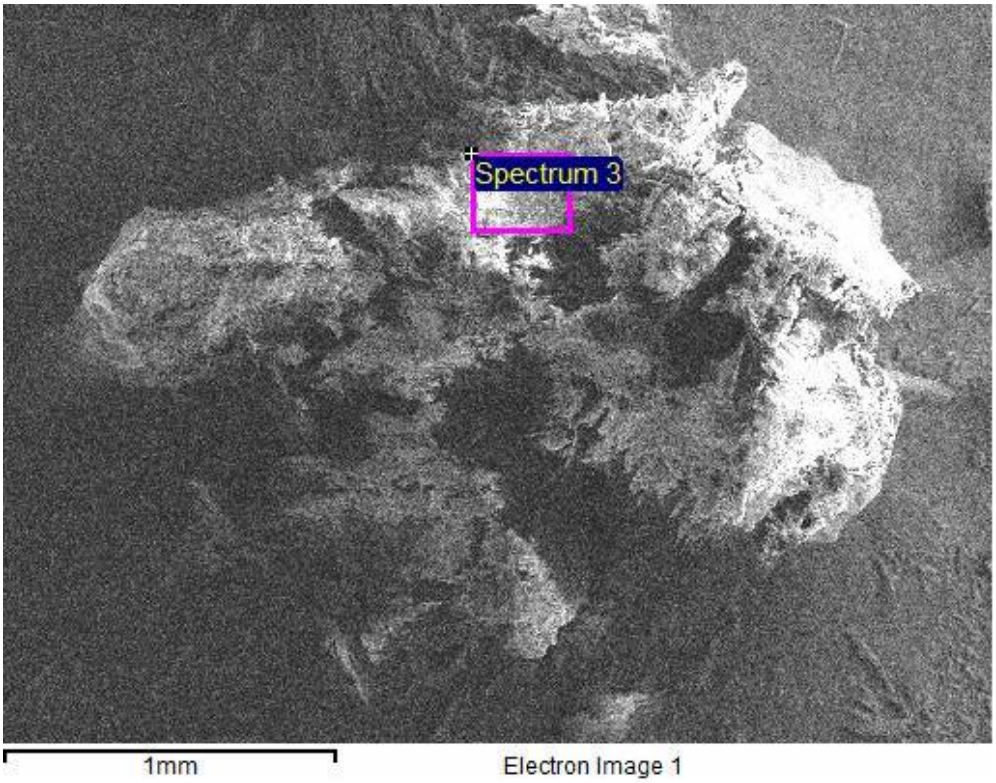


***Figure 4.23**: Electron image of precipitate formed when applying a 5 %NaTPB mixture to a solution containing dissolved Fe and Ti ions. Analysis at 1mm, 25 nA and 15kV.*

This analysis was conducted in order to analyze the composition of Ti and Fe in the precipitate. No precipiate formed when 2 %NaTPB was added to the mixture. **Figure 4.23** represent the electron image of the cake when 5 vol% NaTPB was used. The square labelled spectrum 3 is the area that was used to analyzed the sample composition.The results of this sample are shown in **Figure 4.24** as printed by the SEM.

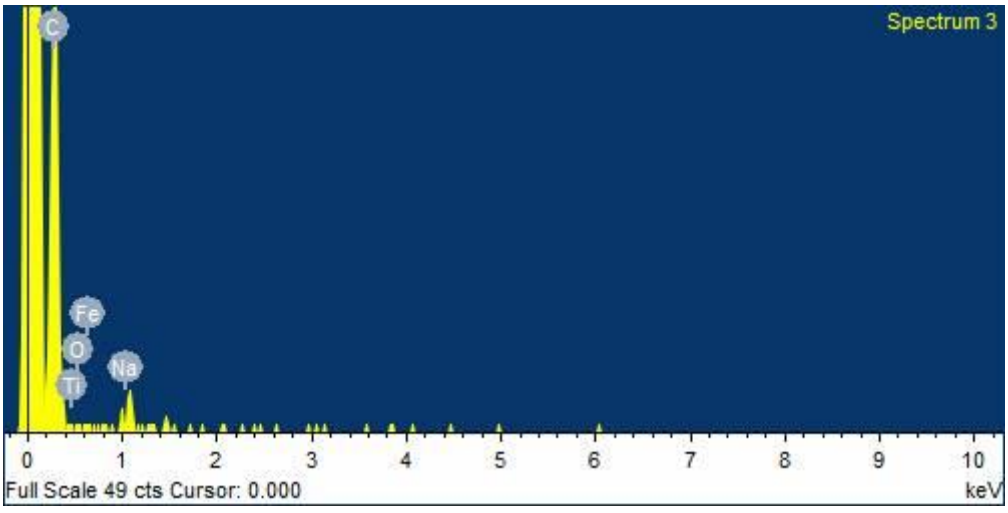


***Figure 4.24**: Graphical precipitate composition results of Fe and Ti for 5 % NaTPB mixture.*

Elements such as sodium were also present(1.28%), since NaTPB contains sodium.The aim was to precipitate Ti and in this way separate it from iron..The results in Table 4.15 represent low residual amounts of Ti and Fe in the precipitates and are not very satisfactory to determine whether the precipitation was successful or not in each case.

***Table 4.14*:** Fe and Ti % quantities on filtered cake.

[NaTBP added(%)]	Fe (mass %)	Ti (mass %)
2	-	-
5	0.02	0.15
10	0.30	-
15	0.15	0.19
20	0.50	0.30

4.4. Experimental Conclusion

The dissolution using H_2O_2 additions was successful at leaching ilmenite favourably as more Ti was dissolved than iron. The separation methods were also successful at separating Ti and Fe. Selective precipitation using NaTPB was successful at precipitating more than 90 % of Ti while leaving more than 95 % of Fe in solution. Solvent extraction using acac and 1-octanol was successful at separating Fe and Ti where more than 95 % of Ti was extracted to the organic phase and more than 95 % of Fe remaining in aqueous solution. Ion exchange resins were also successful at separating the two metals. Breakthrough curves suggested that complete separation for DMCH and IRA-67 was achieved at breakthrough point of 2minutes and 3.3 minutes for IRA-900.Based on these results, any of these results may be taken to preliminary process design. Solvent extraction was taken to preliminary design as it is a well known technology with wide application in metals extractions and separation.

CHAPTER 5—PROCESS FLOWSHEET & UTILITY STRUCTURE

This section provides information that was taken from the experimental observations and used for the flowsheet design. A **conceptual** flowsheet design was constructed to estimate the possible plant structure and general equipment required, which is essential before conducting a complete conceptual design. This section provides information on the planned plant utility structure, as it is aimed that the plant will be a greenfield plant. Furthermore, an economic comparison between the separation methods of this study was conducted. This was done in order to evaluate the potential profitability of each method if incorporated in a continuous process discussed in **section 5.3.** Typical industry operational assumptions and conceptual economic analysis are discussed in **section 5.5**.

5.1. Experiments Conclusion & Information Taken To Preliminary Process

Dissolution

The average Fe dissolution was approximately 1 % and was around 76 % for Ti in sulphuric acid and hydrogen peroxide mixtures. For phosphoric acid with hydrogen peroxide addition,the average Fe dissolution was approximately 1 % and for Ti was around 42 %. H_2SO_4 was selected as the best acid for ilmenite dissolution as it had a higher Ti recovery percentage than H_3PO_4. H_2SO_4 and 15 vol% H_2O_2 was selected as the optimmum mixture for dissolution.. This mixture achieved the highest Ti dissolution (approximately 81%) with only trace amounts of Fe.

Separation

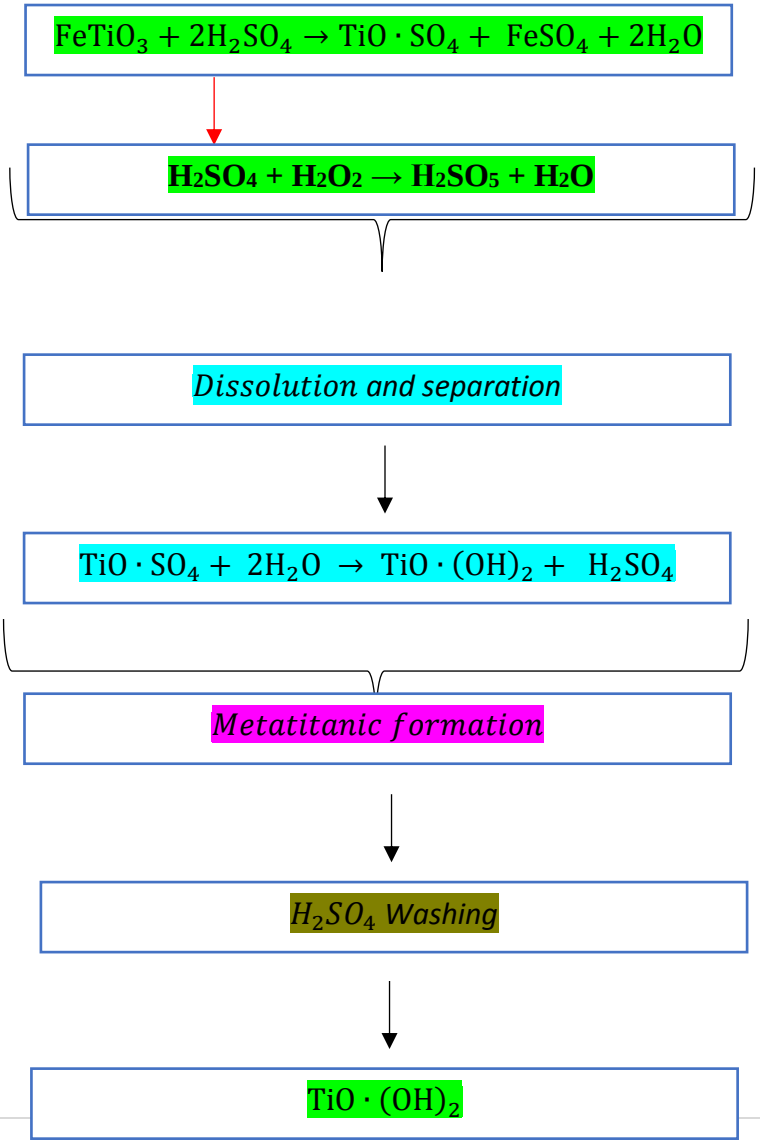
Information taken into consideration for the preliminary design process

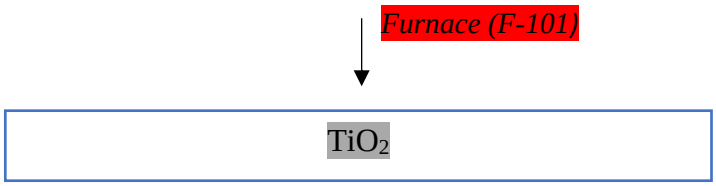
- H_2SO_4 and 15 vol% H_2O_2 was used for dissolution.
- Maximum dissolution temperature was 150°C.
- The separation methods all obtained high recoveries as mentioned in **section 4.4**. Solvent extraction was taken to preliminary design, as it seemed to be a well known and widely applicable technology According to literature, recovery of the chelating reagents is less complex which aids with reducing raw material costs (Dipaloy, 2015).

5.2. General Assumptions Process—Flowsheet and Utility Structure requirements

- Steady state operation.
- Components not included have negligible impact.
- Negligible kinetic and potential energies (very small compared to other terms).
- For initial stages, the pump efficiency was specified at 85%.
- Negligible heat losses from process unit operators.
- Absorption column achieves total recovery of solvent extraction medium.
- Raw materials used are identical to those used in the experimental stage.
- The work extracted from the turbine of the steam generation cycle is sufficient to power all the process equipment.

General Chemical Reaction Scheme (Krishen, 1965):





5.3. Overview of the plant description and flowsheet

Mixer (M-101) mixes the ilmenite and hydrogen peroxide streams at 1 atm and 25 °C. Mixer M-102 mixes the $FeTiO_3$-H_2O_2 stream with H_2SO_4. The dissolution chamber (R-101) receives the resulting stream at 150 °C due to the rapid dissolution temperature increase. R-101 operates adiabatically. A screen is used to remove solids and recycled back to M-101 to increase raw material utilization. To protect the screen from possible wear caused by high temperatures, a heat exchanger (E-101) is used to cool the hot stream to 25 °C before passing through the screen (Pearson, 2013). The cooling performed by E-101 simultaneously meets the operating temperatures of the screen and solvent extraction agitator. The residence time for this agitator is specified to be 30 min, as this was the time allowed for the experimental solvent extraction to take place. Furthermore, this time was found to be sufficient for equilibrium to occur in the extraction process.

In order to recover the chelating reagents, an absorber operating at the typical 10 atm operating pressure was incorporated (Bonet, 2006). A pump (P-101) was used to pump the solution from the absorber inlet to the absorber operating pressure. Distillation column D-101 operates at 121 °C and 1 atm. The differences in boiling points allows peroxymonosulfuric acid (formed in the dissolution phase) to report as the bottoms product (Steudel, 2000). A pressure release valve (V-101) and a heat exchanger (E-101) are used to vent off the pressure from the absorber and increase the temperature to the required column operating conditions. The top product of the column is cooled by the heat exchanger E-104 and enters a boiling water chamber R-102 for the formation of metatitanic acid as recommended in literature (Krishen, 1965). Water is sourced from an external supply. The water is first heated using a heat exchanger to the operating temperature of R-102. The formation of metatitanic acid also forms significant amounts of sulphuric acid. Sulphuric acid affects the purity of titanium oxide after dissolution of the ilmenite. A H_2SO_4 washing stage at 5 atm and 25 °C is used to remove the sulphuric acid (Titanium processing Center, 2017). A heat exchanger and pump was used to transport the boiling water chamber outlet solution to the H_2SO_4 washing stage.

For optimum process efficiency, material have to enter vessels at vessel operating conditions. Pressure release valve V-102 was used to bring the washing stage outlet pressure to the operating pressure of the furnace (F-101) that was used. The furnace is used to form titanium oxide hydroxide $TiO \cdot (OH)_2$(metatitanic acid). Steam is also formed in the furnace. Energy from this steam can be recovered and used in column re-boilers and heat exchangers to reduce heating requirements. The produced titanium oxide is also cooled to approximately 25 °C and the removed energy can be used in other sections of the plant. Apart from reducing costs in heat requirements, recovering heat also aids in minimizing thermal pollution, and hence reduced pollution tax (Nordell, 2020). **Equation 16** shows the mass efficiency formula that was used to calculate the plant mass efficiency for titanium oxide production. The mass efficiency of titanium oxide production was calculated to be approximately 50 % (ratio of the mass of desired product to mass of raw material input), which correlates well with the mass efficiency literature value of 47.5 % for titanium oxide production (Dahe, 2004).

$$Mass\ efficiency\ (\%) = \frac{M_{desired\ product}}{M_{raw\ material\ input}} \times 100 \quad \text{(16)}$$

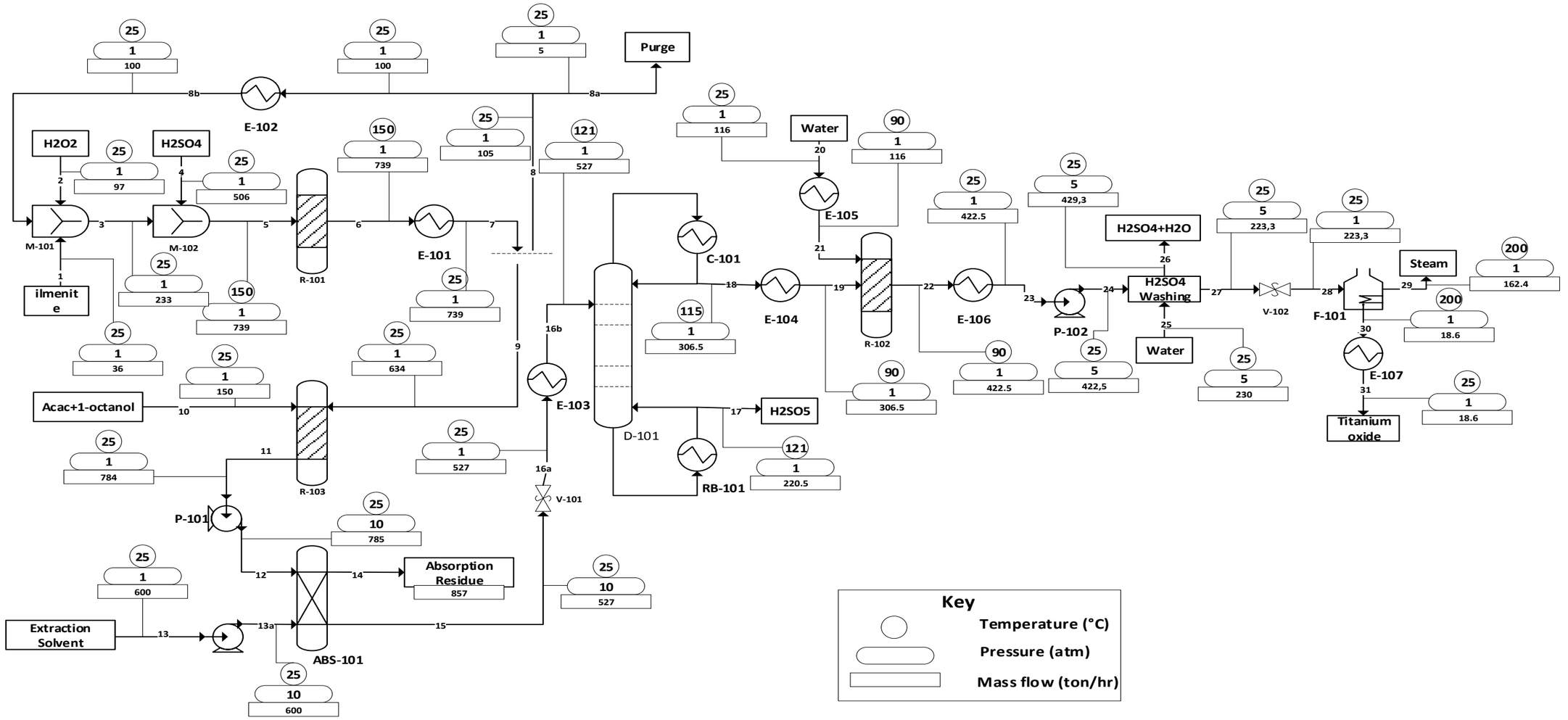
$$= \frac{18 ton/hr}{36 ton/hr} \times 100$$

$$= 50\%$$

Titanium Oxide Plant with Stream Conditions

ABS-101 Absorber	D-101 Distillation column	V-101-102 Pressure release valves	E-101-105 Heat Exchangers	C-101 Condenser	RB-101 Reboiler	R-101 Dissolution Chamber	R102 TiOSO4 Converter	R-103 Solvent Extraction Agitator	M-101-102 Mixer	F-101 Furnace

Figure 5.1



Stream	1	2	3	4	5	6	7	8	8a(pu	8b	9	10	11	12	13	13a	14	15	16a	16b	17	18	19	20	21	22	23	24	25	26	27	28	29	30	31
Temperature C	25	25	25	25	150	150	25	25	25	25	25	25	25	25	25	25	25	25	25	121	121	115	90	25	90	90	25	25	25	25	25	25	200	200	25
Pressure (atm)	1	1	1	1	1	1	1	1	1	1	1	1	1	10	1	10	10	10	1	1	1	1	1	1	1	1	1	5	5	5	5	1	1	1	1
Component mass frac.																																			
Fe2TiO3	33	0	36	0	36	3	3	3	0	3	0	0	0	0	0	0	0	0	0	0	0	0	0	0	0	0	0	0	0	0	0	0	0	0	0
H2O2	0	97	97	0	97	0	0	0	0	0	0	0	0	0	0	0	0	0	0	0	0	0	0	0	0	0	0	0	0	0	0	0	0	0	0
H2SO4	0	0	0	506	506	0	0	0	0	0	0	0	0	0	0	0	0	0	0	0	0	0	0	0	0	0	211	211	211	0	211	0	0	0	0
H2SO5	0	0	40	0	0	263	263	42	1	40	221	0	221	221	0	0	0	221	221	221	221	0	0	0	0	0	0	0	0	0	0	0	0	0	0
H2O	0	0	44	0	0	238	238	46	2	44	192	0	192	192	0	0	0	192	192	192	0	192	192	116	116	0	0	0	230	218	12	12	162	0	0
FeSO4	0	0	13	0	0	121	121	14	1	13	107	0	107	107	0	0	107	0	0	0	0	0	0	0	0	0	0	0	0	0	0	0	0	0	0
TiOSO4	0	0	0	0	0	115	115	0	0	0	115	0	115	115	0	0	0	115	115	115	0	115	115	0	0	0	0	0	0	0	0	0	0	0	0
TiO(OH)2	0	0	0	0	0	0	0	0	0	0	0	0	0	0	0	0	0	0	0	0	0	0	0	0	0	0	211	211	211	0	0	211	211,3	0	0
C5H8O2	0	0	0	0	0	0	0	0	0	0	0	22,5	22,5	22,5	0	0	22,5	0	0	0	0	0	0	0	0	0	0	0	0	0	0	0	0	0	0
TiO2	0	0	0	0	0	0	0	0	0	0	0	0	0	0	0	0	0	0	0	0	0	0	0	0	0	0	0	0	0	0	0	0	0	18,6	18,6
C8H18O	0	0	0	0	0	0	0	0	0	0	0	128	128	128	0	0	128	0	0	0	0	0	0	0	0	0	0	0	0	0	0	0	0	0	0
Extraction sol.	0	0	0	0	0	0	0	0	0	0	0	0	0	0	600	600	600	0	0	0	0	0	0	0	0	0	0	0	0	0	0	0	0	0	0
Mass (kg/hr)	33	97	233	506	739	739	739	105	5	100	634	150	784	784	600	600	857	527	527	527	221	307	307	116	116	423	423	423	230	429	223	223,3	162	18,6	18,6

5.4. Plant Utility Structure

5.4.1 Steam Generation

A fired heater is used to produce high pressure steam in order to provide heating requirements to the plant. The steam is produced from water extracted from the Mhlathuze River as the plant will be located at the Richards Bay Industrial Zone 4 (RBIDZ, 2020). The high pressure steam is distributed to the respective process equipment. Producing high pressure steam increases capital cost. According to literature the steam pressure should be around 60 bar—which is a good trade-off between cost and efficiency (Carcasci & Pacifici, 2015). High pressure steam above 60 bar not only results in high power consumption, but also increases equipment costs as special equipment materials are required.

Natural gas is used to fuel the fired heater. An effective energy percentage of 75 % was assumed for natural gas. The stack gas from the fired heater is required to be cooled before being discharged to the atmosphere in order to avoid thermal pollution (Nordell, 2020). After the distribution of the steam, the used steam streams are mixed at 400 °C and 34 bar. The mixed steam stream is then passed through a turbine where work is extracted.

The steam leaves the turbine at typical conditions of 400 °C and 10 bar. This steam is then fed to a de-aerator where water losses occur. The de-aerator aids with removing oxygen from the cycle in order to prevent aggressive oxidation of process equipment. The outlet of the de-aerator is then mixed with make-up water as presented in the utility structure diagram. This mixture is pumped from 10 bar to 60 bar before entering the fired heater.. This cycle is in essence like a Rankine cycle, but uses a de-aerator instead of a normal condenser. A typical example of a Rankine cycle is show in **Figure 5.2**:

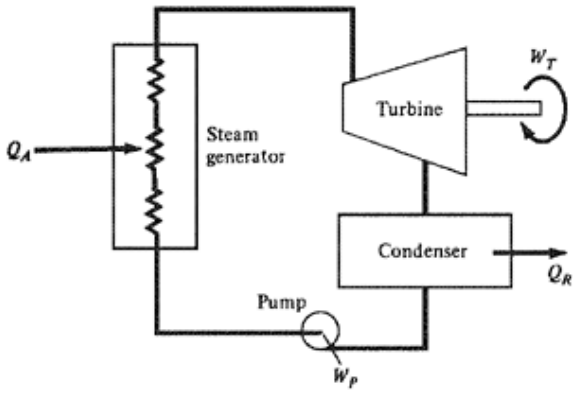


Figure 5.2: *Rankine Cycle diagram.*

As presented in **Figure 5.2**, the steam is expanded in the turbine. The maximum amount of work which can be extracted from the steam is calculated using **Equations 17** and **18**.

$$\eta_{carnot} = 1 - \frac{T_C}{T_H} \quad \text{..... (17)}$$

$$\dot{W}_{MAX} = \eta_{carnot} \times \dot{q}_H \quad \text{..... (18)}$$

Typical Rankine cycles operate at efficiencies of 42 % (Messadi, 2018). For this design, the work extracted from the turbine of the steam generation cycle was sufficient to power all the process equipment.

The utility structure above did not take into account the exact water requirements for the utility structure. Necessary equations for such calculations are given below. The log mean temperature is calculated in order to obtain heat exchanger area requirements. Upon detailed design, the default heat transfer coefficient in Aspen energy analysis should be used for these calculations. **Equation 19** below represents the equation that is used to calculate the respective matched streams' heat exchanger areas.

$$A = Q/U\Delta T_{LM} \quad \text{..... (20)}$$

Where:

$$\Delta T_{LM} = \frac{(T_{hot,in} - T_{cold,out}) - (T_{hot,out} - T_{cold,in})}{\ln\frac{(T_{hot,in} - T_{cold,out})}{(T_{hot,out} - T_{cold,in})}} \quad \text{..... (21)}$$

The utility structure is governed by the amount of water required as steam (heating) and water at ambient temperature (cooing).The amount of water m is calculated using **Equation 22** in order to provide the required water.

$$Q = mc_p\Delta T \quad \text{..... (22)}$$

For temperature and phase change:

$$Q = m(\int_{T_{ref}}^{T} C_P\, dt + H_{VAP}) \quad \text{..... (23)}$$

The equation below is used in the calculations of steam required for heating.

$$Q = m_{steam} \times \hat{h} \quad \text{..... (24)}$$

The $\hat{h}$ values are found in the steam table:

$$\hat{h} = 3564.8\ \frac{kJ}{kg}\ at\ T = 560°C\ and\ P = 60\ bar$$

$$\hat{h} = 3223.2\ \frac{kJ}{kg}\ at\ T = 400°C\ and\ P = 34\ bar$$

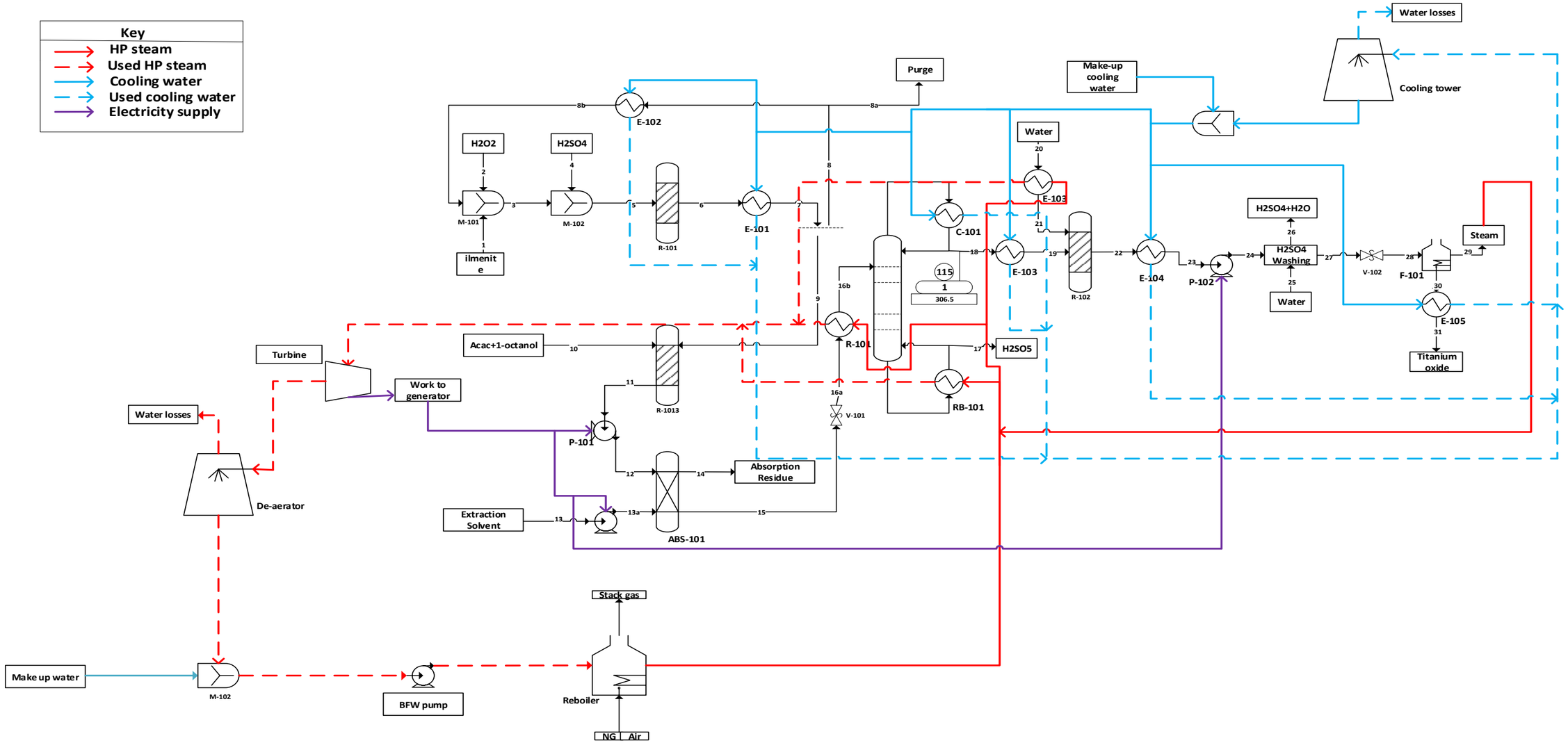
5.4.2. Cooling Tower

The Richards Bay River is used as a source for process water. The cooling water is distributed to process units requiring cooling such as condensers and heat exchangers. The used cooling water is then mixed and passed into a cooling tower. The cooling tower cools the used water before supplying the process units. A make-up water stream is used as the cooling tower also has water losses that occur during cooling. **Figure 5.3** represents the above-described utility structure.

Titanium Oxide Plant with Utility Structure

ABS-101 Absorber	D-101 Distillation column	V-101-102 Pressure release valves	E-101-105 Heat Exchangers	C-101 Condenser	RB-101 Reboiler	R-101 Dissolution Chamber	R102 TiOSO4 Converter	F-101 Furnace	M-101-102 Mixer

Figure 5.3



5.5. Economic Comparison

A preliminary economic calculation excluding any capital and operating costs, and just focussing on the raw materials costs, yielded large differences for the various processes. In these comparisons, the following assumptions have been made:

1. A full-scale commercial plant produces 20 000 tonnes/year of TiO_2. To cater for plant down time due to maintenance and breakages, provision is made for a production of 18 000 tonnes/year.
2. The plant operates for 330 days per year.
3. The ilmenite used as a raw material costs R4.06/kg. (Creamer Media, 2013)
4. Pure grade titanium oxide powder sells for R320/kg.($20/kg) (Alibaba.com, 2020).

$$Annual\ Gross\ Profit\ Margin = [Product\ price \times yield] - [Raw\ material\ cost \times\ consumption]$$

$$= \left[\left(\frac{R320}{kg}\right) * \left(\frac{1000kg}{ton}\right) * \left(\frac{18\,000ton}{yr}\right) * 330/365\right] - \left[\left(\frac{R4.06}{kg}\right) * \left(\frac{18000kg}{ton}\right) * \left(\frac{1000kg}{ton}\right) * 330/360\right]$$

= R 5.141 x 10^9/yr.

= R5.141 billion gross profit.

For consumable costs, the following were taken into account for the two viable separation options of selective precipitation and solvent extraction:

1. The solvents costs of 1-octanol and acetylacetone are R24/kg and R60/kg .
   Cost of 1-octanol and acetylacetone as mixed based on the best experiments results:
   = [(R24/kg.oct)×0.90 + (R60/kg.acac)×0.10]x 18 000 ton/a x 1000kg/ton x (330/365)a
   = R449.2 x 10^6 solvent extraction mixture/s
   = R0.449 x 10^9 (billion rands)
   Gross profit per year = Titanium revenue per year – (Solvent mixture cost per year + Raw material cost)
   = R4.692 x 10^9 (billion rands).

2. The cost of NaTPB, which was used in selective precipitation, is R1296/kg.
   Cost of NATBP based on the best experiments results (15%):
   = R1296 x 0.15 /kg x 18 000 ton/a x 1000kg/ton x (330/365)a
   =R 3.499 x 10^9
   = R3.449 billion.
   Gross profit per year = Titanium revenue per year – (Solvent mixture cost per year + Raw material cost)
   = R1.692 billion.

According Rand Project Air Force, a 446 000 tonne/year production capacity plant will require a capital investment cost of approximately R40 billion (Somi, 2009). If calculated on a pro-rata basis, a 18 000 tonne/year plant will then require R1.614 billion.

This capital expense, plus the cost of the consumables in the selective precipitation process, amounts to R5.06 billion. However, the cost of sulphuric acid and hydrogen peroxide to dissolve the ilmenite first before it goes through the plant, has not been taken into account, which will probably make the selective precipitation route economically non-feasible. This leave the solvent extraction route as the only realistic possibility to pursue, even if the cost for the sulphuric acid and hydrogen peroxide for the initial dissolution step is taken into account.

CHAPTER 6 – CONCLUSIONS AND RECOMMENDATIONS

6.1. Conclusions

The study aimed at finding titanium recovery methods that offer a good trade-off between optimum operations and costs.

- The first objective of the study was to find ilmenite's optimum dissolution route.This also had to take into account the ease of titanium and iron separation.H_2SO_4 was selected as the best acid for ilmenite dissolution as it had a higher Ti recovery percentage than H_3PO_4. H_2SO_4 and 15 vol%H_2O_2 was the optimum mixture for dissolution. The temperature for the dissolution increased rapidly to a temperature of about 155 °C and no heat was added until the end of the 30min period. This mixture achieved the highest Ti dissolution(81%) with only trace amounts of Fe. Through techno-economic analysis this dissolution technique proved to be expensive ($870 million) as a continuous dissolution process.

- The second objective of the study was to determine the optimal separation route for titanium and iron in the ilmenite solution. Solvent extraction was selected to be the best separation method. With solvent extraction when using a combination of 1-octanol and 2 % acac, 90-95 % Fe reported to the aqueous layer over the 30 min period. All the titanium in the respective mixtures was chelated and extracted into the organic layer. The separation kinetics was found to be second order with a rate constant of 0.03 $M^{-1}min^{-1}$.

- The final objective was to convert the optimal dissolution and separation routes into a process.This objective was also met as a process flowsheet was designed with a mass efficiency of approximately 50 %. A plant utility structure was also constructed as the plant is aimed at being a greenfield plant.

- The solvent extraction method was compared to the Becher process, which is the current process used to separate titanium oxide from iron oxide. The solvent extraction method had similar economic indicators as the Becher process.

The payback period of the solvent extraction method was calculated to be approximately 5.3 years at a return on investment of 18.7 %. The optimization performed together with plant power generation as depicted in the utility structure aids with reducing costs. The study was therefore successful at converting the most efficient dissolution and separation method into a process with a nett profit annually and a reasonably good rate on return. Labour costs, disposal of waste and environmental legislations were not taken into account. Although subject to change in the detailed design phase, return on investment for the conceptual design is well above the South African inflation rate of 2.43 % (2020).The design is therefore potentially profitable.

6.2. Recommendations for Future Work

Experiments on raw material fineness (cm^2/g) should be conducted in order to set raw material fineness feed limits as this affects leaching degree.

The conceptual design followed by a detailed design should be done where the sizing of process equipment is considered. An analysis on health and environmental impact should also be conducted included in a plant layout. Furthermore, a detailed economic analysis and process control should also be conducted. This will aid in conducting a HAZOP, plant layout and land requirement. It is therefore important to note that values calculated in flowsheet design are subject to change.

6.3. Value and Contribution of this Work

This study has investigated the separation of iron and titanium in ilmenite from each other. One of the variables considered, was effect of hydrogen peroxide on ilmenite dissolution. It was found that hydrogen peroxide additions favour the dissolution of titanium more than iron. This, on its own, reduces the separation difficulty of titanium and iron. The study has also provided data on separation performance of selective precipitation, solvent extraction and ion exchange resins. A flowsheet design and utility structure that can be taken to full conceptual design and detailed design, has been developed. An economic comparison including the payback period, rate of return on investment and cumulative cash position has been performed and indicated a very profitable process.

Introducing this process will boost the country's economy, because of creating job opportunities, and delivering tax to the Treasury. Furthermore, the favourable profit and return on investment figures could help to attract foreign investments.

7. References

Air Products. (2005, May 17). *Air Products and Chemicals.* Retrieved from http://www.airproducts.com/~/media/Files/PDF/company/safetygram-6.pdf

Alafara, A. (2011). SIMULTANEOUS RECOVERY OF TOTAL IRON AND TITANIUM FROM ILMENITE ORE BY HYDROMETALLURGICAL PROCESSING. *Association of Metallurgical Engineers of Serbia*, 67-70.

Alibaba.com. (2020, June 16). Retrieved from https://www.alibaba.com/product-detail/titanium-dioxide-tio2-nano-powder-price_62217987011.html?spm=a2700.7724857.normalList.46.3278492eWnOZOo

Arkema. (2016, November 6). *The Essential Chemical Industry.* Retrieved from Centre for Industry: http://www.essentialchemicalindustry.org/chemicals/hydrogen-peroxide.html

Arthur, A. (1984, January). *Strategies for Staying Cost Competitive*. Retrieved from Havard Business Review: https://hbr.org/1984/01/strategies-for-staying-cost-competitive

Barthelmy, D. (2014). *Mineralogy database*. Retrieved from Ilmenite mineral data: http://www.webmineral.com/data/Ilmenite.shtml#.XMF3VKdLjs5

Beatriz, F. (2019). Atomic Absorpton Spectrometry,Fundumentals,Instrumentation and Capabilities. *Encyclopedia of Analytical Science*, 43-81.

Bonet, J. (2006). Pressure Optimization of an Original System of Pressure Swing with a Reactive Column. *IChemE*,symposium series no.152, 334-350.

Carcasci, C., & Pacifici, B. (2015). Thermoeconomic Analysis of a One-Pressure Level Heat Recovery Steam Generator Considering Real Steam Turbine Cost . *Energy Procedia*, 591-598.

Carvalho, F. (2002). *Selective precipitation of Mo(VI) with a, a"-bypiridineand 1,10-phenanthroline:Application to molybdenum and radiomolybdenum chemistry. Radioanalytical and Nuclear Chemistry*.Vol.9, 633-636.

Centre for Industry. (2016, October 5). *The essential chemical industry-online*. Retrieved from http://www.essentialchemicalindustry.org/metals/titanium.html

Chemicool. (2017). *Chemicool Dictionary*. Retrieved from What is Chelation?: https://www.chemicool.com/definition/chelation.html

Chen. (2008). THERMAL DECOMPOSITION OF HYDROGEN PEROXIDE IN THE PRESENCE OF SULFURIC ACID. *Journal of Thermal Analysis and Calorimetry.Vol.93*, 115-120.

Chen, D. (2014, January 13). *Utility systems.* Retrieved from https://processdesign.mccormick.northwestern.edu/index.php/Utility_systems

Chipich, T. (1988). A simple, vivid demonstration of selective precipitation. *Chemical Education.Vol.65*, 359.

Christian, G. (1991). Analytical Chemistry. *5th edition*, 145-161.

Creamer Media's. (2013, August 30). *Enineering News*. Retrieved from Speed Space: http://www.engineeringnews.co.za/article/sa-moves-to-use-titanium-ores-base-to-build-new-high-tech-industry-2013-08-30

Dahe, X. (2004).MAGNETIC SEPARATORS APPLIED IN THE ILMENITE PROCESSING INDUSTRY. *Physical Separation in Science and Engineering.Vol.12*, 119-126.

Das, J. (1990). Separation of titanium, iron and aluminium on a chelating resin with benzoylphenylhydroxylamine group and application to bauxite and clay, . *Fresenius Journal of Analytical Chemistry.Vol.336*, 578-581.

Dennis, C. (2001). The synthesis and complexation of a cobaltocenium-based redox-active cryptand containing the phenanthroline unit. *Journal of Organometallic Chemistry.Vol.648*, 1-319.

Dipaloy, D. (2015). Status of the Reactive Extraction as a Method of Separation. *Journal of Chemistry.Vol.2015*, 1-16.

Emsley, J. (2014, December 2). Nature's Building Blocks: An A-Z Guide to the Elements. New York, Oxford University Press, United States of America.

Erik, K. (1993). Determination of acetylacetone and alcohols in titanium chelates . *Analytica Chimica Acta*, 385-389.

Expatica.com. (2020, April 21). *Corporate tax in South Africa*. Retrieved from https://www.expatica.com/za/finance/taxes/corporate-tax-in-south-africa-949408/#:~:text=The%20corporate%20tax%20rate%20in,of%2028%25%20for%20all%20companies.

Hauchard, D. (1997). Solvent extraction of titanium by tributylphosphate, trioctylphosphine oxide and decanol from chloride media . *Hydrometallurgy.Vol.45*, 113-128.

Hobart, M. (2005). *Geoscience News and Information*. Retrieved from Geology.com: https://geology.com/minerals/ilmenite.shtml

Jailson, B. (1997). Spectrophotometric and inductively coupled plasma atomic emission spectrometric determination of titanium in ilmenites after rapid dissolution with phosphoric acid. *Talanta.Vol.44*, 165-168.

Jonglertjunya, W. (2013). Titanium and iron dissolution from ilmenite by acid leaching and microbiological oxidation techniques. *Asia-Pacific Journal of chemical Engineering.Vol.8*, 33-323.

Khan, H. U. (2012, November 7). The Role of Ion Exchange Chromatography in Purification and Characterization of Molecules. Pakistan, Khyber Pakhtunkhwa, Pakistan.

Krishen, A. (1965). Dissolution of ilmenite in sulphuric acid under reducing conditions with controlled abrasion.Metallurgy.Vol.1, 10-77.

Liebenberg, C. (1947). Determination of Ten Major and Minor Elements in Silicate Rocks Based on Separation by Cation Exchange Chromatography on a Single Column. *Analytical Chemistry.Vol.46*, 13-1409.

Liu, W. (2017). Preparation of synthetic rutile via selective sulfation of ilmenite with (NH4)2SO4 followed by targeted removal of impurities. *Chinese Journal of Chemical Engineering.Vol.25*, 821-828.

Mamchenko, A. (2000). Analysis of the Potentiometric Titration Curves. *SAGE Journals.Vol.18*, 881-890.

Martinez, E. (2016). Probability-Based Design of Experiments for Batch Process Optimization with End-Point Specifications. *Industrial & Engineering Chemistry Research.Vol.55*, 1254-1265.

Messadi, A. (2018). Improvement of the Solar Rankine Cycle Applying to the Solar Power Station: Solar II. *Innovative Energy & Research*, 1-12.

Molbase.com. (2020, June 16). Retrieved from http://www.molbase.com/en/cas-143-66-8-cate-p7n10-p4n2.html

Mukhopadhyay, N. (2007). Dissolution studies of mechanically activated Manavalakurichi ilmenite with HCl and H_2SO_4. *Hydrometallurgy.Vol.88*, 154-69.

Neil, G. (1996). Chemical Redox Agents for Organometallic Chemistry. *ACS Publications.Chemical Reviews*, 877-910.

Nel, J. (2010). The plasma manufacturing of titania pigment and nano-titania in a pilot plant . *The Journal of The Southern African Institute of Mining and Metallurgy.Vol.110* , 235-238.

Nordell, B. (2020). Thermal pollution causes global warming. *Global and planetary change.Vol.38*, 305-312.

oanda. (2020, June 16). *Live exchange rates*. Retrieved from USDZAR: https://www1.oanda.com/currency/live-exchange-rates/USDZAR/

Pearson, S. (2013). The effect of temperature on wear and friction of high strength steel in fretting. *Wear.Vol.303*, 622-631.

Poison Control. (2019). *National Capital Poison Centre.* Retrieved from Hydrogen Peroxide: https://www.poison.org/articles/2012-jun/hydrogen-peroxide

PubChem. (2016). *U.S. National Library of Medicine.* Retrieved from https://pubchem.ncbi.nlm.nih.gov/compound/Hydrogen-peroxide

Purcell, W. (2019). Selective precipitation study for the separation of iron and titanium from ilmenite. *Hydrometallurgy.Vol.191*, 1-8.

RBIDZ. (2020, June 27). *Richards Bay Industrial Developments Zone*. Retrieved from KwaZulu-Natal Top Business: https://provincialgovernment.co.za/units/view/151/kwazulu-natal/richards-bay-industrial-development-zone-rbidz

Robertson, M. (2019). *Periodic table.* Retrieved from Royal Society of Chemistry: http://www.rsc.org/periodic-table/element/9/fluorine

Sachkov, V. (2017). Hydrometallurgical Processing Technology of Titanomagnetite Ores. *Minerals.Vol.8*, 1-12.

Sanjeev. (2013). History,Introduction,and Kinetics of Ion Exchange Materials. *Journal of Chemistry.Vol.2013*, 1-13.

Saphan, O. (2018). Qualitative and quantitative analysis of pesticide residues in flower farms soils around lake Naivasha basin, Kenya. *International Journal of Chemical Studies.Vol.6*, 1615-1623.

Siddle, G. (1975). The prospects for titanium dioxide in the paint industry. *Pigment & Resin Technology.Vol.4*, 4-12.

Sinnott, R. (2005). *Coulson & Richardson's Chemical Engineering Series.* Oxford: British Library Cataloguing in Publication Data.

Skoog, D. (2014). Fundamental of Analytical Chemistry. *9th edition*, 773-871.

Solvent Extraction. (2016, 11 06). Retrieved from http://userpages.umbc.edu/~dfrey1/ench445/regular.pdf

Somi, S. (2009). Titanium. *Rand Project Air Force*, 21-45. Retrieved from RAND Project Air Force.

Steudel, R. (2000). Geometries,acidities,and Dissociation Reactions of the Gaseous Superacids. *Chemistry Europe.Vol.2000*, 213.

Stevic, P. (2018, May 18). *Kavli Nanolab Delit.* Retrieved from https://d1rkab7tlqy5f1.cloudfront.net/TNW/Afdelingen/Quantum%20Nanoscience/Kavli%20Nanolab%20Delft/Equipment/Piranha%20SOP.pdf

Taiji, O. (2013). Fundamental Study on Titanium Production Process by the Disproportionation. 113-8656.

Theeraporn, R. (2013). Titanium and iron dissolutions from ilmenite by acid leaching and microbiological oxidation techniques. *Asia-Pacific Journal of Chemical Engineering.Vol.8*, 323-330.

Titanium processing Center. (2017, September 28). *Michelle Chambers*. Retrieved from https://titaniumprocessingcenter.com/what-is-the-kroll-process/

Total materia. (2019). *The world's most comprehensive materials database*. Retrieved from Toal meteria.com: https://www.totalmateria.com/page.aspx?ID=TitaniumProperties&LN=EN

Turker, L. (1988). The Dissolution of Ilmenite in HCI-H_20, HCI-CH_30H and HCI-C_2H_5OH Systems - A Theoretical Approach . *International Journal of Mineral Processing.Vol.24*, 173-184.

Woranart, J. (2013). Kinetics of the dissolution of ilmenite in oxalic and sulfuric acid solutions. *Asia-Pacific Journal of Chemical Engineering.Vol.9*, 24-30.

8. Appendix

8.1. Appendix A- Results in terms of concentration

Some of the results were presented in terms of concentration in order to show that the concentration profile and mass profile of Fe and Ti have the same trend.

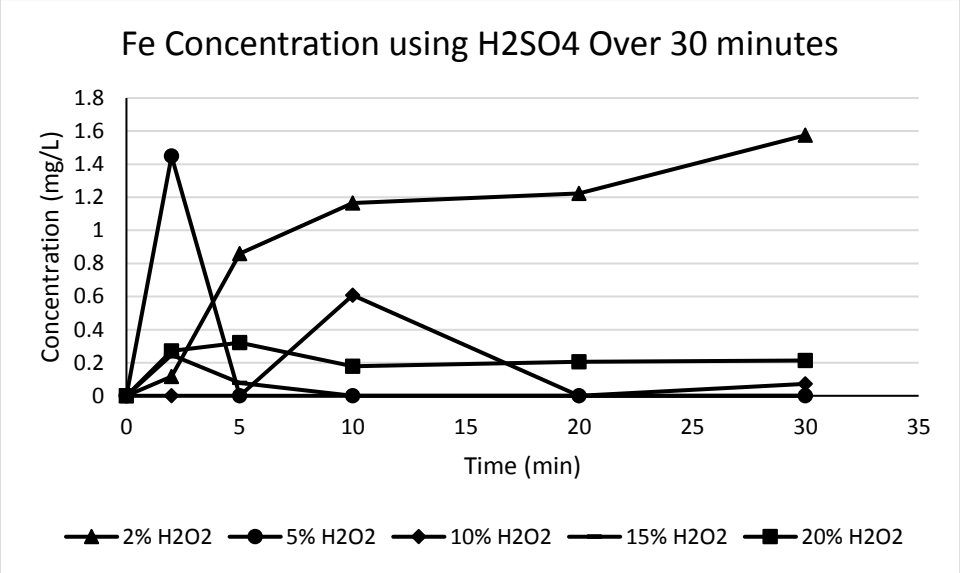


Figure A1: Fe concentration in solution when using H_2SO_4 and H_2O_2 at varied vol%.

The results depict that less iron was dissolved in solution for the mixtures with higher H_2O_2 concentration (vol%).The mixture of 2 % H_2O_2 had the highest Fe concentration at the end of 30min - a concentration of 1.57 mg/L. The mixture of 5,10 and 15 % H_2O_2 had trace amounts of Fe at the end of the 30min duration. The mixture of 20 % H_2O_2 had more Fe dissolved in solution (0.2mg/L) than the lower H_2O_2 concentration mixtures.

From these observations, the optimum H_2O_2 concentration range would approximately be 5 to 15 % provided that more titanium is dissolved in solution at this range. This would make the separation less complex because the iron would be present in the solid phase while titanium would be present in solution. The concentration of titanium was analysed in order to obtain the titanium concentration profile. **Figure A2** represents the titanium concentration profile for the mixtures described above.

The results from **figure A2** depict that more titanium was dissolved in solution for the mixtures with higher H_2O_2 concentration (vol%).The mixture of 2 % H_2O_2 had the least Ti concentration at the end of 30 min—a concentration of 22 mg/L. The mixture of 5 and 10 % H_2O_2 had the

same concentration of Ti (28mg/L) at the end of the 30min duration. Higher concentration shifts were only observed in the 15 and 20 % H_2O_2 mixture. This signified that more H_2O_2 was required in order to dissolve more Ti. The mixture of 20 % H_2O_2 had the highest Ti dissolved in solution (39mg/L).Figure 4.1 and figure 4.2 show that a high amount of titanium was dissolved in solution while small amounts of iron were dissolved. Ore dissolution processes with such characteristics make separation processes less complicated.

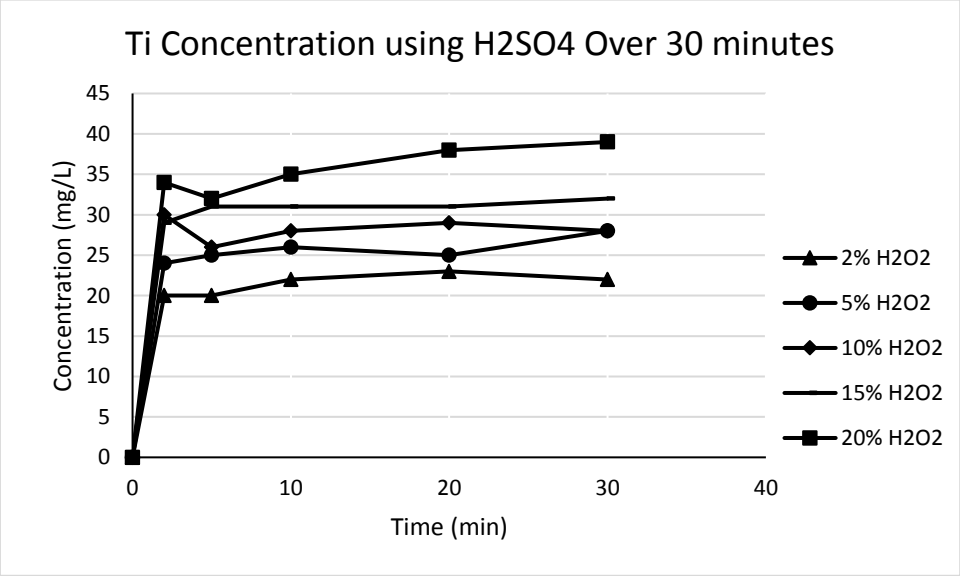


Figure A2: Ti concentration in solution when using H_2SO_4 and H_2O_2 at varied vol%.

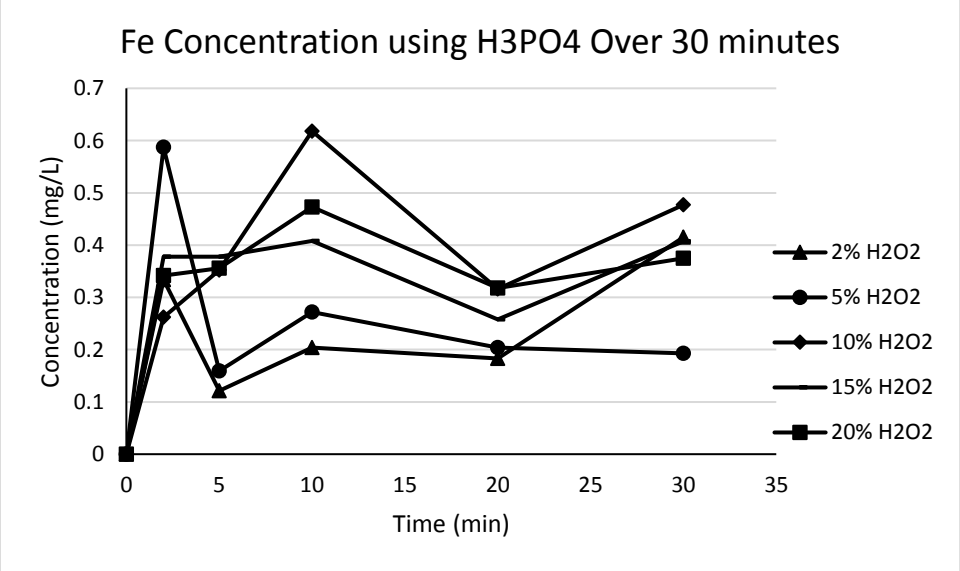


Figure A3: Fe concentration in solution when using H_3PO_4 and H_2O_2 at varied vol%.

The results for when H_3PO_4 was used as an acid suggest that the optimum H_2O_2 concentration range is narrower than when H_2SO_4 was used. From the results,5 % H_2O_2 is the only H_2O_2

concentration that results in the lowest Fe concentration (0.2mg/L) in solution. Furthermore, the results suggest that using H_2SO_4 and H_2O_2 at optimum concentrations can aid with dissolving less Fe than when H_3PO_4 and H_2SO_4 are used. Using H_2SO_4 and H_2O_2 at 5 % H_2O_2 dissolved no Fe while H_3PO_4 and H_2SO_4 at 5 % H_2O_2 (optimum) dissolved 0.2 mg/L.

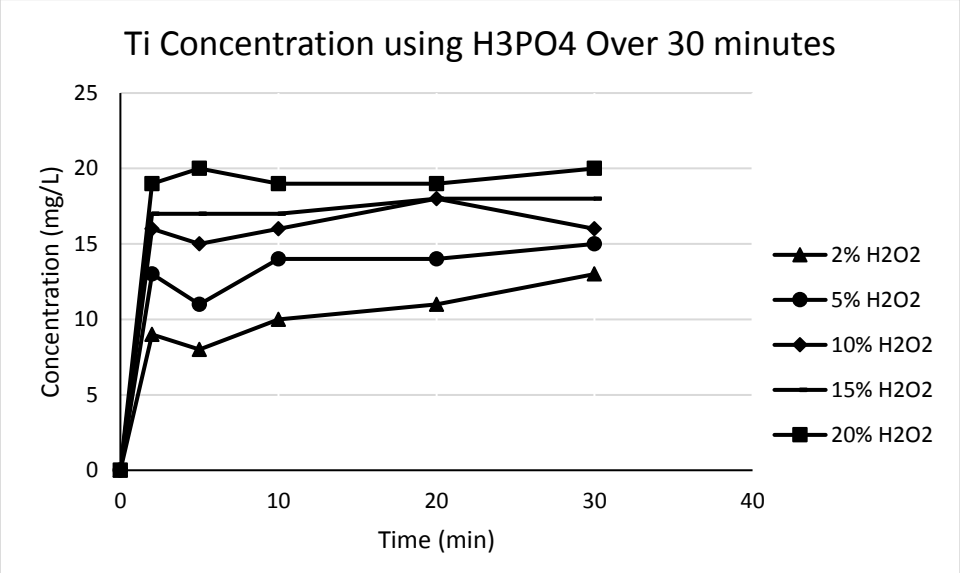


Figure A4: Ti concentration in solution when using H_3PO_4 and H_2O_2 at varied vol%.

Using H_3PO_4 and H_2O_2 resulted in less dissolved Ti compared to when H_2SO_4 and H_2O_2 were used. Based on the 2-20 % H_2O_2 concentration range the minimum dissolved Ti for when H_3PO_4 and H_2O_2 were used was around 13 mg/L while the minimum dissolved Ti for when H_2SO_4 and H_2O_2 were used was around 22 mg/L. The maximum dissolved Ti for when H_3PO_4 and H_2O_2 were used was around 20 mg/L while the maximum dissolved Ti for when H_2SO_4 and H_2O_2 were used was around 39 mg/L.

This project aims at separating titanium and iron and recovering as much titanium as possible. Based on these results, hydrogen peroxide aids with dissolving more titanium and less iron. This observation helped at making the separation of these metals less complex. Using H_3PO_4 and H_2O_2, the lowest achievable Fe concentration that was in solution was 0.2 mg/L while for H_2SO_4 and H_2O_2 it was approximately 0 mg/L. The maximum dissolved Ti for when H_3PO_4 and H_2O_2 were used was around 20 mg/L while the maximum dissolved Ti for when H_2SO_4 and H_2O_2 were used was around 39 mg/L. This observation suggested that it was better to dissolve ilmenite using H_2SO_4 and H_2O_2 than using H_3PO_4 and H_2O_2.With using H_2SO_4 and H_2O_2 it was important to also determine the H_2O_2 concentration that helps achieve a good trade-off between the dissolution of the two metals. **Table A1** represents the exact concentrations of Fe and Ti for when H_2SO_4 and H_2O_2 was used.

***Table A1**: Ti and Fe concentration in solution when using H_2SO_4 and H_2O_2 at varied vol%.*

Fe Concentration using H2SO4					
Time	H2O2 2.vol%	H2O2 5.vol%	H2O2 10.vol%	H2O2 15.vol%	H2O2 20.vol%
0	0	0	0	0	0
2	0,116	1,449	0	0,247	0,272
5	0,859	0	0	0,077	0,321
10	1,166	0	0,608	0	0,179
20	1,223	0	0	0	0,205
30	1,575	0	0,073	0	0,214
Ti Concentration using H2SO4					
0	0	0	0	0	0
2	50	60	75	72,5	85
5	50	62,5	65	77,5	80
10	55	65	70	77,5	87,5
20	57,5	62,5	72,5	77,5	95
30	55	70	70	80	97,5

8.2. Appendix B-Lab Plan

This section provides the schedule that was used to conduct the experiments of this project.

8.2.1. Dissolution

***Table B1**: Ilmenite dissolution guide using H_2SO_4 and H_3SO_4 through H_2O_2 concentration optimization.*

Ilmenite Dissolution			
Time (min)	H2SO4+H2O2	H3PO4+H2O2	H2O2
0	✓	✓	5 %
2	✓	✓	2 %
5	✓	✓	5 %
10	✓	✓	10 %
20	✓	✓	15 %
30	✓	✓	20 %

Ilmenite (0.5g) was placed in a beaker.H_2SO_4 (20mL) and H_2O_2 at 5.vol% were added to the ilmenite beaker and the solution was stirred.0.5ml of the solution was extracted for the time intervals shown in **Table B1.**The extracted samples were poured in 100mL volumetric flasks.Deionized water was poured into the flasks and filled to the 100mL mark.This was done

in order to dilute the sample and to not damage the AA spectroscopy.The AA spectroscopy was used to analyzed the concentrations of Ti and Fe present in solution.The dillution was taken into consideration in order to track back the original concentration that was in each of the 0.5mL samples in order to calculate the amount(mass) of dissolved Ti and Fe.The following equation was used (Saphan, 2018):

$C_1V_1 = C_2V_2$ ……..(B1)

Sample Calculation:

Fe concentration at 2min when H_3PO_4 was used to dissolve ilmenite at 2 %H_2O_2:

$$C_1V_1 = C_2V_2$$

$$C_1 = \frac{C_2V_2}{V_1}$$

$$\boldsymbol{m = (\frac{C_2V_2}{V_1}) \times V_{original}} \text{ ..... (B2)}$$

$$= (\frac{(\frac{0.334mg}{L}) \times 0.1L}{0.0005L}) \times 0.2L$$

$$= 1.3mg$$

8.2.2. Separation

***Table B2**: Selective precipitation using Phenenthroline (Phen).*

Selective Precipitation					
Time (min)	2%Phen	5%Phen	10%Phen	15%Phen	20%Phen
0	✓	✓	✓	✓	✓
2	✓	✓	✓	✓	✓
5	✓	✓	✓	✓	✓
10	✓	✓	✓	✓	✓
20	✓	✓	✓	✓	✓
30	✓	✓	✓	✓	✓

***Table B3**: Selective precipitation using sodium tetra-phenyl borate (NaTPB).*

Selective Precipitation					
Time (min)	2%NaTPB	5%NaTPB	10%NaTPB	15%NaTPB	20%NaTPB
0	✓	✓	✓	✓	✓
2	✓	✓	✓	✓	✓

5	✓	✓	✓	✓	✓
10	✓	✓	✓	✓	✓
20	✓	✓	✓	✓	✓
30	✓	✓	✓	✓	✓

Table B4*: Solvent Extraction using acetyl-acetone(acac) in 1-octanol.*

Solvent Extraction					
Time (min)	2%acac	5%acac	10%acac	15%acac	20%acac
0	✓	✓	✓	✓	✓
2	✓	✓	✓	✓	✓
5	✓	✓	✓	✓	✓
10	✓	✓	✓	✓	✓
20	✓	✓	✓	✓	✓
30	✓	✓	✓	✓	✓

Table B5*: Ion Exchange using Dowex Marathon C Hydrogen (DMCH).*

Ion Exchange					
Time (min)	2%DMCH	5%DMCH	10%DMCH	15%DMCH	20%DMCH
0	✓	✓	✓	✓	✓
2	✓	✓	✓	✓	✓
5	✓	✓	✓	✓	✓
10	✓	✓	✓	✓	✓
20	✓	✓	✓	✓	✓
30	✓	✓	✓	✓	✓

Table B6*: Ion Exchange using Amberlite IRA-67.*

Amberlite IRA-67					
Time (min)	2%IRA-67	5%IRA-67	10%IRA-67	15%IRA-67	20%IRA-67
0	✓	✓	✓	✓	✓
2	✓	✓	✓	✓	✓
5	✓	✓	✓	✓	✓
10	✓	✓	✓	✓	✓
20	✓	✓	✓	✓	✓
30	✓	✓	✓	✓	✓

Table B7*: Ion Exchange using Amberlite IRA-900.*

Amberlite IRA-900					
Time (min)	2%IRA-900	5%IRA-900	10%IRA-900	15%IRA-900	20%IRA-900
0	✓	✓	✓	✓	✓
2	✓	✓	✓	✓	✓
5	✓	✓	✓	✓	✓
10	✓	✓	✓	✓	✓

20	✓	✓	✓	✓	✓
30	✓	✓	✓	✓	✓

8.3.Appendix C-Images of Prepared Solutions

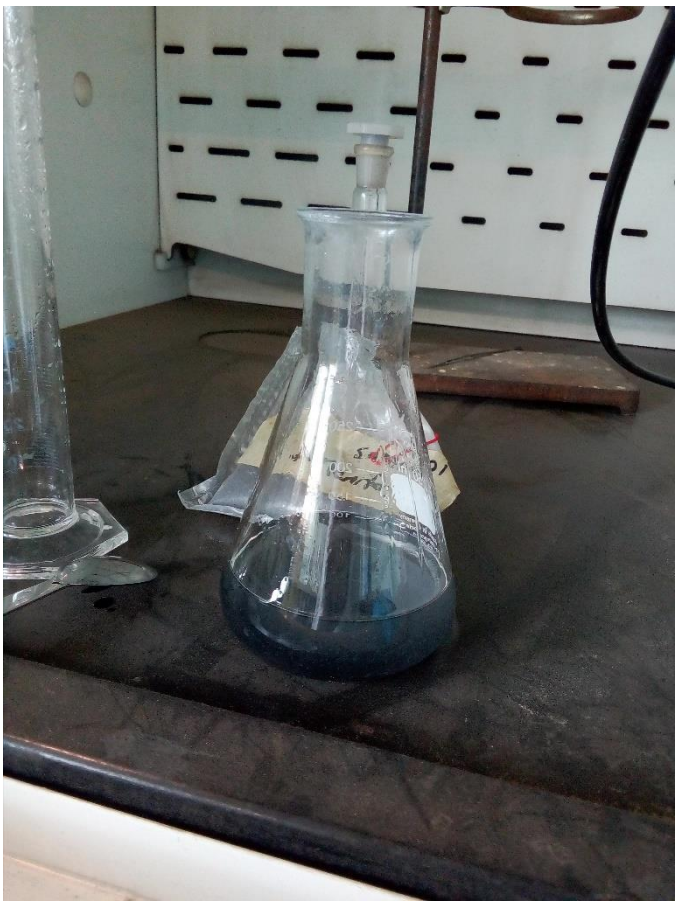


Figure C1: Ilmenite being dissolved by H_2SO_4 and H_2O_2.



Figure C2: Precipitation formed when NaTPB was used.



Figure C3: Image of NaTPB taken during experiments of this project.



Figure C4: Solvent extraction using acetyl-acetone in 1-octanol.

Figure C4 shows how the aqueous layer separated with the organic layer. During this separation process 0.5 mL sample were extracted as presented in **Appendix B**.



Figure C5: Ion exchange using Amberlite IRA-900.

Figure C5 shows the solutions that were extracted at time intervals presented in **appendix B**. The resulting cakes shown in **figure C5** were taken to SEM for composition analysis.

8.4.Appendix D-Mass & Concentration Profile Tables (Raw Data)

The mass profile of Fe and Ti in the tables below was calculated as discussed in **Appendix B**. These tables include the dissolution mass profiles and separation mass profiles.

8.4.1. Dissolution

***Table D1**: Fe mass in solution when using H_2SO_4 and H_2O_2 at varied vol%.*

Fe mass(mg) in solution using H_2SO_4					
Time	H_2O_2 2.vol%	H_2O_2 5.vol%	H_2O_2 10.vol%	H_2O_2 15.vol%	H_2O_2 20.vol%
0	0	0	0	0	0
2	0.464	5.796	0	0.988	1.088
5	3.436	0	0	0.308	1.284
10	4.664	0	2.432	0	0.716
20	4.892	0	0	0	0.820
30	6.300	0	0.292	0	0.856

***Table D2**: Fe mass in solution when using H_3PO_4 and H_2O_2 at varied vol%.*

Fe mass(mg) in solution using H3PO4					
Time	H_2O_2 2.vol%	H_2O_2 5.vol%	H_2O_2 10.vol%	H_2O_2 15.vol%	H_2O_2 20.vol%
0	0	0	0	0	0
2	1.336	2.348	1.048	1.512	1.368
5	0.484	0.636	1.408	1.512	1.424
10	0.816	1.088	2.472	1.632	1.892
20	0.732	0.816	1.264	1.032	1.272
30	1.660	0.772	1.908	1.628	1.500

***Table D3**: Ti mass in solution when using H_3PO_4 and H_2O_2 at varied vol%.*

Ti mass(mg) in solution using H3PO4					
Time	H_2O_2 2.vol%	H_2O_2 5.vol%	H_2O_2 10.vol%	H_2O_2 15.vol%	H_2O_2 20.vol%
0	0	0	0	0	0
2	36	52	64	68	76
5	32	44	60	68	80
10	40	56	64	68	76
20	44	56	72	72	76
30	52	60	64	72	80

***Table D4**: Ti mass in solution when using H_2SO_4 and H_2O_2 at varied vol%.*

Ti mass(mg) in solution using H2SO4					
Time	H_2O_2 2.vol%	H_2O_2 5.vol%	H_2O_2 10.vol%	H_2O_2 15.vol%	H_2O_2 20.vol%
0	0	0	0	0	0
2	80	96	120	116	136
5	80	100	104	124	128
10	88	104	112	124	140
20	92	100	116	124	152
30	88	112	112	128	156

8.4.2.Separation

***Table D5**: Fe mass in solution in selective precipitation when using phenanthroline at varied vol%.*

Fe Mass(mg) in Solution using Phenanthroline					
Time	Phen 2.vol%	Phen 5.vol%	Phen 10.vol%	Phen 15.vol%	Phen 20.vol%
0	1.254	1.364	1.218	1.307	1.298
2	0.826	0.946	0.967	1.092	0.852
5	1.254	1.161	1.055	1.097	1.283
10	1.050	0.984	1.241	1.216	1.316
20	1.296	1.131	1.087	1.307	1.226
30	1.0924	1.364	1.218	1.187	1.298

***Table D6**: Fe mass in solution in selective precipitation when using NaTPB at varied vol%.*

Fe Mass(mg) in Solution using NaTPB					
Time	NaTPB 2.vol%	NaTPB 5.vol%	NaTPB 10.vol%	NaTPB 15.vol%	NaTPB 20.vol%
0	1.272	1.192	1.086	0.949	0.910
2	1.272	1.192	1.086	0.949	0.910
5	1.694	2.108	2.478	2.266	0.517
10	2.35	2.00	2.260	1.927	0.958
20	2.156	2.613	2.273	2.038	1.113
30	2.662	2.452	2.664	2.657	0.759

***Table D7**: Fe Concentration in Aqueous layer using Acetylacetone in 1-Octanol.*

Fe Concentration(mg/L) in Aqueous layer using Acetylacetone in 1-Octanol					
Time	acac 2.vol%	acac 5.vol%	acac 10.vol%	acac 15.vol%	acac 20.vol%
0	0	0	0	0	0
2	3.182	2.981	2.716	2.373	2.276
5	4.237	5.272	6,.197	5.665	1.294
10	5.89	5.015	5.651	4.818	2.397
20	5.391	6.534	5.683	5.095	2.783
30	6.656	6.131	6.661	6.643	1.898

***Table D8**: Ti Concentration in Aqueous layer using Acetylacetone in 1-Octanol.*

Ti Concentration(mg/L) in Aqueous layer using Acetylacetone in 1-Octanol					
Time	acac 2.vol%	acac 5.vol%	acac 10.vol%	acac 15.vol%	acac 20.vol%
0	0	0	0	0	0
2	7.387	6.922	5.233	5.010	5.800
5	6.682	6.348	5.100	5.000	5.100
10	4.989	3.871	3.220	4.230	5.700
20	1.911	1.022	0.980	4.230	5.700
30	0	0	0	0	3.700

***Table D8**: Fe Concentration in solution when using DMCH.*

Fe Concentration(mg/L) in solution when using DMCH					
Time (min)	2%DMCH	5%DMCH	10%DMCH	15%DMCH	20%DMCH
0	0	0	0	0	0
2	5.147	4.470	4.749	4.222	1.509
5	4.219	6.987	8.218	7.406	1.350
10	7.783	7.807	8.550	8.206	2.239
20	7.484	7.587	8.106	7.937	3.145
30	8.856	9.412	8.580	10.149	4.858

***Table D9**: Ti Concentration in solution when using DMCH.*

Ti Concentration(mg/L) in solution when using DMCH					
Time (min)	2%DMCH	5%DMCH	10%DMCH	15%DMCH	20%DMCH
0	0	0	0	0	0
2	4.300	4.500	5.300	4.900	7.500
5	9.400	5.400	5.700	5.700	7.500
10	11.500	5.500	5.500	6.100	7.900
20	10.400	5.900	4.800	6.500	7.600
30	8.100	5.400	4.300	6.500	7.300

***Table D10**: Fe Concentration in solution when Amberlite IRA-67.*

Fe Concentration(mg/L) in solution when Amberlite IRA-67					
Time (min)	2%IRA-67	5%IRA-67	10%IRA-67	15%IRA-67	20%IRA-67
0	0	0	0	0	0
2	6,176	5,364	5,699	5,066	1,811
5	5,063	8,384	9,862	8,887	1,620
10	9,340	9,368	10,260	9,847	2,687
20	8,981	9,104	9,727	9,524	3,774
30	10,627	11,294	10,296	12,179	5,830

***Table D11**: Fe Concentration in solution when Amberlite IRA-67.*

Ti Concentration(mg/L) in solution when Amberlite IRA-67					
Time (min)	2%IRA-67	5%IRA-67	10%IRA-67	15%IRA-67	20%IRA-67
0	0	0	0	0	0
2	8,2352	7,152	7,5984	6,7552	2,4144
5	6,7504	11,1792	13,1488	11,8496	2,16
10	12,4528	12,4912	13,68	13,1296	3,5824
20	11,9744	12,1392	12,9696	12,6992	5,032
30	14,1696	15,0592	13,728	16,2384	7,7728

***Table D12**: Fe Concentration in solution when Amberlite IRA-900.*

Fe Concentration(mg/L) in solution when Amberlite IRA-900					
Time (min)	2%IRA-900	5%IRA-900	10%IRA-900	15%IRA-900	20%IRA-900
0	0	0	0	0	0
2	6,691	6,691	6,173	5,488	1,961
5	5,487	5,484	10,683	9,627	1,755
10	10,117	10,117	11,115	10,667	2,910
20	9,729	9,729	10,537	10,318	4,088
30	11,512	11,512	11,154	13,193	6,315

***Table D13**: Ti Concentration in solution when Amberlite IRA-900.*

Ti Concentration(mg/L) in solution when Amberlite IRA-900					
Time (min)	2%IRA-900	5%IRA-900	10%IRA-900	15%IRA-900	20%IRA-900
0	0	0	0	0	0
2	8,646	7,596	7,978	7,092	2,535
5	7,0872	11,731	13,806	12,442	2,268
10	13,075	13,117	14,364	13,786	3,761
20	12,572	12,741	13,618	13,334	5,283
30	14,878	15,811	14,414	17,050	8,161

8.6 Appendix F-SEM Results

The separation methods that resulted in the formation of a cake were analysed by SEM for composition analysis. When phenanthroline was used as a precipitant in selective precipitation, there was no precipitation observed. However, when NaTPB was used, there was some precipitate seen, as the images below indicate. (see appendix C).

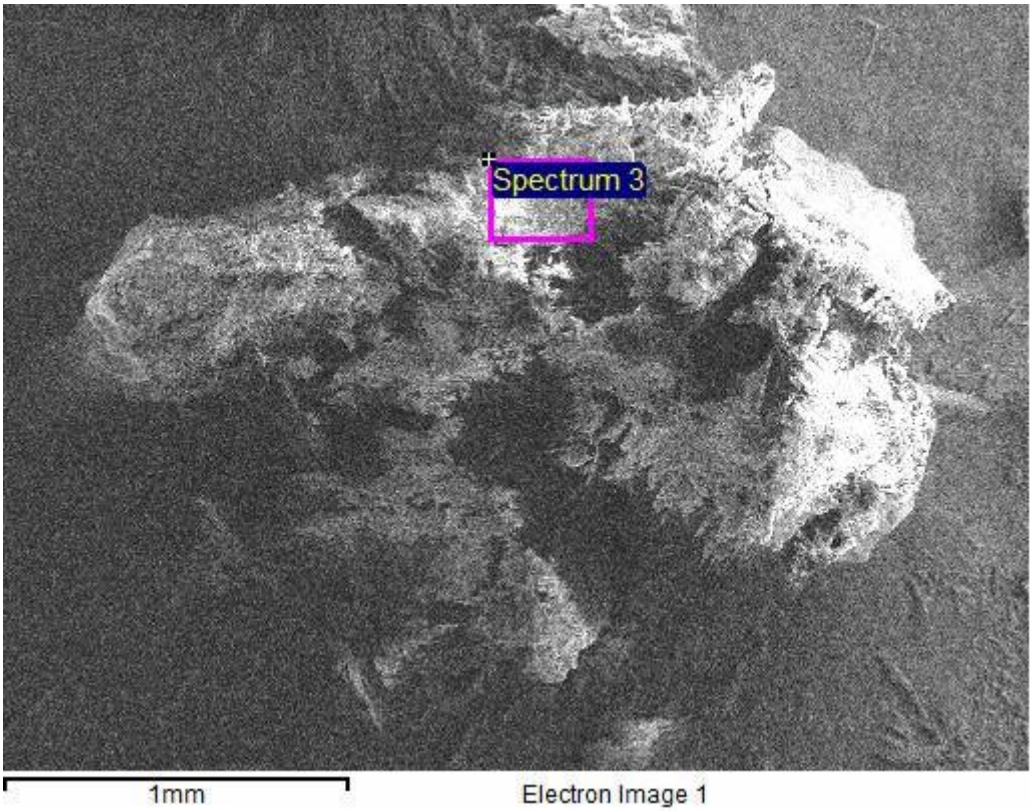


Figure F1: Electron image of precipitate formed when applying a 5 %NaTPB mixture. for precipitation in a sulphuric 15% peroxide solution.

This analysis was conducted in order to analyze the composition of Ti and Fe in the precipitate. No precipiate formed when 2 %NaTPB was added to the mixture. **Figure F1** represent the electron image of the cake when 5 vol%.NaTPB was usedThe square labelled spectrum 3 is the area that was used to analyzed the sample composition.The results of this sample are shown on **figure F2** as printed by the SEM.

Element	Weight%	Atomic%
C K	83.29	87.26
O K	15.25	12.00
Na K	1.28	0.70
Ti K	0.15	0.04
Fe K	0.02	0.00
Totals	100.00	

Figure F1: SEM composition results of precipitate form from 5%NaTPB mixture.

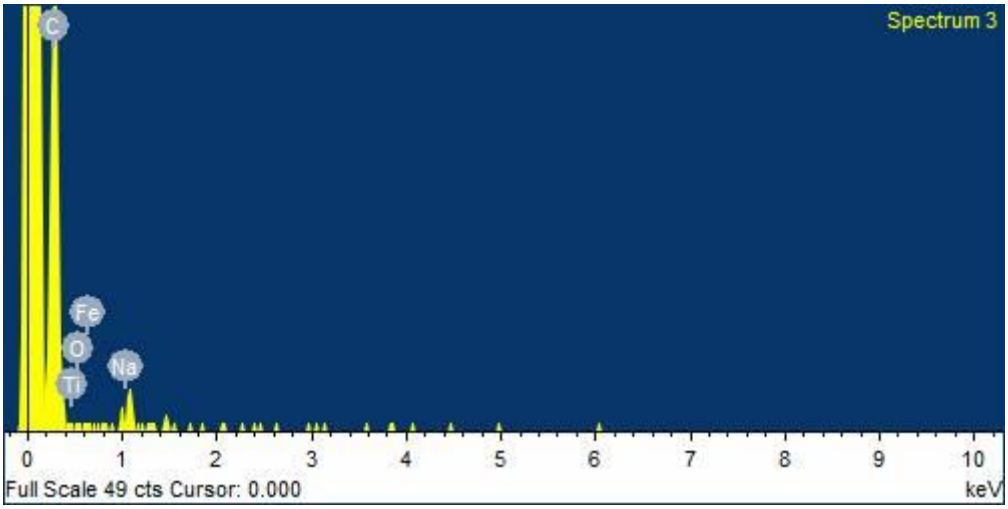


Figure F2: Graphical precipitate composition results of Fe and Ti for 5 %NaTPB mixture.

Elements such as sodium were also present(1.28%) since NaTPB contains sodium.The aim was to precipitate Ti and in this way separate it from iron.The sample had more Ti than Fe which were present at 0.15 % and 0.02 % respectively. The selectivity in precipitating Ti was therefore 7,5 times more than that of Fe.

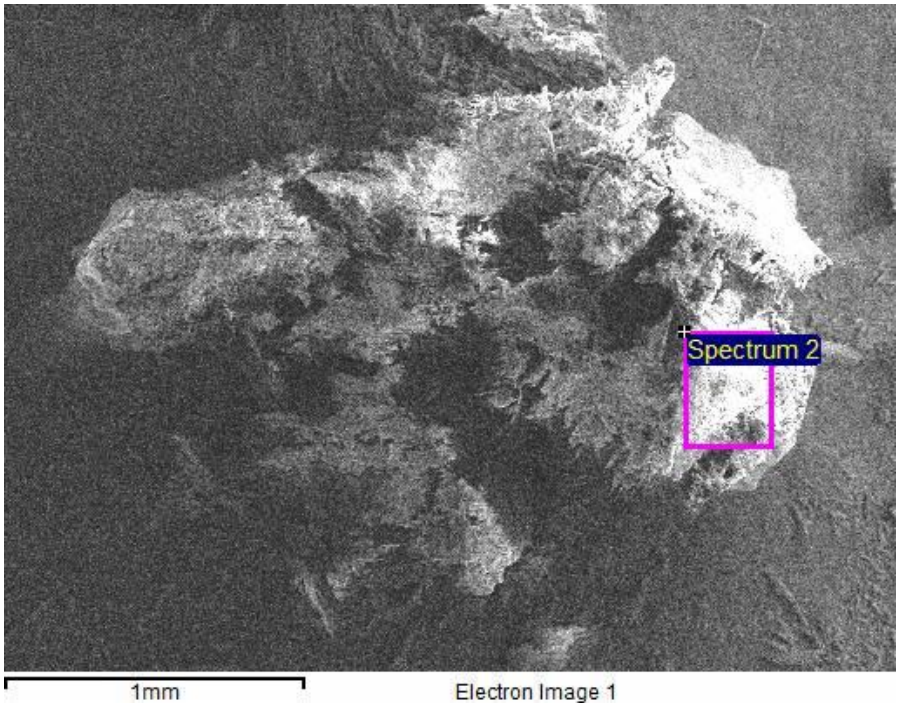


Figure F3: Electron image of precipitate form from 10 %NaTPB mixture.

Figure F3 represent the electron image that was taken for the mixture where NaTPB was added at 10 vol%.The square labelled spectrum 2 is the area that was used to analyzed the sample composition.The results of this sample are shown in **figure F4** as printed by the SEM.

Element	Weight%	Atomic%
C K	91.10	93.88
O K	5.70	4.41
Na K	3.18	1.71
Ti K	-0.27	-0.07
Fe K	0.30	0.07
Totals	100.00	

Figure F4: Composition results of precipitate form from 10%NaTPB mixture.

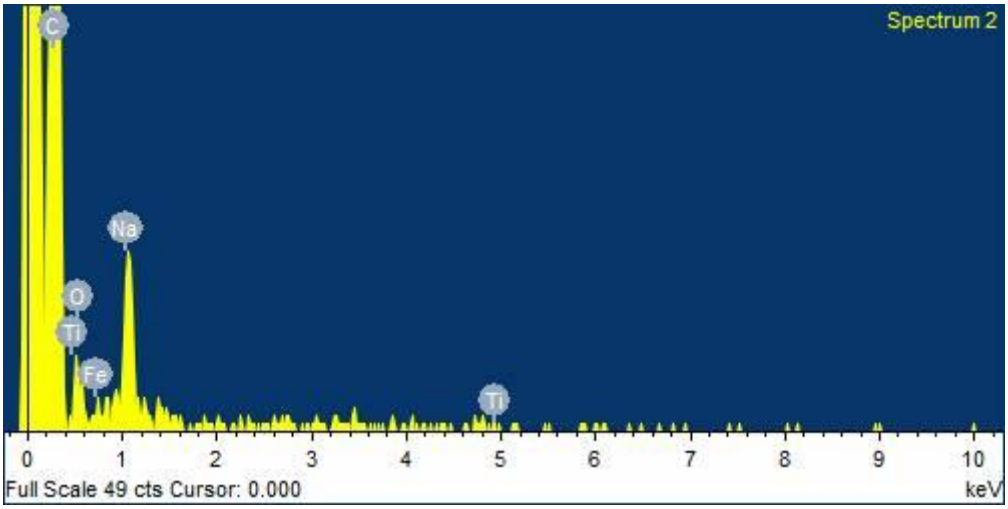


Figure F5: Graphical precipitate composition results of Fe and Ti for 10%NaTPB mixture.

The composition of Ti was a negative value (-0.27%).This meant that NaTPB at 10.vol% did not precipitate any Ti(see **section 6.1**).The composition of Fe was 0.3 % which meant that NaTPB at 10.vol% precipitated some Fe without precipitating Ti.In terms of precipitation selectivity for these 2 metals, NaTPB at 10.vol% had 100 % precipitation selectitity.

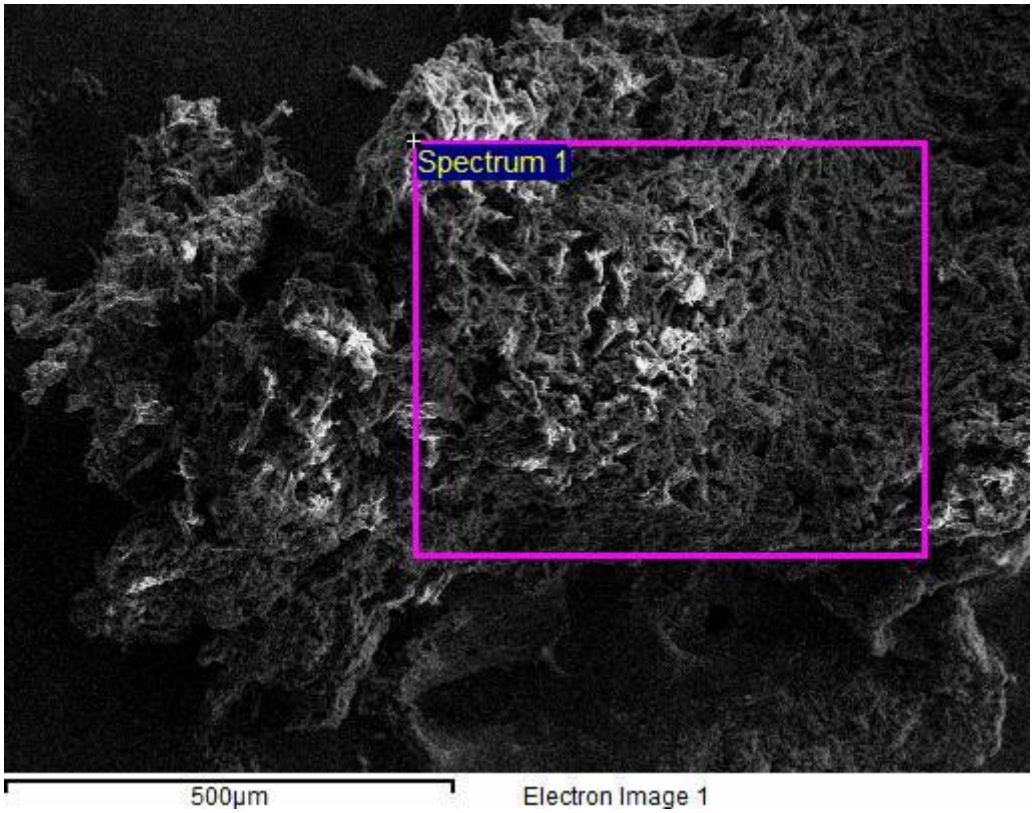


Figure F6: Electron image of precipitate form from 15 %NaTPB mixture.

Element	Weight%	Atomic%
C K	44.39	54.10
O K	45.38	41.51
Al K	0.45	0.24
Si K	0.54	0.28
S K	5.58	2.55
Ca K	3.31	1.21
Ti K	0.19	0.06
Fe K	0.15	0.04
Totals	100.00	

Figure F7: Composition results of precipitate form from 15 %NaTPB mixture.

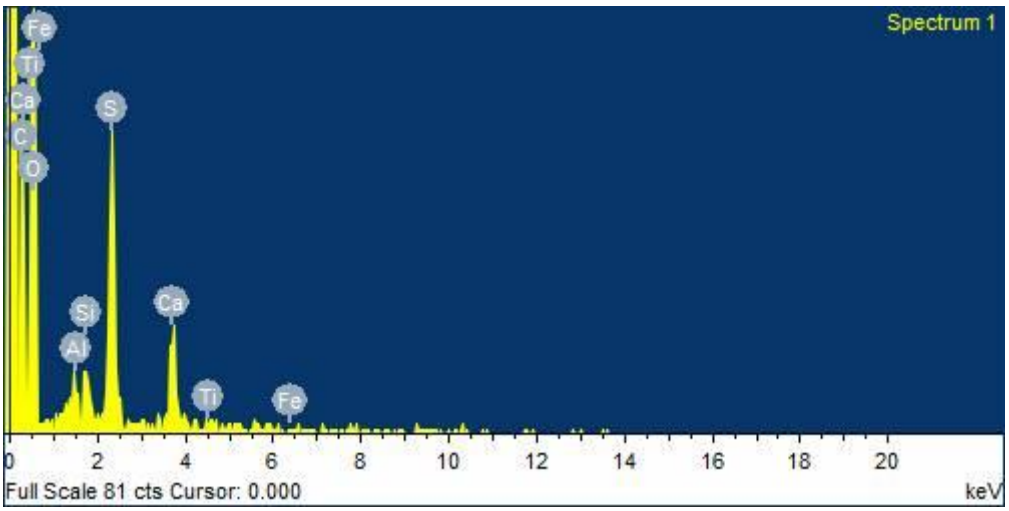


Figure F8: Graphical precipitate composition results of Fe and Ti for 15 %NaTPB mixture.

Ti and Fe were present almost at the same amounts.Ti was present at 0.19 % and Fe was presenta at 0.15 %.This was observed as a poor precipitation selectivity as this menat that for every 1.2 mg of Ti that was precipitated,1 mg of Fe was also precipitated.This then defeats the aim of separating these metals.

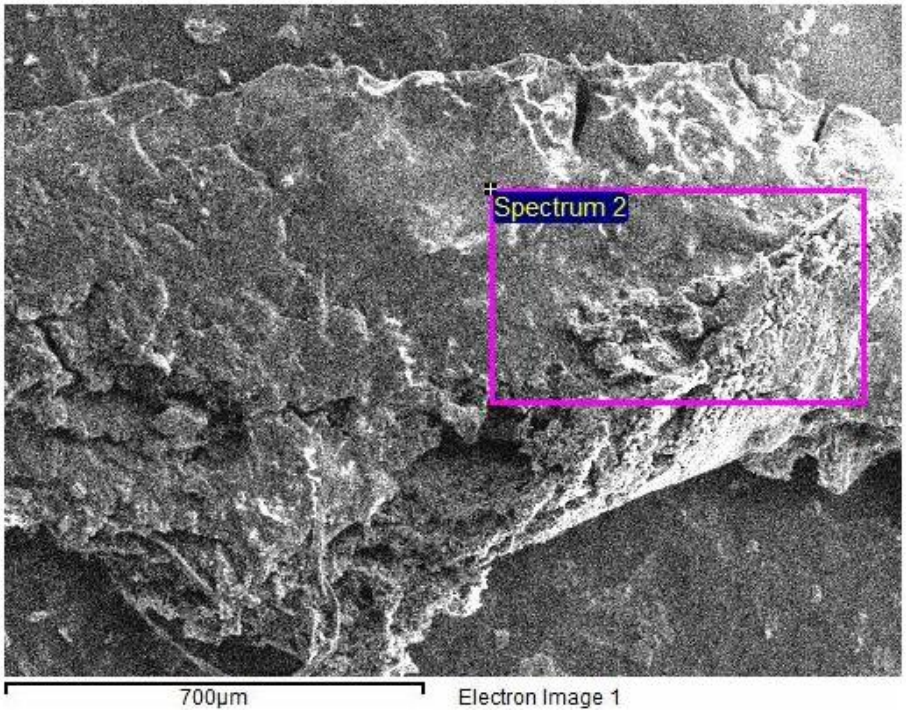


Figure F9: Electron image of precipitate form from 20 %NaTPB mixture.

Element	Weight%	Atomic%
C K	68.21	75.81
O K	26.22	21.88
Al K	0.49	0.24
Si K	1.87	0.89
S K	2.16	0.90
Ca K	0.23	0.08
Ti K	0.30	0.08
Fe K	0.50	0.12
Totals	100.00	

Figure F10: Composition results of precipitate form from 20 %NaTPB mixture.

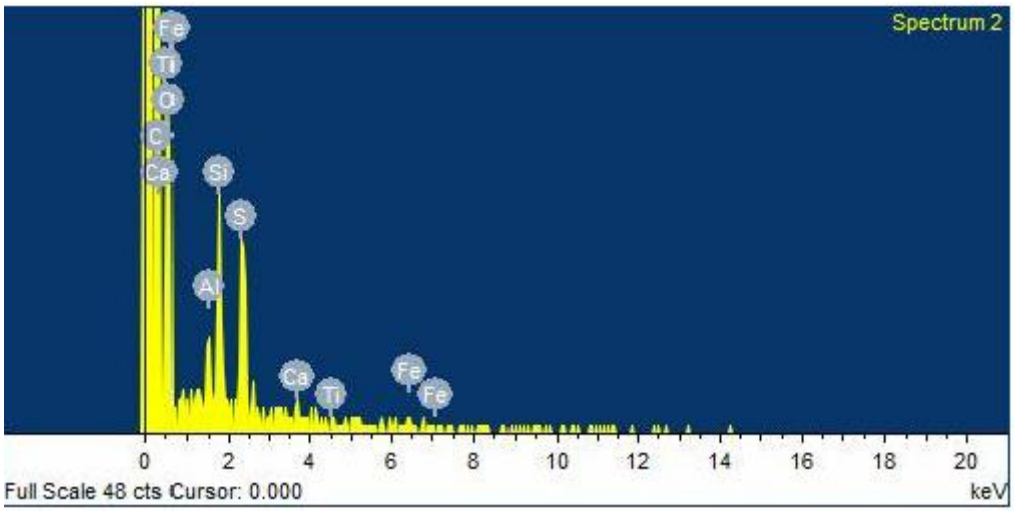


Figure F11: Graphical precipitate composition results of Fe and Ti for 20 %NaTPB mixture.

Elements from alumium down to calcium were present in small fractions.Aluminium was detected from the SEM aluminium stub and the other elements could possibly be picked up during the sample drying process(see **figure F10**).The composition difference of Ti and Fe for the 20 % NaTPB mixture was more than that of the 15 %NaTPB mixture. Ti was present at 0.5% and Fe was present at 0.3 %.This was observed as a better precipitation selectivity (compared to the 15 %NaTPB mixture) as this menat that for every 1.6 mg of Ti that was precipitated,1mg of Fe was also precipitated.